The Stripe Phase in 4-Leg Ladders and Quantum Impurity Entanglement

by

Ming-Shyang Chang

M.Sc., National Tsing Hua University, Taiwan, 2003

A THESIS SUBMITTED IN PARTIAL FULFILMENT OF
THE REQUIREMENTS FOR THE DEGREE OF

Doctor of Philosophy

in

The Faculty of Graduate Studies

(Physics)

The University Of British Columbia

September 11, 2007

Abstract

The physics of ladder systems and the Kondo problem have an essentially one-dimensional nature. There are powerful tools, such as bosonization and conformal field theory, applicable to these systems. In the first part of this dissertation, the stripe phase in 4-leg ladders is investigated by bosonization and weak-coupling renormalization group equations. A new type of charge-four correlation, bipairing, is proposed and gives a simple explanation of the stripe phase. In the second part, we discuss boundary effects on the entanglement entropy in quantum spin chains and calculate the entanglement entropy in the Kondo-like quantum impurity model. The result on impurity entanglement entropy is generalized to the system with finite size or finite temperature by employing conformal field theory methods. The theoretical calculations are also compared with numerical results obtained by density matrix renormalization group methods.

Contents

List of Tables

List of Figures

List of Abbreviations

1D	one dimension
2D	two dimesnion
ARPES	angle-resolved photoemission spectroscopy
BCS	Bardeen-Cooper-Schrieffer
CDW	charge density wave
CFT	conformal field theory
CnSm	n gapless charge modes and m gapless spin modes
DMRG	density matrix renormalization group
FLT	Fermi liquid theory
FSS	finite size spectrum
LSCO	$La_{2-\delta}Sr_{\delta}CuO_4$
OBC	open boundary conditions
PBC	periodic boundary conditions
RG	renormalization group

Acknowledgements

I would like to acknowledge all the good teachers I have met throughout my educations. They are the reason that I can enjoy learning. Especially, I would like to thank George Sawatzky, Mona Berciu and Gordon Semenoff for their nice lectures from which I learn a lot. I also want to acknowledge my committee Andrea Damascelli, Mark Van Raamsdonk and Fei Zhou for their effort during my PhD.

The most important person to thank is my advisor, Ian Affleck. This thesis won't exist without him. I appreciate his teaching during these three years. It's really an exciting and unforgettable experience to work with him. Besides my advisor, my collaborators Erik Sørensen and Nicolas Laflorencie are also important to this thesis. I enjoy the time working with them. I also want to thank my former advisor during my M.Sc., Hsiu-Hau Lin for the private communication about his unpublished results.

I would like to acknowledge all my friends at UBC, Tom Davis, Suman Hossain, Henry Lin, Yoshitaka Maeda, Justin Malecki, Dominic Marchand, Rodrigo Pereira, Brian Shieh, Lara Thompson, Greg Van Anders and Conan Weeks. I also want to thank the support from my friends Hsin-Ying Chiu, Chang-Yu Hou, Bo-Young Lin, Chi-Chang Lau, Shao-Hwai Tasi and Chen Chih-Yu.

The last but not the least, I thank my family's long time support for me to be a physicist, especially to my girlfriend Chien-Hsin Tso.

Co-Authorship Statement

The results in Chapters 2-5 have been accepted for publication: "Bipairing and the Stripe Phase in 4-Leg Ladders" in Physical Review B (2007) [1]. This work was done in collaboration with my advisor Professor Ian Affleck. The results in Chapter 6 have been published: "Boundary effects in the critical scaling of entanglement entropy in 1D systems" in Physical Review Letters (2006) [2] and "Impurity Entanglement Entropy and the Kondo Screening Cloud" in Journal of Statistical Mechanics (2007) [3] and "Quantum Impurity Entanglement" accepted by Journal of Statistical Mechanics (2007) [4]. These works are done in the collaboration with Professor Erik Sørensen (McMaster University), Dr. Nicolas Laflorencie and my advisor Professor Ian Affleck. The numerical results of density matrix renormalization group in Chapter 6 are obtained by Professor Erik Sørensen. Figure (6.3), (6.4), (6.5) and Table (6.1), (6.2) are also used courtesy of him.

Chapter 1

Introduction

The physics of ladder systems and the Kondo problem have an essentially one-dimensional (1D) nature. There are powerful tools, such as bosonization and conformal field theory (CFT), applicable to these systems. In the first part of this dissertation, the stripe phase in the 4-leg ladders is investigated by bosonization and weak-coupling renormalization group equations. A new type of charge four correlation, bipairing, is proposed, which gives a simple explanation of the stripe phase. In the second part, we discuss the boundary effects on the entanglement entropy in quantum spin chains and calculate the entanglement entropy in Kondo-like quantum impurity models. The result on impurity entanglement entropy is generalized to the system with finite size or finite temperature by employing conformal field theory methods. The theoretical calculations are also compared with numerical results obtained by density matrix renormalization group by Professor Erik Sørensen.

Strongly correlated systems in low dimension have been active research fields for more than two decades [5, 6, 7, 8]. The theoretical calculations become more tractable with the help of bosonization and conformal field theory. In general, the numerical methods can also reach larger system size compared to the problems in two dimensions (2D). One powerful tool, density matrix renormalization group (DMRG), works specially well for the low dimensional systems [9]. Besides being the intersection of theoretical and numerical methods, the experimental realization of ladder systems is accessible in some materials [10, 11, 12, 13].

The nonvanishing spin gap and d-wave pairing correlations in the slightly doped 2-leg ladder $t-J$ model are reminiscent of the pseudo gap phase in high critical temperature (high Tc) superconducting materials [14]. This result attracted a lot of attention to the ladder systems and pointed toward a possible connection to the high Tc physics. Later on, DMRG found "stripes", the charge density oscillations at incommensurate filling in the $t-J$ ladders and small 2D clusters [14, 15, 16, 17, 18, 19, 20]. These clear numerical results again remind people about the stripe phase found in cuprates [21, 22]. While whether the stripes phases in the $t-J$ ladders and cuprates share the same physics remains an open question, there is not even a satisfactory understanding of the stripe phase in the $t-J$ ladders. The stripe phase in 2-leg $t-J$ ladders can be well understood as generalized Friedel oscillations in bosonization language [23]. In the first part of this thesis, we will adopt a scheme similar to that used in [23] to study the stripe phase in 4-leg $t-J$ ladders. By this means, we may be able to extract some physics relevant to 2D systems when the number of legs is increased.

The second part of this thesis is about the entanglement entropy in quantum spin

chains and the Kondo model [2, 3]. Entanglement entropy is basically the von Neumann entropy for the reduced density matrix instead of the full density matrix. It was proposed as one measurement of quantum entanglement between two subsystems [24]. The entanglement entropy for 1D systems at quantum critical points has universal scaling behaviors characterized by the central charge in conformal field theory (CFT) associated with the phase transitions [25]. Moreover, the scaling form can be calculated explicitly by CFT methods [26, 27]. There is a well-known CFT approach to the Kondo problem and we will study the impurity contribution to the entanglement entropy.

Chapter 1 to 5 contain the work about the stripe phase in 4-leg ladders. In Chapter 1, we introduce the motivations, models of our systems and the theoretical background. Chapter 2 presents the proof that pairing and stripes can't coexist in 4-leg ladders based on bosonization. Chapter 3 supports this result by investigating finite size spectrum (FSS). Chapter 4 proposes a candidate for the stripe phase found in the analysis of weak coupling renormalization group (RG) equations. Chapter 5 establishes the effective 2-leg bosonic description to the original 4-leg fermionic problem and another stripe phase is found in this approach. Chapter 6 contains the other project about the impurity entanglement entropy. We will introduce the impurity model and CFT methods to calculate the impurity contribution to entanglement entropy.

1.1 Stripes and High Temperature Superconductors

Besides the DMRG data on $t-J$ ladders, the project about the ladder stripes is largely motivated by the experimental results that (2D) stripes exist in the high critical temperature superconductor materials. Therefore, we will first review the relevant results in high temperature superconductors [28].

Conventional superconductors are good metal in their normal states (when the temperature is higher than the critical temperature) and these metallic states are well described by Fermi liquid theory. When the interactions between electrons are attractive (even infinitesimally small), the Fermi surface is unstable and electrons will form Cooper pairs. Later on, people realized that the attractive interactions between electrons are mediated by phonons. This is the celebrated Bardeen-Cooper-Schrieffer (BCS) theory [29]. This superconductivity instability is in general weak and the theory is valid when $E_F \gg \hbar\omega_D \gg k_B T_c$, where E_F, ω_D and T_c are the Fermi energy, Debye frequency and superconducting transition temperature, respectively. That's why T_c is usually less than 20K in conventional superconductors.

The discovery of superconductivity in layered copper-oxide compounds (cuprates) was a great surprise [30]. It's not only because of their high transition temperatures but also because the "parent" compounds of the materials are in fact insulators [31]. These superconductors are obtained by electronically doping (mostly hole doping) "parent" compounds that are antiferromagnetic Mott insulators. Mott insulators are insulators due to electron interactions, which are different from simple band insulators. The fact that undoped materials have antiferromagnetic order and insulating behavior indicates the

electron-electron correlations are important. In other words, they are so-called strongly correlated systems with strong repulsive interactions. Besides antiferromagnetism and superconductivity, there are various types of low temperature orders in the cuprates due to the strong correlations. These proposed orders can either compete or coexist with superconductivity. Since the nonsuperconducting states are not Fermi liquid, the superconductivity mechanism is surely different from the canonical BCS theory. Then the question for theorists is how to get superconductivity from doped antiferromagnetic Mott insulators [32, 33].

The typical phase diagram is shown in the Fig. (1.1). When the holes are doped into the system, the antiferromagnetic order is destroyed rather fast. Then the system becomes superconducting above the critical hole density δ. The transition temperature is first increased with higher doping and reaches its maximum at the optimal doping. After the optimal doping, the transition temperature goes down again. The superconductivity region is called underdoped or overdoped for the doping lower or higher than the optimal doping, respectively. In the underdoped regime, there are a variety of crossover phenomena observed at temperatures above T_c where the low energy single particle spectral weight is suppressed [34]. This indicates that there is an energy gap opened in the system. This energy gap has similar feature to the superconducting gap observed in the same materials at temperatures below T_c. This energy gap above T_c is called a "pseudogap" [35, 36, 37]. Superconductivity is the result of two distinct quantum phenomena: pairing and long range phase coherence. In conventional superconductors, these two things occur at the same time. The observation of a pseudogap strongly suggests that pairs are formed first at higher temperature then move coherently at the lower temperature in the high temperature superconducting materials. If preformed pairs really exist, then phase fluctuation will be important. There are many experimental facts related to the pseudogap from angle-resolved photoemission spectroscopy (ARPES) [35, 36, 37], tunnelling [38], resistivity [39] and specific heat [40] measurements. However, this crossover phenomena is not sharply defined and there is still debate on it boundary of onset.

The symmetry of the pair wavefunction is another distinct feature of high temperature superconductors. In the conventional superconductors, the phonon-mediated pairs have zero angular momentum quantum number. The pair wavefunction and gap function are invariant under rotations and it's called "s-wave" pairing [29]. Around the same time as the discovery of high temperature superconductivity in the cuprates, the possibility of superconductivity in the two dimensional Hubbard model near the antiferromagnetic state at half filling was discussed [41]. That work concluded that the dominant superconducting instability should have $d_{x^2-y^2}$ symmetry instead of s symmetry. The d-wave pairing was later confirmed from the temperature dependence of the penetration depth [42] and by various phase sensitive measurements [43, 44].

In the conventional superconductors, if the superconductivity is suppressed by either a magnetic field or higher temperatures, then the system remains a metallic Fermi liquid [29]. The situation becomes much more complex for high temperature superconductors due to the strong interactions between electrons. In this case, the suppressed supercon-

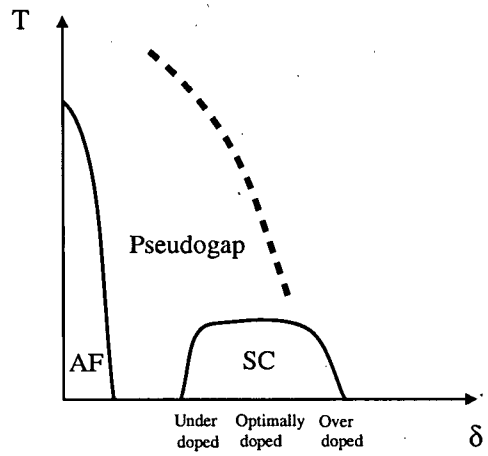

Figure 1.1: This is a schematic phase diagram of high temperature superconductors as a function of temperature T and hole doping δ. AF and SC are antiferromagnetic and superconducting states, respectively. The solid lines are the phase boundaries. The dashed lines is the boundary where a pseudogap is opened, which is not sharply defined and is still under debate.

ductivity can not be described as a Fermi liquid and many possible phases compete [45]. One would generally expect various sorts of electronic density waves, including charge and spin ordered phases such as Wigner crystal and antiferromagnetic Néel state. Charge and spin orders can coexist with the metallic or even superconducting transport if the density wave order opens a gap on only part of the Fermi surface, leaving other parts gapless [46]. This seems similar to what happens in the pseudogap region.

One particular class of competing orders is known as "stripes" and is observed widely in experiments. Stripe order refers to unidirectional density wave order, that is, the order which spontaneously breaks translational symmetry in one direction but not in others. It's a charge stripe order, if the broken symmetry results in charge density modulations or a spin stripe order, if the broken symmetry results in spin density modulations. In particular, the occurrence of stripe phases in the high temperature superconductors or more generally doped antiferromagnetic was predicted by theory before the experimental observations [47, 48].

Neutron scattering is one of the most useful probes to detect stripe orders [21, 22, 49]. Neutrons are spin 1/2 but charge neutral particles and can scatter directly from the electrons spins. Diffraction of a neutron beam by spin stripes yields extra Bragg peaks. However, neutrons can only detect charge stripes indirectly by imaging the induced lattice (i.e. nuclei) distortions. For two dimensional stripes, the stripe direction is referred to as the direction in which translational symmetry is not broken. The stripe period is the period of the density along the direction in which translational symmetry is broken. Since stripe order is unidirectional, the new Bragg peaks are at positions $\vec{k}_{\pm} = \vec{Q} \pm 2\pi\hat{e}/\lambda$

where $\hat{e}$ is the unit vector perpendicular to the stripe direction, λ is the stripe period, and $\vec{Q}$ is an appropriate point [21, 50]. For charge stripes, $\vec{Q}$ is any reciprocal lattice vector of the underlying crystal, such as $(2\pi/a, 2\pi/a)$ where a is the lattice spacing. For spin stripes, $\vec{Q}$ is the antiferromagnetic wave vector $(\pi/a, \pi/a)$. One striking feature of stripes in high Tc materials is that the stripe period changes with the hole density. This indicates that the periods of stripes don't match up with the underlying lattice structure. Thus, stripes are incommensurate density waves.

The first indication of incommensurate spin modulation was provided by inelastic neutron scattering on superconducting $La_{2-\delta}Sr_\delta CuO_4$ (LSCO) [51]. Superconductivity coexists with the incommensurate spin correlations but T_c is strongly depressed. The suppression of superconductivity is maximum for $\delta \approx 1/8$, which is the 1/8 anomaly in high temperature superconductivity [52]. It certainly suggests that an order with incommensurate spin structures competes with superconductivity. The first experiment to see both charge and spin stripes was done by Tranquada and co-workers on a LSCO material ($La_{1.6-\delta}Nd_{0.4}Sr_\delta CuO_4$) in which Nd was added to freeze the fluctuating spins and charges into a static structure [21]. As we mentioned before, the charge configuration can not be seen directly by neutrons but indirectly by the atoms that move in response to the charges. The shifted wave vector of charge stripes is twice that of spin stripes, i.e. $\vec{k}_{charge} = 2\vec{k}_{spin}$ or equivalent $\lambda_{spin} = 2\lambda_{charge}$. They concluded that spin correlations have a π phase shift (e.g. spin up to down) across the 1D like charge domain of the stripes. Moreover, they showed that the inverse stripe period $1/\lambda_{spin} \approx \delta$ for various hole doping δ [21]. In general, charge stripes form at a higher temperature than spin stripes. Note also that static charge and spin stripes coexist with superconductivity throughout the superconducting dome. Recently, charge and spin peaks have also been detected in $La_{1.875}Ba_{0.125-\delta}Sr_\delta CuO_4$ in neutron scattering studies [53].

One thing to notice is that the experiments actually revealed quartets (two pairs) of Bragg peaks at $\vec{Q} \pm 2\pi\hat{x}/\lambda$ and $\vec{Q} \pm 2\pi\hat{y}/\lambda$. This peaks can be also interpreted as due to the checkerboard order in the system, which was also discussed in the papers by Tranquada and co-workers [21, 49]. Base on the material structure and the analogy of the stripe phase found in a similar (nonsuperconducting) compound, they concluded that the system more likely has the stripe order on each Cu-O planes but the stripe orders on neighboring planes tend to be oriented at right angles to each other. Recently, the checkerboard order has been observed in $Bi_2Sr_2CaCu_2O_{8+\delta}$ by scanning tunneling microscopy [54, 55]. Whether one should change the stripe interpretation in LSCO and other compounds relies on further studies.

There are many interesting experimental results regarding stripes in the cuprates. The spin stripe order has also been observed in LSCO for dopings between $\delta = 0.02$ and $\delta = 0.05$ where the system is not superconductding at any temperature. These stripes are called diagonal because they lie along a direction rotated 45 degrees to the Cu-O bond direction [56]. Above $\delta = 0.05$, the stripes become vertical (along the Cu-O bond direction) and the material are superconductiviting at low temperature [57]. Spin stripes also exist in $La_2CuO_{4+\delta}$ with $\delta = 0.12$. In this material, static stripes coexist with

superconductivity even at optimal doping [58]. Neutron scattering evidence has been found of static charge stripes in underdoped $YBaCu_2O_{6+\delta}$ (YBCO) with $\delta = 0.35$, and $T_c = 39$K. The charge peaks persist to at least 300K [59]. These experiments indicate that the charge stripes form at higher temperature before the spin stripe formation at lower temperature. Also, the charge stripe formation occurs at a higher temperature than the formation of the pairing gap (pseudogap) in those observed results.

Apparently, stripes are important bridges between the antiferromagnetic and superconducting orders. Then two questions emerge immediately. The first one is why do we see stripes in these materials? The other one is whether stripes play important roles in the mechanism for high temperature superconductivity? To date, there is no definite answers to these two questions. We will review some theories addressing these issues.

The undoped state of the cuprate superconductors is an insulating antiferromagnet. This is now widely believed to be an essential feature of high temperature superconductivity. However, the doped antiferromagnet is a complicated theoretical problem. The most important local interactions in a doped antiferromagnet are well represented by the $t - J$ model, resulting from the infinitely large repulsive on-site interaction, where t is the hopping amplitude of holes from one to its neighboring sites and J is the antiferromagnetic exchange coupling between spins. The physics of several simple situations is well understood. When there is no hole, the ground state is antiferromagnetic. The motion of a single hole in an antiferromagnet is highly frustrated. When a hole hops to it neighboring site, the system gains kinetic energy $-t$. However, the spin which exchanges with the hole will increase the total energy by $(d-1)J$, where d is the dimension of the system. The motion of a hole creates a string of "defect" in an antiferromagnet and costs a large energy. It turns out the hole can move through a sixth or higher order process called a Trugman path but the effective hopping matrix elements is much smaller than t [60]. It seems that a pair of holes can move without frustration since the other hole cures the string created by the first one. Actually, this was suggested to be a new mechanism of pairing [61]. However, Trugman showed that this mode of propagation of the hole pair is still frustrated by a quantum effect [60]. If there are many holes and $J \gg t$, then phase separation happens [62]. The holes will tend to stay together in order to maximize the number of spin bonds. In fact, phase separation occurs for a wide range of parameters in the phase diagram.

There are proposals to explain stripes as the compromise between phase separation and long range Coulomb interactions [28, 63]. However, these proposals are not consistent with the DMRG result where there is only short range (screened) Coulomb interaction [15]. If the holes carry charge, the full phase separation will cost a huge energy due to the Coulomb repulsion. In general, Coulomb interactions don't favor charge accumulations. Therefore, there is a competition between the short range tendency to phase separation and the long range repulsion of the Coulomb interaction. The compromise between the charge aggregation on short length scales and the required homogeneity on long length scales results in an emergent crossover length scale [64]. Many solutions with inhomogeneous behaviour on intermediate length scales are possible, such as checkerboard

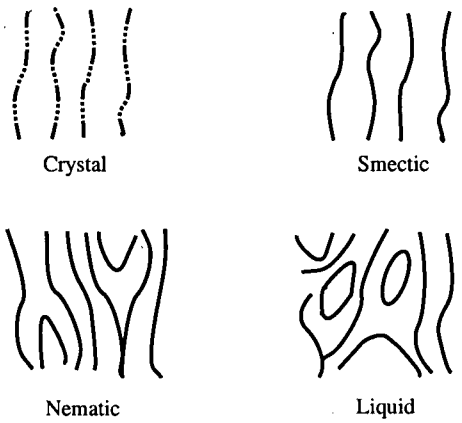

Figure 1.2: This is a schematic view of electronic liquid crystals. Solid lines represent metallic stripes along which electrons can flow. The dashed lines represent density modulations. In the crystal phase, the phases of density modulations between neighboring stripes are locked. It's an insulating phase and breaks translational symmetry in all directions.The smectic phase breaks translation symmetries in only one direction, which is a static stripe phase. When the transverse fluctuations along the stripes increase, the system is driven into the nematic phase. There is only local stripe order in the nematic phase and it can be thought as a melted or fluctuating stripe phase. The liquid phase breaks no spatial symmetry and is isotropic.

patterns, stripes and others [63, 65].

The stripe solution is very stable in some models and is widely observed in the cuprates. Also, the fact that charge stripes form before the spin stripes in the cuprates suggests that stripes are driven by charges. When doping is not large in the cuprates, the screening may be poor and long range Coulomb interaction becomes important. These are consistent with the mechanism of Coulomb frustrated phase separation mentioned above. However, stripes are also found in the DMRG works on 2D $t-J$ model [15], where the long range Coulomb interaction is absolutely absent. Quantum Monte Carlo methods find the ground state of 2D $t-J$ model has superconductivity instead of stripes [66]. The main criticism of DMRG work is that the stripes may be the artifacts due to the open boundary conditions or finite size effects. Quantum Monte Carlo methods are also biased by the trial wave function chosen at the beginning. Whether long range Coulomb interactions are important for the stripe formations in cuprates remains controversial.

Although the origin of stripes in the cuprates is still not clear, is it possible that stripes play important roles in the mechanism for high temperature superconductivity? Or more precisely, how can a stripe phase becomes a high temperature superconductor? There is a theory proposal by Kivelson and collaborators based on the quantum analogy of classical liquid crystals [50, 67]. Liquid crystals exhibit a state of matter whose properties are between conventional liquid and solid. For example, a liquid crystal can flow like

liquid but have the molecules arranged or oriented in the same direction like a crystal. The phases of classical liquid crystals are characterized by the broken symmetries, like the quantum analogy. According to the possible broken symmetry, an electronic liquid crystal has the following phases: (1) a *liquid*, which breaks no spatial symmetries and is a conductor or a superconductor when there is no disorder; (2) a *nematic*, or anisotropic liquid, which breaks the rotation symmetry of the lattice but the translational symmetry is unbroken; (3) a *smectic*, which breaks translational symmetry in only one direction. Otherwise, it is an electron liquid in other directions; (4) an *insulator*, which breaks translational symmetries in all directions and has the character of an electronic solid. The schematic views of these phases are shown in Fig. (1.2). They identify smectic phases as the static stripes and nematic as the melted or fluctuating stripes. Of course, a nematic phase can be superconducting.

They model each one dimensional electron "river" in a smectic phase as a Luttinger liquid and allow the transverse displacement as the density fluctuation in the Luttinger liquid. A Luttinger liquid is the low energy effective theory for 1D electron systems with forward scattering type of interactions and is exactly solvable. More detailed properties will be given in the section (1.2.1). In each Luttinger liquid, there are quasi-long-ranged pairing and charge density orders. Then the interactions between the one dimension electron rivers are the Josphenson coupling (hopping of electron pairs) and the density-density interactions. If the Josphenson coupling dominates, then the electron pairs move coherently and the system is driven into superconductivity. If the density-density interactions dominate, then the system exhibits static stripes. It's clear that a stripes based mechanism of high temperature superconductivity predicts competition between static stripes and superconductivity. Their idea is simply to think of the cuprates as quasi-one-dimensional superconductors [67].

Some ARPES experiments show the features of the cuprates are reminiscent of a quasi-one-dimensional superconductor [37, 68, 69]. However, it's difficult to compare the parameters in this stripes based mechanism of high temperature superconductivity with the experiments. The detailed predictions from the model depend on the Luttinger parameter of each 1D electron river. Unfortunately, it's unknown. Therefore, there is no quantitative prediction for the phase diagram and the critical transition temperature T_c since they can be quite different for different Luttingter parameters. Another more important issue is that whether stripes are universal phenomena in high temperature superconductors is not clear. If stripes are not universal, then it's very unlikely that the stripes based mechanism of high temperature superconductivity is the final story.

To sum up, the stripes in the cuprates is still an active field in the research, not only the mechanism of stripes but also their connection to superconductivity. The study of related questions about the stripes phases in t-J ladders should shine some light on the stripes in the cuprates.

1.2 The Stripe Phase in 4-Leg Ladders

Numerical evidence for stripes has also been found in Hubbard and t-J ladders, which contain only short range interactions [14, 15, 16, 17, 18, 19, 20]. Ladder stripes are incommensurate density modulations. Particularly, for the number of legs less than or equal to four, the wave length of charge stripes λ is the inverse of hole density δ, that is, $\lambda \sim 1/\delta$ [14, 16, 17, 18]. For the 2D t-J model (on a 8×19 lattice) [15], the periods of charge and spin stripes are $1/2\delta$ and $1/\delta$, respectively, which are the same as the those observed in the neutron scattering experiments [21, 49]. Although the wave length of the charge stripes in the ladder systems is twice that of stripes in the cuprates, nonetheless, it's the first step toward the two dimensional system. An understanding of the occurrence of stripes in these ladder models, whether or not long-range Coulomb interactions are required for their existence and their connection with superconductivity are important open questions.

There are experimental realizations of the ladder systems [10, 11, 12, 13]. Recently, a stripe phase has also been observed by a resonant X-ray scattering technique in the 2-leg ladder [70]. Numerical evidence for ladder stripes comes from DMRG work [14, 16, 17, 18, 19, 20, 23]. Since this method, as originally formulated, is intrinsically one-dimensional (1D), the results have been presented for "ladders" i.e. finite systems in which the number of rungs is considerably greater than the number of legs. (For instance, results exhibiting stripes have been presented for systems of size 6×21 [20].) In the limit where the length of the ladders (number of rungs) is much larger than their width (number of legs) they become 1D systems and a corresponding arsenal of field theory methods, such as bosonization, can be applied. Combining DMRG results with field theory methods to extrapolate to the limit of infinitely long ladders is an important step towards reaching the two dimensional (2D) limit. Of course, an extrapolation in the number of legs must finally be taken.

DMRG works much more efficiently with open boundary conditions (OBC) and most work on ladders has used OBC in the leg direction. Such boundary conditions can induce "generalized Friedel oscillations", meaning oscillations in the electron density which decay away from the boundary with a non-trivial power law and oscillate with an incommensurate wave-vector, often related to the hole density [23]. While sometimes regarded as an unphysical nuisance, we regard OBC as a useful diagnostic tool. According to bosonization results, the density-density correlation function for an infinite length ladder decays with twice the exponent, the same wave-vector and the square of the amplitude, governing the Friedel oscillations. Thus the Friedel oscillations are giving information about correlations in the infinite system. Furthermore, in the 2D limit of an infinite number of legs, these Friedel oscillations could turn into a static incommensurate CDW or else fluctuating stripes.

While a true long-range CDW is possible at commensurate filling even in 1D, bosonization/field theory methods suggest that it is not possible at incommensurate filling in 1D, giving way instead to boundary induced Friedel oscillations [23, 71, 72, 73]. (A long-

range CDW at p/q filling, where p and q are integers, becomes increasingly suppressed as q increases.) This assertion is related to Coleman's or Mermin-Wager's theorem about the impossibility of spontaneous breaking of continuous symmetries (and the impossibility of the existence of the corresponding Goldstone modes) in Lorentz invariant 1D systems even at zero temperature (or correspondingly 2D classical systems at any finite temperature). A true long-range incommensurate CDW leads to spontaneous breaking of translational symmetry by any integer number of lattice spacings, no matter how large, whereas a commensurate CDW only breaks a finite dimensional symmetry. Taking the low energy continuum limit, translational symmetry at incommensurate filling is promoted to a true continuous $U(1)$ symmetry and Coleman's theorem apparently applies.

"Stripes" or boundary-induced Friedel oscillations, have been observed in the t-J model, related to the $U \to \infty$ limit of the Hubbard model, on 2-leg ladders [23]. These Friedel oscillations, at $x \gg 1$, are of the form:

$$\sum_{a=1}^{2} < n_a(x) > \to \frac{A\cos(2\pi n x + \alpha)}{|x|^{2K_{+\rho}}}. \tag{1.1}$$

Here the average electron density is,

$$n \equiv N_e/(2L), \tag{1.2}$$

where N_e is the total number of electrons. $K_{+\rho}$ is the Luttinger parameter for the charge boson (ρ) which is the sum (+) of the 2 charge bosons corresponding to the two bands in a weak coupling analysis. A and α are constants. Note that we may replace the oscillation wave-vector by:

$$2\pi n \to -2\pi\delta, \tag{1.3}$$

where $\delta \equiv 1 - n$, is the hole density, measured from half-filling, since x is always integer. "Snapshots" of typical configurations within the DMRG calculations show pairs of nearby holes, one from each leg, well-separated from other pairs. An appealing picture is that the holes are pairing into bosons, 1 hole from each leg. (Here we refer to bosons with a conserved particle number, such as atoms, not the bosons arising from bosonization.) This phase is of C1S0 type, indicating that only 1 gapless charge boson survives and zero gapless spin bosons, out of the 2 charge and 2 spin bosons introduced in bosonizing the 2 leg ladder. (In general, CnSm means there are n gapless charge modes and m gapless spin modes) This phase exhibits exponential decay for the single electron Green's function but power law decay for the electron pair Green's function. One may approximately map the 2-leg fermionic ladder into a (single leg) bosonic chain. The standard superfluid phase of this boson model exhibits Friedel oscillations at wave-vector $2\pi\delta$ where $\delta = N_b/L$, is the number of bosons (i.e. hole pairs) per unit length and the number of bosons is: $N_b = N_h/2$, were N_h is the number of holes. These Friedel oscillations in the bosonic model just correspond to a sort of quasi-solid behavior. We can think of the bosons as almost forming a solid near the boundary with a uniform spacing between all nearest neighbor bosons. This, of course, coexists with quasi-superfluid behavior since the phase correlations also

decay with a power law. Thus it could be called quasi-supersolid behavior and is typical of many 1D systems. In general the density profile will contain other Fourier modes besides the $2\pi n$ mode kept in Eq. (1.1). This $2\pi n$ mode dominates in the sense that it has both the smallest wave-vector and also the smallest power law decay exponent. Note that this behavior is quite different than what we might expect in a C2S0 phase, for example, or which occurs at zero interaction strength in the C2S2 phase. Then we expect density oscillations at wave-vector $2k_{F,e}$ and also $2k_{F,o}$ where $k_{,Fe/o}$ are the Fermi wave-vectors for the even and odd bands. (They are even or odd under the parity transformation that interchanges the two legs.) In the C1S0 phase that is observed in 2-leg ladders, the oscillation wave-vector can be written as $2\pi n = 2(k_{F,e} + k_{F,o}) = 4\bar{k}_F$ where $\bar{k}_F$ is the average Fermi wave-vector.

DMRG works on the doped 4-leg t-J model exhibited two phases, both of which appear to have a spin gap [17, 18, 74, 75]. At low doping, the dominant Friedel oscillation wave-vector appears to be $4\pi n$, where n, the average electron density is now:

$$n \equiv N_e/(4L). \tag{1.4}$$

Above a critical doping δ_c, corresponding to $\delta_c \approx 1/8$, for $J = 0.35t$ and $0.5t$, the oscillation wave-vector changes to $2\pi n$. DMRG "snapshots" of typical configurations suggest well separated pair holes in the lower density phase but 4-hole clusters (1 hole on each leg) in the higher density phase. This is consistent with the $2\pi n$ Friedel oscillation wave-vector since the average separation along the ladder of the equally spaced 4-hole clusters would be $1/n$. This higher density phase with $2\pi n$ oscillation wave-vector has been referred as a stripe phase.

In the standard weak coupling approach we assume that all the interactions are small compared to the hopping. Thus we first solve for the band structure of the non-interacting model and then take the continuum limit of the interacting model, yielding right and left moving fermions from each band. These continuum limit fermions are then bosonized. Letting k_{Fi} be the Fermi wave-vector of the 4 bands ($i = 1, 2, 3$ or 4) the number of electrons in each band (summing over both spins) is:

$$N_e^i = L(2k_{Fi}/\pi), \quad (i = 1, 2, 3, 4). \tag{1.5}$$

Thus we see that the electron density n is:

$$n = N/4L = \sum_{i=1}^{4} k_{Fi}/(2\pi), \tag{1.6}$$

so

$$2\pi n = \sum_{i=1}^{4} k_{Fi} = 4\bar{k}_F. \tag{1.7}$$

Thus the stripe phase again corresponds to Friedel oscillations at a wave-vector of $4\bar{k}_F$. Using the equivalence of $2\pi n$ with $-2\pi\delta$, the physical picture of the stripe phase is well-separated clusters of 4 holes (one on each leg). If such 4-hole clusters are equally spaced

we obtain a Friedel oscillation wave-vector of $2\pi n$, since the average separation along the legs of the clusters is $1/n$. On the other hand, the lower density phase shows no evidence for Friedel oscillations at wave-vector $2\pi n$ and instead $4\pi n$ ($8\bar{k}_F$) oscillations appear to dominate. (We note that, when interactions are included, we expect the Fermi wave-vectors to be renormalized or lose their significance entirely. However, the sum of all Fermi wave-vectors, $4\bar{k}_F = 2\pi n$, is known to still be a meaningful and "unrenormalized" wave-vector even in the presence of interactions. This follows from the 1D version of Luttinger's theorem, proven in Ref. [76].)

This stripe phase appears to have a spin gap. Limited DMRG results have been presented on the decay of the pair correlation function. Pairing correlations appear to go through a maximum, as a function of doping, at a somewhat higher doping than δ_c where their behavior appears consistent with power-law decay [17, 18].

However, based on bosonization and finite size spectrum (FSS) in Chapter 2 and 3, we find that stripes, $2\pi n$ Friedel oscillations, can not coexist with the power-law decaying pair-pair correlations in 4-leg ladders. Instead, stripes can accompany a new type of charge-four correlations, bipairing. Precisely speaking, in a bipairing phase, the pair-pair correlations decay exponentially and bipair-bipair correlations decay with power-law. We then explore 4-leg ladder models in two different limits, weak coupling limit in Chapter 4 and decoupled two 2-leg ladders limit in Chapter 5. We find the results are consistent with bosonization and FSS. If this bipairing assumption is correct it finally yields a remarkably simple picture of the stripe phase in 4-leg ladders. It is a phase in which electrons do not form pairs, but rather bipairs. While the usual pairing does not occur in this phase, it tends towards a more exotic form of superconductivity based on condensed charge-four objects (see Fig. (1.3)). There are proposals in the literature that some systems like a frustrated Josephson junction chain [77, 78], strongly coupled fermions [79] and spin 3/2 fermionic chains [80] can have unusual pairs composed of Cooper pairs or four-particle condensations. They are very similar but not exactly the same as bipairing here. Starting with a four band system, the phase we propose is more like the generalized Luther-Emery phase with four-holes.

1.2.1 Continuum Limit and Bosonization

Now we would like to review the bosonization treatment of the Hamiltonian on a ladder with N legs and L rungs with open boundary conditions in both rung and leg directions. The Hamilonian is $H = H_0 + H_{int}$, with

$$H_0 = -\sum_{\alpha=\pm}\left[\sum_{x=1}^{L-1}\sum_{a=1}^{N} t c^{\dagger}_{a,\alpha}(x)c_{a,\alpha}(x+1) + \sum_{x=1}^{L}\sum_{a=1}^{N-1} t_{\perp} c^{\dagger}_{a,\alpha}(x)c_{a+1,\alpha}(x)\right] + h.c. \qquad (1.8)$$

and

$$H_{int} = U\sum_{x=1}^{N}\sum_{a=1}^{L} n_{a,\uparrow}(x)n_{a,\downarrow}(x) \qquad (1.9)$$

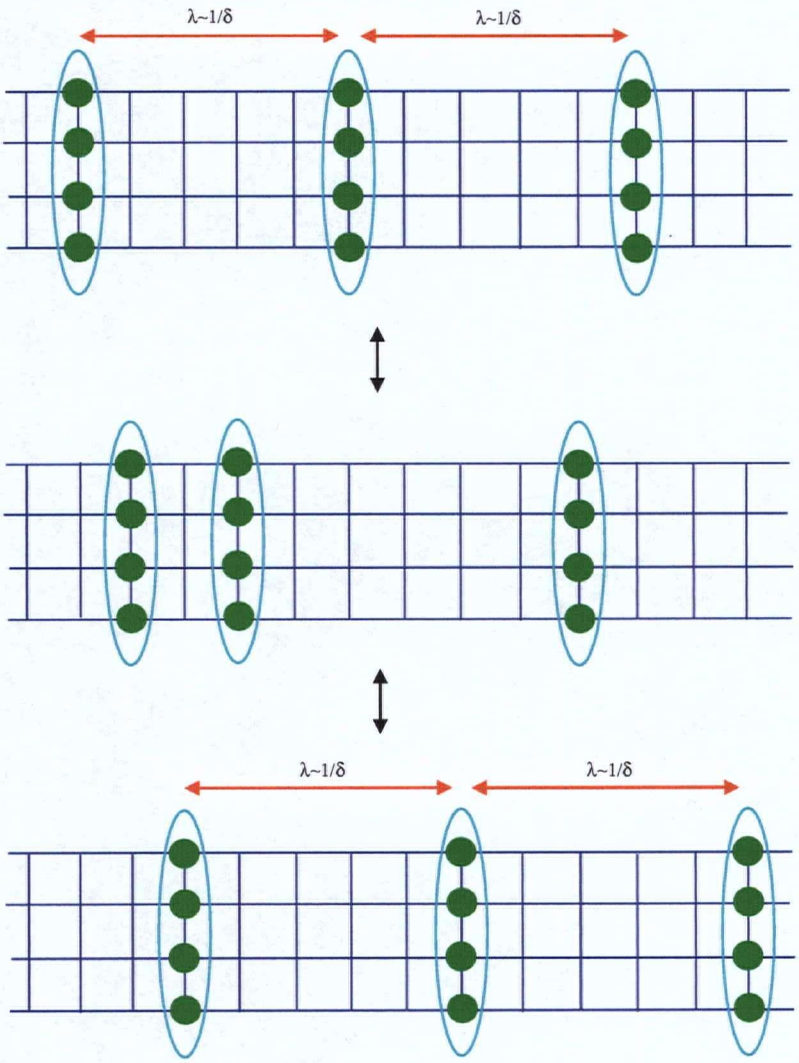

Figure 1.3: The stripe phase forms four-hole clusters along the rungs, well-separated from each other with the wave length $1/\delta$. Instead of moving as hole pairs, four holes can be created or annihilated in a bipairing phase. We suggest that stripes will accompany bipairing in 4-leg ladders.

Here $n_{a,\alpha} \equiv c^{\dagger}_{a,\alpha} c_{a,\alpha}$ and *h.c.* stands for Hermitian conjugate. We first diagonalize the rung hopping terms, Eq. (1.8) in the Hamiltonian by transforming from leg fermions $c_{a,\alpha}$ to the band basis, $\psi_{j,\alpha}$, for $i = 1, 2,...,N$:

$$\psi_{j,\alpha} \equiv \sum_{a=1}^{N} S_{ja} c_{a,\alpha}, \tag{1.10}$$

where S is a unitary matrix:

$$S_{ja} = \sqrt{\frac{2}{N+1}} \sin(\frac{\pi}{N+1}\, j * a). \tag{1.11}$$

Now Eq. (1.8) becomes diagonal in momentum space:

$$H_0 = \sum_{j,\alpha} \int_{-\pi}^{\pi} \frac{dk}{2\pi} \epsilon_j(k)\ \psi^{\dagger}_{j\alpha}(k) \psi_{j\alpha}(k) \tag{1.12}$$

and the dispersion relation for the j^{th} band is

$$\epsilon_j(k) = -2t \cos k - 2t_{\perp} \cos(k_{yj}), \text{ and } k_{yj} = \frac{j\pi}{N+1},\ j = 1, 2, ..., N. \tag{1.13}$$

We have a system with N-bands filled up to some chemical potential μ. We may take the continuum limit, to study the low energy physics, by introducing right/left moving fermions fields, $\psi_{R/Lj\alpha}(x)$ (sometimes called chiral fermions) which contain wave-vectors of the original band fermion fields near the Fermi points,

$$\psi_{j\alpha}(x) \ \sim\ \psi_{Rj\alpha}(x)\, e^{ik_{Fi}x} \ +\ \psi_{Lj\alpha}(x)\, e^{-ik_{Fi}x}, \tag{1.14}$$

where k_{Fj} is the Fermi wave vector for band j. Since the dispersion relations near the Fermi points are approximately linear and $\psi_{R/Lj\alpha}(x)$ vary slowly over a lattice constant, the effective low energy Hamiltonian in terms of chiral fermions is then

$$H_0 = \sum_{j,\alpha} \int dx[\ -iv_j \psi^{\dagger}_{Rj\alpha}(x) \partial_x \psi_{Rj\alpha}(x) + iv_j \psi^{\dagger}_{Lj\alpha}(x) \partial_x \psi_{Lj\alpha}(x)], \tag{1.15}$$

where $v_j = 2t \sin(k_{yj})$. At this point, the problem is formulated as an N-channel 1D fermion system (see Fig. (1.4)). Note that we should also express the interaction H_{int}, Eq. (1.9), in terms of right and left moving fermions fields. However, we will leave that part to Chapter 4 when we discuss the RG equations. Now we should introduce the bosonization scheme for the N-channel 1D fermion system.

It's well known that 1D fermion models can be rewritten as bosonic ones. In the low energy limit, particle-hole excitations in 1D are coherent and thus the (bosonic) density fluctuation fields create propagating particles. One can find more details in [81] and we only summarize some important results here.

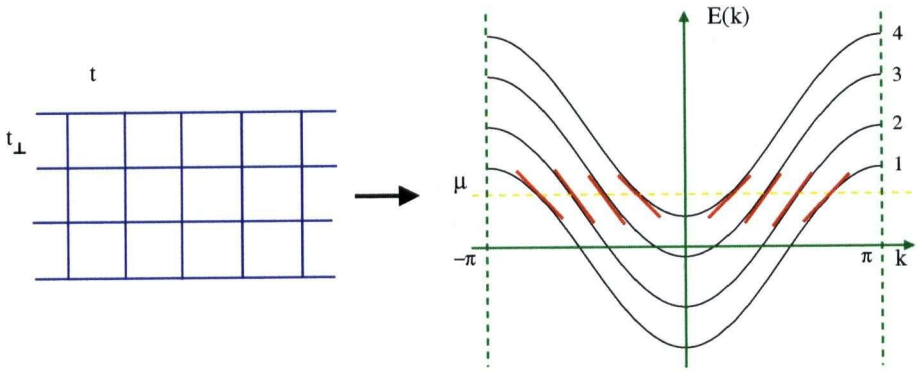

Figure 1.4: Diagonalizing the hopping terms, Eq. (1.8) on the 4-leg ladder, we get four cosine bands (black lines) filled up to the chemical potential μ. In the low energy limit, the excitations are only close to the Fermi points and the energy dispersions can be approximated by linear functions (red lines). In the end, the ladder system is described by four pairs of chiral fermions.

We can bosonize these right and left fermions by the dictionary

$$\psi_{R/Lj\alpha} \sim \eta_j e^{i\sqrt{4\pi}\varphi_{R/Lj\alpha}}, \tag{1.16}$$

where $\varphi_{Ri\alpha}$ and $\varphi_{Lj\beta}$ are boson fields with the commutator

$$[\varphi_{Ri\alpha}, \varphi_{Lj\beta}] = i\delta_{ij}\delta_{\alpha\beta}/4, \tag{1.17}$$

and η_j are Klein factors with $\{\eta_i, \eta_j\} = 2\delta_{ij}$ which make sure that the fermions in different bands anticommute with each other. The derivatives of boson fields are related to right and left moving densities defined as

$$n_{Rj\alpha} = \frac{1}{\sqrt{\pi}}\partial_x\varphi_{Rj\alpha}, \tag{1.18}$$

$$n_{Lj\alpha} = \frac{-1}{\sqrt{\pi}}\partial_x\varphi_{Lj\alpha}. \tag{1.19}$$

Now we have two chiral bosons and it's more convenient to describe physics by the conventional bosonic field ϕ and its dual field θ,

$$\theta_{j\alpha} = \varphi_{Rj\alpha} - \varphi_{Lj\alpha}, \ \phi_{j\alpha} = \varphi_{Rj\alpha} + \varphi_{Lj\alpha}. \tag{1.20}$$

Then the derivatives of $\theta_{j\alpha}$ and $\phi_{j\alpha}$ are the density $N_{j\alpha}$ and current $J_{j\alpha}$ in band j:

$$N_{j\alpha} = n_{Rj\alpha} + n_{Lj\alpha} = \frac{1}{\sqrt{\pi}}\partial_x\theta_{j\alpha}, \tag{1.21}$$

$$J_{j\alpha} = n_{Rj\alpha} - n_{Lj\alpha} = \frac{1}{\sqrt{\pi}}\partial_x\phi_{j\alpha}. \tag{1.22}$$

We can also separate the charge ρ and spin σ degrees of freedom by introducing the following fields,

$$\phi_{j\rho} = \frac{1}{\sqrt{2}}(\phi_{j\uparrow} + \phi_{j\downarrow}), \tag{1.23}$$

$$\phi_{j\sigma} = \frac{1}{\sqrt{2}}(\phi_{j\uparrow} - \phi_{j\downarrow}) \tag{1.24}$$

and similarly for θ fields. Then Eq. (1.8) becomes

$$H_0 = \sum_{i,\nu} \frac{v_i}{2} \int dx[(\partial_x \phi_{i\nu})^2 + (\partial_x \theta_{i\nu})^2], \tag{1.25}$$

where $\nu = \rho$ or σ and v_i is the Fermi velocity of band i. We define new fields from the linear combinations of the bosons from different bands:

$$\phi_{ij}^{\rho,\sigma\pm} = \frac{1}{\sqrt{2}}(\phi_{i\rho,\sigma} \pm \phi_{j\rho,\sigma}), \tag{1.26}$$

and the same for $\theta_{ij}^{\rho\pm}$ and $\theta_{ij}^{\sigma\pm}$. Eq. (1.26) is convenient when we express the bosonized interactions but not necessarily the final basis to describe the system. The final basis should be in principle determined by the interactions. We know that there should be four mutually orthogonal charge and spin bosons for 4-leg ladders. That is to say, starting with bosons in the band basis, Eq. (1.23) and (1.24), guided by the interactions, we should be able to find the proper new basis, some linear combinations of band bosons. The new basis only differs by an orthogonal transformation from the band basis. In general, the transformations of charge and spin fields don't have to be the same.

Due to the different Fermi velocities in Eq. (1.25), after changing to a new basis, mixing terms of the derivative of boson fields appear in the Hamiltonian. These mixing derivative terms are quadratic in boson fields. Spinless fermions on 2-leg ladders were studied in Ref. [82] and they found that the mixing terms only modify the exponents of correlation functions within the conventional bosonization analysis. We are mainly concerned about whether the correlation function of an operator is power-law or exponentially decaying but not its exponent. In the later sections, we only discuss the mixing terms if it's necessary.

Eq. (1.25) is a Gaussian type Hamiltonian for free boson fields and many correlation functions can be computed easily [81]. The basic correlation functions, given by the straightforward mode expansion in an infinite system, are

$$\langle \varphi_{Rj\alpha}(z)\varphi_{Rj\alpha}(z')\rangle = \frac{-1}{4\pi}\ln(z - z') + \text{const}, \tag{1.27}$$

$$\langle \varphi_{Lj\alpha}(\overline{z})\varphi_{Lj\alpha}(\overline{z}')\rangle = \frac{-1}{4\pi}\ln(\overline{z} - \overline{z}') + \text{const}, \tag{1.28}$$

where $z = -i(x - v_j t)$ and $\overline{z} = i(x + v_j t)$. The constant is cut-off dependent and we will drop it. Following the definition in Eq. (1.20), we then easily get

$$\langle \theta_{j\alpha}(x,t)\theta_{j\alpha}(0)\rangle = \langle \phi_{j\alpha}(x,t)\phi_{j\alpha}(0)\rangle = \frac{-1}{4\pi}\ln z\overline{z} = \frac{-1}{4\pi}\ln(x^2 - v_j^2 t^2). \tag{1.29}$$

The most important correlation functions are those for vertex operators, which are exponentials of boson fields, such as $e^{ia\phi_{j\alpha}}$ or $e^{ia\theta_{j\alpha}}$ where a is a constant.

The normal order for a operator is to move its creation part to the left and annihilation part to the right. For a operator A, the expectation value of its normal ordered form $:A:$ with respect to the ground state will be zero, i.e. $\langle 0|:A:|0\rangle = 0$. For two operators A and B, with c-number commutator $[A,B]$, by using Baker-Hausdorff formula $e^A e^B = e^{A+B}e^{[A,B]/2}$, one can show that

$$:e^A::e^B:=:e^{A+B}:e^{\langle AB\rangle}, \tag{1.30}$$

where :: means normal ordering the operator inside [83]. Then Eq. (1.29) and (1.30) will enable us to calculate correlation functions like

$$\begin{aligned}\left\langle :e^{ia\theta_{j\alpha}(z)}::e^{-ia\theta_{j\alpha}(0)}:\right\rangle &= \left\langle :e^{ia[\theta_{j\alpha}(z)-\theta_{j\alpha}(0)]}:\right\rangle e^{-a^2\langle\theta_{j\alpha}(z)\theta_{j\alpha}(0)\rangle} \\ &= (x^2-v_j^2t^2)^{-a^2/4\pi},\end{aligned} \tag{1.31}$$

where a is a constant. Similarly,

$$\left\langle :e^{ia\phi_{j\alpha}(z)}::e^{-ia\phi_{j\alpha}(0)}:\right\rangle = (x^2-v_j^2t^2)^{-a^2/4\pi}.$$

This normal ordering is only a way to avoid the infinity due to the ultraviolet cutoff and we won't write it explicitly in the later discussion.

In particular, for the equal time correlation functions

$$\left\langle e^{ia\theta_{j\alpha}(x)}e^{-ia\theta_{j\alpha}(0)}\right\rangle = \left\langle e^{ia\phi_{j\alpha}(x)}e^{-ia\phi_{j\alpha}(0)}\right\rangle = x^{-a^2/2\pi}. \tag{1.32}$$

The power of bosonization is that some four fermion interactions like $N_{j\alpha}N_{j\alpha}$, $J_{j\alpha}J_{j\alpha}$ and $N_{j\alpha}J_{j\alpha}$, according to Eq. (1.21) and (1.22), are just the cross terms of boson field and the whole Hamiltonian including these interactions is still quadratic. In general, the system becomes the N-channel Tomonaga-Luttinger model,

$$H_{TL} = \sum_{j,\nu}\frac{v_{j\nu}}{2}\int dx[K_{j\nu}(\partial_x\phi_{j\nu})^2 + \frac{1}{K_{j\nu}}(\partial_x\theta_{j\nu})^2], \tag{1.33}$$

where $v_{j\nu}$ and $K_{j\nu}$ are the renormalized Fermi velocity and Luttinger parameter, respectively. Their exactly values depends on the coefficients of those four fermion interactions and unrenormalized Fermi velocities v_j but we don't care about them too much here. The boson field $\theta_{j\nu}$ (or $\phi_{j\nu}$) with the Hamiltonian Eq. (1.33) is called a gapless field.

The way to calculate the correlation functions in Eq. (1.32) with the Tomonaga-Luttinger Hamiltonian Eq. (1.33) is by rescaling the fields by

$$\phi_{j\nu} \rightarrow \frac{\phi_{j\nu}}{\sqrt{K_{j\nu}}}, \tag{1.34}$$

$$\theta_{j\nu} \rightarrow \sqrt{K_{j\nu}}\theta_{j\nu}, \tag{1.35}$$

then Eq. (1.33) is back to the non-interacting Hamiltonian Eq. (1.25) but with renormalized Fermi velocities $v_{j\nu}$. The correlation functions are also rescaled by the Luttinger parameters $K_{j\nu}$ and become:

$$\left\langle e^{ia\phi_{j\nu}(x)} e^{-ia\phi_{j\nu}(0)} \right\rangle \rightarrow \left\langle e^{ia\phi_{j\nu}(x)/\sqrt{K_{j\nu}}} e^{-ia\phi_{j\nu}(0)/\sqrt{K_{j\nu}}} \right\rangle = x^{-a^2/2\pi K_{j\nu}}, \quad (1.36)$$

$$\left\langle e^{ia\theta_{j\nu}(x)} e^{-ia\theta_{j\nu}(0)} \right\rangle \rightarrow \left\langle e^{ia\sqrt{K_{j\nu}}\theta_{j\nu}(x)} e^{-ia\sqrt{K_{j\nu}}\theta_{j\nu}(0)} \right\rangle = x^{-a^2 K_{j\nu}/2\pi}. \quad (1.37)$$

The operators with the correlation function forms like Eq. (1.36) and (1.37) are said to decay with a power law and have quasi-long-ranged order. The correlation functions involving gapless boson fields will be power-law decaying and we usually say the operator $e^{ia\phi_{j\nu}(x)}$ (or $e^{ia\theta_{j\nu}(x)}$) has the scaling dimension $a^2/4\pi K_{j\nu}$ (or $a^2 K_{j\nu}/4\pi$).

If a cosine interaction term containing $\phi_{j\nu}(x)$ is present,

$$H_{int} = \int dx \cos[\beta\phi_{j\nu}(x)], \quad (1.38)$$

the effect depends on its scaling dimension $\beta^2/4\pi K_{j\nu}$. This is the widely studied sine-Gordon model. More details can be found in Ref. [81]. If $\beta^2/4\pi K_{j\nu} > 2$, then it's an irrelevant operator. The correlation functions of vertex operators are still given by Eq. (1.36) and (1.37). If $\beta^2/4\pi K_{j\nu} < 2$, then it's a relevant operator. $\phi_{j\nu}(x)$ will tend to be "pinned" to a constant so as to minimize the ground state energy in the semiclassical sense. We can replace $\phi_{j\nu}(x)$ by its pinned value when calculate the correlation function for the operator $e^{ia\phi_{j\nu}(x)}$. Instead of decaying with a power-law, Eq. (1.36) becomes a constant and the $e^{ia\phi_{j\nu}(x)}$ operator has true long-ranged order. On the other hand, if $\phi_{j\nu}(x)$ is pinned, its conjugated field $\theta_{j\nu}(x)$ will fluctuate violently. The correlation function of the operator $e^{ia\theta_{j\nu}(x)}$ will decay exponentially. Instead of $\cos[\beta\phi_{j\nu}(x)]$, if the term $\cos[\beta\theta_{j\nu}(x)]$ is in Eq. (1.38), now the scaling dimension is $\beta^2 K_{j\nu}/4\pi$. If it's relevant, then Eq. (1.37) becomes a constant and Eq. (1.36) decay exponentially. In general, there is more than one interaction in the Hamiltonian. We will analyze the RG equations to see which interactions are relevant in Chapter 4.

OBC along the rung direction are taken care of by the values of S_{ja} in Eq. (1.11). We should consider what's the consequence of OBC in the leg direction. The system is from site 1 to L. OBC on site 1 and L are equivalent to vanishing boundary conditions at the extra "phantom" site 0 and $L+1$. For $x = 0$, $\psi_{ja}(0) = 0$, and in terms of chiral fermions becomes

$$\psi_{Rja}(0) = -\psi_{Lja}(0). \quad (1.39)$$

Upon bosonizing we obtain

$$\theta_{ja}(0,t) = \phi_{Rja}(0,t) - \phi_{Lja}(0,t) = \text{const.} \quad (1.40)$$

Because ϕ_{Rja} is only a function of $v_j t - x$ and ϕ_{Lja} a function of $v_j t + x$, we can regard ϕ_{Rja} as the analytic continuation of ϕ_{Lja} to the negative axis

$$\phi_{Rja}(x) = \phi_{Lja}(-x) + \text{const.} \quad (1.41)$$

The innocent-looking result Eq. (1.41) will change the properties of correlation functions dramatically. The one point function for a gapless mode $\left\langle e^{ia\theta_{j\alpha}(x)}\right\rangle = 0$ for periodic boundary condition in the leg direction. Now with OBC, by using Eq. (1.41), the one point function reduces to a two point function of the operators with half scaling dimension (only left moving fields):

$$\left\langle e^{ia\theta_{j\alpha}(x)}\right\rangle_{OBC} \sim \left\langle e^{ia\phi_{Lj\alpha}(-x)}e^{-ia\phi_{Lj\alpha}(x)}\right\rangle = (2x)^{-a^2K_{j\alpha}/4\pi}. \tag{1.42}$$

The density operators usually involve $\theta_{j\alpha}$ fields. So the boundary-induced generalized Friedel oscillations, such as Eq. (1.1), can be regarded as a useful tool to diagnose the Luttinger parameter.

Note that Eq. (1.41) doesn't significantly change the one point functions of non-zero charge operators involving $\phi_{j\alpha}$ fields, such as pair and bipair operators. The sign change in Eq. (1.42) will leave the one point function zero. What we describe here is very general and $\theta_{j\alpha}$ is not only limited to a band boson field. For any gapless boson field, the results here are still applicable.

Chapter 2

Stripes and Bipairing

In this Chapter we wish to prove a general result that would apply to any of these phases that are candidates for a stripe phase, regardless of what basis for the boson fields we use. Stripes are incommensurate density oscillations with the lowest wave-vector $2\pi n$ (e.g. no πn density oscillations) [17, 18]. The wave-vector $2\pi n$ is equivalent to $4\bar{k}_F$ via the 1D Luttinger theorem [76]. Stripes thus can be described as the generalized Friedel oscillations induced by the boundary [23]. A derivation of the $4\bar{k}_F$ components of density operators is given in Appendix A. At incommensurate filling, the 1D Luttinger theorem states that at least one gapless charge mode always exists. Stripe phases appear to have a spin gap in DMRG works and we expect that phases with more than 1 gapless charge mode are generically unstable. So we restrict out attention to C1S0 phases.

We then argue that *any* phase exhibiting stripes (i.e. $2\pi n$ oscillations) cannot exhibit pairing (i.e. power law pair correlations and gapless pair excitations) but can exhibit bipairing (charge four operators).

In a C1S0 phase, 7 out of 8 boson fields are pinned due to interactions. We will consider all possible four fermion interactions written in terms of right and left moving fields $\psi_{R/L}$, including those that are ignored in the conventional weak coupling analysis. Similarly to what we discussed in the previous Chapter, after bosonizing, if the interaction is relevant, the boson fields in the interaction will tend to be pinned to constants. Before we proceed, we should explain explicitly what we mean by a boson field θ (or ϕ) being pinned. Consider a vertex operator of a boson field, $e^{ia\theta}$, where a is a constant. If $\langle e^{ia\theta} \rangle$ = const $\neq 0$, then we say θ is "pinned" to some constant modulo $2\pi/a$. On the other hand, we say θ is "unpinned" if $\langle e^{ia\theta} \rangle = 0$. There could be three situations for θ to be unpinned. First, θ is gapless. Second, a part of it is gapless and the rest is pinned. For example, if $\theta_{1\rho}$ is gapless and $\theta_{2\rho}$ is pinned, then $\left\langle e^{i(\theta_{1\rho}+\theta_{2\rho})/\sqrt{2}} \right\rangle$ is still zero since we can replace the pinned fields by their pinned values. Thirdly, its dual field ϕ or part of its dual field is pinned and therefore θ will fluctuate violently.

There are many such phases characterized by which fields are pinned. In general, it is not appropriate to simply label the pinned fields as $\phi_{i\nu}$ or $\theta_{i\nu}$ in terms of the band basis. The interaction terms in the Hamiltonian involve various linear combinations of these fields and it is generally necessary to characterize phases by first going to a different basis of boson fields:

$$\vec{\theta}'_\rho = R_\rho \vec{\theta}_\rho, \ \vec{\phi}'_\rho = R_\rho \vec{\phi}_\rho, \ \vec{\theta}'_\sigma = R_\sigma \vec{\theta}_\sigma, \ \vec{\phi}'_\sigma = R_\sigma \vec{\phi}_\sigma, \tag{2.1}$$

where $\vec{\theta}_\rho = (\theta_{1\rho}, \theta_{2\rho}, \theta_{3\rho}, \theta_{4\rho})$ etc and R_ρ and R_σ are orthogonal matrices. We will refer to the basis $(\theta'_{i\rho}, \phi'_{i\rho})$ and $(\theta'_{i\sigma}, \phi'_{i\sigma})$ as the "pinning basis". One of the 4 charge bosons

in the new basis $(\theta'_{i\rho}, \phi'_{i\rho})$ remains gapless in a C1S0 phase. All of the other 7 bosons are gapped. However, for each of these 7 bosons we must specify whether it is $\theta'_{i\nu}$ or $\phi'_{i\nu}$ which is pinned. We refer to this choice of which bosons are pinned as a "pinning pattern". Each pinning pattern corresponds to a distinct phase. (Actually the number of distinct phases is even larger than this since the points, $c_{i\nu}$ at which a boson is pinned, eg. $\langle\theta'_{i\nu}\rangle = c_{i\nu}$, can also characterize the phase.)

Our basic strategy is to check through all possible pinning patterns for a C1S0 phase and see if any pinning pattern can make the correlation functions of pair and $4\bar{k}_F$ density operators decay with a power-law at the same time. As we discussed before, with a pinning pattern, we can replace the pinned bosons by constants inside the correlation function. The correlation function will decay exponentially if the vertex operator contains the dual of a pinned boson. It will decay with a power-law if the vertex operator only contains the gapless mode and pinned bosons. However, there are three main complications here. The first one is: what is the basis for the boson fields (including the gapless mode)? Even though we know the basis, there are still too many pinning patterns (more than 2^7). The last problem is that the wave-vectors of $4k_F$ density operators can be changed and actually correspond to that of stripes if some Fermi momentum renormalization occurs. For example. the wave-vector $k_{F1} + k_{F2} + 2k_{F3} = 4\bar{k}_F$ if the condition $k_{F3} = k_{F4}$ is satisfied. In this Chapter, we try to solve these problems.

Now we would like to introduce a specific combination of band bosons Eq. (1.23) and (1.24), which is relevant to symmetry. Define the total charge (or spin) field as

$$\Theta_{1\nu} = \frac{1}{2}(\theta_{1\nu} + \theta_{2\nu} + \theta_{3\nu} + \theta_{4\nu}), \tag{2.2}$$

where $\nu = \rho$ or σ and similarly for $\Phi_{1\nu}$ if we replace θ by ϕ.

We can somewhat restrict the possible pinning patterns by symmetry considerations. Charge conservation symmetry, $\psi \to e^{i\gamma}\psi$ for all fermion fields, ψ, corresponds to the translation:

$$\phi_{j\rho} \to \phi_{j\rho} + \sqrt{2/\pi}\gamma. \tag{2.3}$$

Thus, the allowed pinned $\phi'_{i\rho}$ must be the linear combinations of $\phi^{\rho-}_{ij}$, in other words, any pinned $\phi'_{i\rho}$ fields must be orthogonal to $\Phi_{1\rho}$. Similarly, the subgroup of $SU(2)$ symmetry, $\psi_\alpha \to e^{i\alpha\epsilon}\psi_\alpha$ where $\alpha = +$ or $-$ for spin up or down, respectively, corresponds to:

$$\phi_{j\sigma} \to \phi_{j\sigma} + \sqrt{2/\pi}\epsilon. \tag{2.4}$$

Therefore, any pinned $\phi'_{i\sigma}$ can only be the linear combinations of $\phi^{\sigma-}_{ij}$ in order not to violate the $SU(2)$ symmetry. We also expect translation symmetry to be unbroken at incommensurate filling, as discussed in Sec. I. We see from Eq. (1.14), that translation by one site: $x \to x + 1$, corresponds to the symmetry:

$$\psi_{R/Lj\nu} \to e^{\pm ik_{Fj}}\psi_{R/Lj\nu}, \quad (j = 1, 2, 3, 4) \tag{2.5}$$

corresponding to:

$$\theta_{j\rho} \to \theta_{j\rho} + \sqrt{2/\pi}k_{Fj}, \quad (j = 1, 2, 3, 4). \tag{2.6}$$

Consider a vertex operator of a boson field, $e^{ia\theta}$, where a is a constant. Since in general the factors $\sqrt{2/\pi}k_{Fj}$ are not zero modulo $2\pi/a$, this may forbid pinning of *any* of the $\theta'_{j\rho}$ fields. However, it may happen, due perhaps to some renormalization phenomenon, that 2 or more of the k_{Fj} are equal. In that case it might be possible for some of the $\theta'_{j\rho}$ bosons to be pinned. For example if $k_{Fi} = k_{Fj}$, then $\theta^{\rho-}_{ij}$ could be pinned without breaking translational symmetry. We will allow for that possibility since there is no reason to exclude it in the strong coupling region. However, $\Theta_{1\rho}$ can *never* be pinned since it transforms under translation by one site as:

$$\Theta_{1\rho} \to \Theta_{1\rho} + 4\bar{k}_F/\sqrt{2\pi}, \tag{2.7}$$

and $4\bar{k}_F/2\pi = n$ is always non-zero modulo $2\pi/a$ at incommensurate filling. The fact that $\Theta_{1\rho}$ can never be pinned is not exactly equivalent to the statement that the gapless boson in a general C1S0 phase at incommensurate filling has to be $(\Theta_{1\rho}, \Phi_{1\rho})$. There could be exceptions if some pinned $\theta'_{i\rho}$ fields are *not* orthogonal to $\Theta_{1\rho}$. If that happens, then $\Theta_{1\rho}$ can't even be chosen as a basis field. As we know, all the pinned $\phi'_{i\rho}$ must be orthogonal to $\Phi_{1\rho}$ due to the charge conservation. However, translational symmetry doesn't demand all the pinned $\theta'_{i\rho}$ must be orthogonal to $\Theta_{1\rho}$ and in general whether a $\theta'_{i\rho}$ is pinned or not depends on the Fermi momentum. Thus to know whether a $\theta'_{i\rho}$ can be pinned without violating translational symmetry, we have to discuss the possible Fermi momentum renormalization.

However, even though some $\theta'_{i\rho}$ field is allowed to be pinned by symmetry, in practice, whether it really gets pinned or not depends on the interactions in the Hamiltonian. In the weak coupling treatment, the renormalizations of k_{Fj} are assumed not to happen and k_{Fj} are in general all different. The interactions involving $\theta'_{i\rho}$ fields won't be present in the Hamiltonian due to the fast oscillating factors in front of them. Again, if some renormalization of Fermi momentum occurs such that the oscillating factor becomes a constant, then new interaction will appear in the Hamiltonian. For example, if $2(k_{Fi} + k_{Fj}) = 2\pi$, the interaction involving it, such as $e^{-i2(k_{Fi}+k_{Fj})x}\psi^\dagger_{Ri\alpha}\psi^\dagger_{Rj\bar{\alpha}}\psi_{Li\bar{\alpha}}\psi_{Lj\alpha} \propto e^{-i\sqrt{4\pi}(\theta^{\rho+}_{ij} \pm \phi^{\sigma-}_{ij})}$, can be present in the Hamiltonian since the oscillating factor $e^{-i2(k_{Fi}+k_{Fj})x}$ becomes a constant at each lattice site x. In this case the shift of $\theta^{\rho+}_{ij}$ under translation is $2\pi/\sqrt{4\pi}$, which becomes 2π for $\sqrt{4\pi}\theta^{\rho+}_{ij}$.Thus if this interaction is relevant, then then the field $\theta^{\rho+}_{ij}$ will be pinned.

Therefore, whether a $\theta'_{i\rho}$ field is pinned or not depends strongly on the specific renormalizations of Fermi momenta, which could happen in the strong coupling region. Besides these issues related to symmetry and interactions, a general $4k_F$ density operator may correspond to the $4\bar{k}_F$ one if some suitable Fermi momentum renormalization happens. For example, the wave-vector $2(k_{F1}+k_{F2})$ is the same as $4\bar{k}_F$ if $k_{F1} = k_{F3}$ and $k_{F2} = k_{F4}$. So we have to carefully discuss all the possible Fermi momentum renormalizations and their implications.

Our strategy is to first discuss the case when pinned bosons are all orthogonal to the total charge mode. Therefore, the gapless mode is the total charge field. Then we consider cases where some pinned $\theta'_{i\rho}$ fields not orthogonal to the total charge mode $\Theta_{1\rho}$.

The efficient way to check through all the possibilities is by checking all the possible renormalizations of Fermi momentum such that the interaction containing $\theta'_{i\rho}$ will appear in the Hamiltonian. If that interaction is relevant, the gapless charge mode is not $(\Theta_{1\rho}, \Phi_{1\rho})$ anymore since it can't be used as a basis field. These cases will be discussed in a separate section.

2.1 Total Charge Mode Is Gapless

In the following discussion in this subsection, we will only consider the renormalization of k_{Fi} such that the pinned $\theta'_{i\rho}$ bosons are orthogonal to $\Theta_{1\rho}$. In other words, the conditions such as $2(k_{Fi} + k_{Fj}) = 2\pi$, won't occur but other possibilities such as $k_{Fi} - k_{Fj} = 0$ or $k_{F1} - k_{F2} + k_{F3} - k_{F4} = 0$ are allowed. Then θ^{ρ}_{ij} and $(\theta_{1\rho} - \theta_{2\rho} + \theta_{3\rho} - \theta_{4\rho})/2$ may get pinned but they are still orthogonal to $\Theta_{1\rho}$. In this case, the gapless charge mode will be $(\Theta_{1\rho}, \Phi_{1\rho})$ since all pinned $\theta'_{i\rho}$ or $\phi'_{i\rho}$ fields are orthogonal to $\Theta_{1\rho}$ or $\Phi_{1\rho}$, respectively. We can reorder the transformed basis, $\phi'_{i\rho}$, so that $\phi'_{1\rho} = \Phi_{1\rho}$ and $\theta'_{1\rho} = \Theta_{1\rho}$.

First of all, we have to know the conditions so that two (or more) operators can (or can't) be power law decaying at the same time. To find these conditions, consider two arbitrary operators expressed in terms of the band basis and let's rewrite them in the following way:

$$O_A \sim e^{i\left(\vec{u}_{\rho A}\cdot\vec{\theta}_\rho + \vec{v}_{\rho A}\cdot\vec{\phi}_\rho + \vec{u}_{\sigma A}\cdot\vec{\theta}_\sigma + \vec{v}_{\sigma A}\cdot\vec{\phi}_\sigma\right)}, \tag{2.8}$$

$$O_B \sim e^{i\left(\vec{u}_{\rho B}\cdot\vec{\theta}_\rho + \vec{v}_{\rho B}\cdot\vec{\phi}_\rho + \vec{u}_{\sigma B}\cdot\vec{\theta}_\sigma + \vec{v}_{\sigma B}\cdot\vec{\phi}_\sigma\right)}. \tag{2.9}$$

We can represent any vertex operator O_A by four coefficient vectors $\vec{u}_{\rho A}$, $\vec{v}_{\rho A}$, $\vec{u}_{\sigma A}$ and $\vec{v}_{\sigma A}$. For example, if $O_A \sim e^{i\sqrt{2\pi}(\phi_1^\rho + \theta_1^\sigma)}$, then $\vec{v}_{\rho A} = (\sqrt{2\pi}, 0, 0, 0)$, $\vec{u}_{\sigma A} = (\sqrt{2\pi}, 0, 0, 0)$ and both $\vec{u}_{\rho A}$ and $\vec{v}_{\sigma A}$ are $(0, 0, 0, 0)$.

Eq. (2.8) and (2.9) are written in terms of the boson fields in the band basis, which is not necessarily the basis in which boson fields are pinned. At this stage, we may not know what the new basis should be but we know at least that the fields in the transformed basis have to be orthogonal to each other. Then Eq. (2.8) and (2.9) can be rewritten as

$$O_A \sim e^{i\left(\vec{u}'_{\rho A}\cdot\vec{\theta}'_\rho + \vec{v}'_{\rho A}\cdot\vec{\phi}'_\rho + \vec{u}'_{\sigma A}\cdot\vec{\theta}'_\sigma + \vec{v}'_{\sigma A}\cdot\vec{\phi}'_\sigma\right)}, \tag{2.10}$$

$$O_B \sim e^{i\left(\vec{u}'_{\rho B}\cdot\vec{\theta}'_\rho + \vec{v}'_{\rho B}\cdot\vec{\phi}'_\rho + \vec{u}'_{\sigma B}\cdot\vec{\theta}'_\sigma + \vec{v}'_{\sigma B}\cdot\vec{\phi}'_\sigma\right)}, \tag{2.11}$$

where $\vec{\theta}'_\rho = R_\rho\vec{\theta}_\rho$, $\vec{\theta}'_\sigma = R_\sigma\vec{\theta}_\sigma$ and similarly for $\vec{\phi}'_\rho = R_\rho\vec{\phi}_\rho$ and $\vec{\phi}'_\sigma = R_\sigma\vec{\phi}_\sigma$. Here R_ρ and R_σ are two orthogonal 4 by 4 matrices that transform the boson fields from the band basis to a new one. The new corresponding coefficient vectors are $\vec{u}'_{\rho A} = \vec{u}_{\rho A}R^T_\rho$, $\vec{u}'_{\sigma A} = \vec{u}_{\sigma A}R^T_\sigma$... here R^T_ρ and R^T_σ are the transpose of R_ρ and R_σ.

Now assume that the bosons get pinned in this new basis. We know only one of θ'_i and ϕ'_i can be pinned and the presence of the dual of a pinned boson will result in exponential decay. Consider a simple situation in which all bosons are pinned, i.e. a C0S0 phase and

the pinned bosons are $(\phi'_{1\rho}, \theta'_{2\rho}, \theta'_{3\rho}, \phi'_{4\rho})$ in the charge channel and $(\theta'_{1\sigma}, \phi'_{2\sigma}, \phi'_{3\sigma}, \theta'_{4\sigma})$ in the spin channel, even though we don't know explicitly the transformations to the new basis.

This set of pinned bosons enforces some constraints on the coefficient vectors $\vec{u}_{\rho A/B}$, $\vec{v}_{\rho A/B}$, $\vec{u}_{\sigma A/B}$ and $\vec{v}_{\sigma A/B}$ so that O_A and O_B don't decay exponentially. The constraints are simply that the coefficients for the dual of each pinned boson must be zero. In this case, for $X = A$ or B:

$$\begin{aligned}
\vec{u}'_{\rho X} &= (0,-,-,0),\\
\vec{v}'_{\rho X} &= (-,0,0,-),\\
\vec{u}'_{\sigma X} &= (-,0,0,-),\\
\vec{v}'_{\sigma X} &= (0,-,-,0),
\end{aligned}$$

where "$-$" means no constraint. These constraints actually imply the following equations:

$$\vec{u}'_{\rho A} \cdot \vec{v}'_{\rho B} = \vec{u}'_{\sigma A} \cdot \vec{v}'_{\sigma B} = 0, \tag{2.12}$$
$$\vec{v}'_{\rho A} \cdot \vec{u}'_{\rho B} = \vec{v}'_{\sigma A} \cdot \vec{u}'_{\sigma B} = 0, \tag{2.13}$$
$$\vec{u}'_{\rho A} \cdot \vec{v}'_{\rho A} = \vec{u}'_{\sigma A} \cdot \vec{v}'_{\sigma A} = 0, \tag{2.14}$$
$$\vec{u}'_{\rho B} \cdot \vec{v}'_{\rho B} = \vec{u}'_{\sigma B} \cdot \vec{v}'_{\sigma B} = 0. \tag{2.15}$$

One can easily see that different sets of pinned bosons will imply the same equations for inner products. So the actually pinning patterns of boson fields are irrelevant for the constraints here and the crucial point is that all the fields are pinned.

Eq. (2.12)-(2.13) are for the coefficient vectors in the new primed basis. So we don't really know their components. However, we know inner products are invariant under any orthogonal transformation. Thus, the coefficient vectors in the band basis should satisfy the same Eq. (2.12)-(2.13) but without the primes. So for any two operators O_A and O_B written in the band basis, we know the necessary condition on their coefficient vectors for O_A and O_B not to be exponentially decaying.

However, things are slightly different for a C1S0 phase, which is the case we are really interested in. Now the inner products $\vec{u}'_{\rho A} \cdot \vec{v}'_{\rho B}$ and $\vec{v}'_{\rho A} \cdot \vec{u}'_{\rho B}$ in the charge channel are not necessary zero since the overlap is allowed in the subspace of gapless boson fields. For example none of $O_A \sim e^{i\phi'_{1\rho}}$ and $O_B \sim e^{i\theta'_{1\rho}}$ are exponentially decaying if $(\theta'_{1\rho}, \phi'_{1\rho})$ is gapless even though $\vec{v}'_{\rho A} \cdot \vec{u}'_{\rho B} = 1$ in this example. In principle, we even don't know what's the value for the nonzero inner products if the gapless field is arbitrary. However, here we first discuss the case in which gapless mode is the total charge bosons $(\Theta_{1\rho}, \Phi_{1\rho})$. This means, choosing $\phi'_{1\rho} = \Phi_{1\rho}$, that the first row of the orthogonal matrix R_ρ can be chosen to be $(1/2, 1/2, 1/2, 1/2)$. Roughly speaking, for each charge boson field in the band basis, we have

$$\begin{aligned}
\theta_{i\rho} &= \frac{1}{2}\Theta_{1\rho} + \cdots,\\
\phi_{i\rho} &= \frac{1}{2}\Phi_{1\rho} + \cdots.
\end{aligned}$$

Therefore, we find that for all the pairing Δ and $4\bar{k}_F$ density operators $n_{4\bar{k}_F}$, the coefficients of $\Theta_{1\rho}$ and $\Phi_{1\rho}$ are fixed:

$$\Delta \sim e^{i\left(\vec{u}'_{\rho\Delta}\cdot\vec{\theta}'_\rho+\vec{v}'_{\rho\Delta}\cdot\vec{\phi}'_\rho+\vec{u}'_{\sigma\Delta}\cdot\vec{\theta}'_\sigma+\vec{v}'_{\sigma\Delta}\cdot\vec{\phi}'_\sigma\right)} = e^{i\sqrt{\frac{\pi}{2}}\Phi_{1\rho}+\cdots}, \tag{2.16}$$

$$n_{4\bar{k}_F} \sim e^{i\left(\vec{u}'_{\rho n}\cdot\vec{\theta}'_\rho+\vec{v}'_{\rho n}\cdot\vec{\phi}'_\rho+\vec{u}'_{\sigma n}\cdot\vec{\theta}'_\sigma+\vec{v}'_{\sigma n}\cdot\vec{\phi}'_\sigma\right)} = e^{-i\sqrt{2\pi}\Theta_{1\rho}+\cdots}. \tag{2.17}$$

As we mentioned before, the only nonzero part of inner products must come from the gapless boson $(\Theta_{1\rho}, \Phi_{1\rho})$. Although we don't know the full representation of pairing and $4\bar{k}_F$ density operators in the new basis, nonetheless, from Eq. (2.16) and (2.17), it's sufficient to conclude that the only nonzero inner product between $(\vec{v}')$'s and $(\vec{u}')$'s has to be exactly

$$\vec{v}'_{\rho\Delta}\cdot\vec{u}'_{\rho n} = \pm\pi, \tag{2.18}$$

where the positive sign occurs when taking the Hermitian conjugate of one of the operators. In the following convention, we choose $4\bar{k}_F$ density operators so that $-\pi$ is taken in Eq. (2.18). Finally, we get the necessary conditions on the coefficient vectors in the band basis so that a C1S0 phase can have both pairing and stripe correlations:

$$\vec{v}_{\rho\Delta}\cdot\vec{u}_{\rho n} = -\pi, \tag{2.19}$$

$$\vec{u}_{\rho\Delta}\cdot\vec{v}_{\rho n} = 0, \tag{2.20}$$

$$\vec{u}_{\sigma\Delta}\cdot\vec{v}_{\sigma n} = \vec{v}_{\sigma\Delta}\cdot\vec{u}_{\sigma n} = 0, \tag{2.21}$$

$$\vec{u}_{\rho\Delta}\cdot\vec{v}_{\rho\Delta} = \vec{u}_{\sigma\Delta}\cdot\vec{v}_{\sigma\Delta} = 0, \tag{2.22}$$

$$\vec{u}_{\rho n}\cdot\vec{v}_{\rho n} = \vec{u}_{\sigma n}\cdot\vec{v}_{\sigma n} = 0. \tag{2.23}$$

Now we will write down the bosonized expressions for pair and $4\bar{k}_F$ density operators in the band basis and then give our proof that stripes and pairing cannot coexist. First consider pairing. By "pairing" we mean the existence of any operator of charge 2 whose correlation functions exhibit power-law decay. Any pair operator that only contains right or left fermions, such as $\psi_{Ra\uparrow}\psi_{Rb\downarrow}$, can never exhibit power law decay since from Eq. (1.20) we know $\varphi_{Ra\alpha} = (\phi_{a\alpha} + \theta_{a\alpha})/2$ and this will result in $\vec{u}_{\rho\Delta}\cdot\vec{v}_{\rho\Delta}$ and $\vec{u}_{\sigma\Delta}\cdot\vec{v}_{\sigma\Delta}$ $\neq 0$. (Eq. (2.22) is violated.) Furthermore, any pair operator with non-zero total z-component of spin will contain a factor with the exponential of $\Phi_{1\sigma}$ and hence exhibit exponential decay.

So, there are only two types of charge 2 operators, containing only two fermion fields, which are candidates for power-law decay. Ignoring Klein factors, these are:

$$\psi_{Ra\alpha}\psi_{La\bar{\alpha}} \sim e^{i\sqrt{2\pi}(\phi_{a\rho}\pm\theta_{a\sigma})} \tag{2.24}$$

$$\psi_{Ra\alpha}\psi_{Lb\bar{\alpha}} \sim e^{i\sqrt{\pi}(\theta^{\rho-}_{ab}+\phi^{\rho+}_{ab}\pm\theta^{\sigma+}_{ab}\pm\phi^{\sigma-}_{ab})} \quad (a\neq b) \tag{2.25}$$

Here a and b are band indices and $\alpha = \uparrow$ or $\downarrow$, $\bar{\alpha} \equiv -\alpha$. The $+$ or $-$ sign occurs for $\alpha = \uparrow$ or $\downarrow$ respectively. Even though Eq. (2.25) carries non-zero momentum for $k_{F_a} \neq k_{F_b}$, there is no reason to exclude it.

We now consider the $4k_F$ density operators, corresponding to stripes. The following two operators are the most general $4k_F$ density operators:

$$\psi^\dagger_{Ri\alpha}\psi_{Lj\alpha}\psi^\dagger_{Rk\alpha}\psi_{Ll\alpha} \sim e^{-i\sqrt{\pi}[(\theta^{\rho+}_{ij}+\theta^{\rho+}_{kl})+(\phi^{\rho-}_{ij}+\phi^{\rho-}_{kl})\pm(\theta^{\sigma+}_{ij}+\theta^{\sigma+}_{kl})\pm(\phi^{\sigma-}_{ij}+\phi^{\sigma-}_{kl})]}, \quad (2.26)$$

$$\psi^\dagger_{Ri\alpha}\psi_{Lj\alpha}\psi^\dagger_{Rk\bar{\alpha}}\psi_{Ll\bar{\alpha}} \sim e^{-i\sqrt{\pi}[(\theta^{\rho+}_{ij}+\theta^{\rho+}_{kl})+(\phi^{\rho-}_{ij}+\phi^{\rho-}_{kl})\pm(\theta^{\sigma+}_{ij}-\theta^{\sigma+}_{kl})\pm(\phi^{\sigma-}_{ij}-\phi^{\sigma-}_{kl})]}, \quad (2.27)$$

Here i, j, k and l are arbitrary band indices and the $+$ or $-$ sign is for $\alpha = \uparrow$ or $\downarrow$ respectively. Whether i, j, k and l are all different or not actually doesn't change the conclusion. When all the band indices are different, the operators correspond to the oscillation wave-vector of $4\bar{k}_F \equiv k_{F1} + k_{F2} + k_{F3} + k_{F4}$ which is $2\pi n$, the wave-vector of stripes. However, if some special renormalizations of Fermi momentum, such as $k_{F1} = k_{F3}$ and $k_{F2} = k_{F4}$ occur, then the wave vector $2(k_{F1} + k_{F2})$ also corresponds to $2\pi n$. That's the reason why we consider arbitrary rather than assuming they are all different band indices in Eq. (2.26) and (2.27).

Now we are ready to proceed with our proof that pairing and stripes can't coexist. Before we start, please note that we adopt the usual convention for set theory in mathematics. Two sets A and B are said to be equal, if they have the same elements.

Let's first consider whether the pair operator in Eq. (2.24) and $4k_F$ density operators in Eq. (2.26) or (2.27) could both have power law decay. In order to satisfy Eq. (2.19), $\vec{v}_{\rho\Delta} \cdot \vec{u}_{\rho n} = -\pi$, the index a in Eq. (2.24) must be chosen the same as precisely one of the indices from the set $\{i, j, k, l\}$ in Eq. (2.26) or (2.27). For example if $\{i, j, k, l\} = \{1, 1, 2, 3\}$, then a must be either 2 or 3. If such a choice of a exists (one counter example is $\{i, j, k, l\} = \{1, 1, 2, 2\}$, $\vec{v}_{\rho\Delta} \cdot \vec{u}_{\rho n} \neq -\pi$ for any a), however, it implies $\vec{u}_{\sigma\Delta} \cdot \vec{v}_{\sigma n} \neq 0$ due to the term $\theta_{a\sigma}$ in Eq. (2.24) and $(\phi^{\sigma-}_{ij} \pm \phi^{\sigma-}_{kl})$ in Eq. (2.26) or (2.27). Thus, the condition Eq. (2.21) is not satisfied and the pair operator Eq. (2.24) can't coexist with any $4k_F$ density operator of arbitrary $\{i, j, k, l\}$, including stripes.

Things are less trivial for the other type of pair operators Eq. (2.25). The discussion depends on the situations of the indices set $\{i, j, k, l\}$. Eq. (2.26) and (2.27) are reduced to different operator forms depending on the different choices of the indices and the inner products need to be discussed separately. For example, if $i = j$, $k = l$ and $i \neq k$, then Eq. (2.26) and (2.27) contain neither charge nor spin ϕ fields. In the following, we classify all the possible choices of $\{i, j, k, l\}$ and prove there is no pairing operator that can satisfy all the conditions Eq. (2.19)-(2.23) for any choice of $\{i, j, k, l\}$.

We first consider the case where all the indices are different from each other, i.e. $i \neq j \neq k \neq l$. Comparing the coefficient vectors $\vec{u}_{\rho\Delta}$ arising from $\theta^{\rho-}_{ab}$ in Eq. (2.25) and $\vec{v}_{\rho n}$ from $(\phi^{\rho-}_{ij} + \phi^{\rho-}_{kl})$ in Eq. (2.26) and (2.27), in order to have $\vec{u}_{\rho\Delta} \cdot \vec{v}_{\rho n} = 0$, the indices set $\{a, b\}$ have to be chosen the same set as $\{i, k\}$ or $\{j, l\}$. Next when we compare $\theta^{\sigma+}_{ab}$ in Eq. (2.25) with $(\phi^{\sigma-}_{ij} + \phi^{\sigma-}_{kl})$ in Eq. (2.26), we find $\vec{u}_{\sigma\Delta} \cdot \vec{v}_{\sigma n} \neq 0$ since $\{a, b\} = \{i, k\}$ or $\{j, l\}$. Also, when $\phi^{\sigma-}_{ab}$ in Eq. (2.25) is compared with $(\theta^{\sigma+}_{ij} - \theta^{\sigma+}_{kl})$ in Eq. (2.27), we find that $\vec{v}_{\sigma\Delta} \cdot \vec{u}_{\sigma n} \neq 0$ for the same reason. So, the pair operator Eq. (2.25) is not compatible with $4\bar{k}_F$ density operators.

To make the above argument more clearly, we should look at one specific example. For density operators with the choice $i = 1, j = 2, k = 3$ and $l = 4$, we have the

coefficient vector $\vec{v}_{\rho n} = -\sqrt{\pi/2}(1,-1,1,-1)$ from the term $(\phi^{\rho-}_{ij} + \phi^{\rho-}_{kl})$ in Eq. (2.26) and (2.27). If we choose $\{a,b\} = \{1,3\}$ or $\{2,4\}$, the coefficient vector due to $\theta^{\rho-}_{ab}$ is $\vec{u}_{\rho\Delta} = \pm\sqrt{\pi/2}(1,0,-1,0)$ or $\pm\sqrt{\pi/2}(0,1,0,-1)$, which satisfies the condition $\vec{u}_{\rho\Delta}\cdot\vec{v}_{\rho n} = 0$. Now, with this choice of indices, the term $\phi^{\sigma-}_{ab}$ in Eq. (2.25) corresponds to the coefficient vector $\vec{u}_{\sigma\Delta} = \sqrt{\pi/2}(1,0,1,0)$ or $\sqrt{\pi/2}(0,1,0,1)$, up to a negative sign and $\vec{u}_{\sigma\Delta}$ can not satisfy the condition $\vec{u}_{\sigma\Delta}\cdot\vec{v}_{\sigma n} = 0$ with $\vec{v}_{\sigma n} = \pm\sqrt{\pi/2}(1,-1,1,-1)$ from the term $(\phi^{\sigma-}_{ij} + \phi^{\sigma-}_{kl})$ in Eq. (2.26). Similarly, Eq. (2.25) and (2.27) can not satisfy another condition $\vec{v}_{\sigma\Delta}\cdot\vec{u}_{\sigma n} = 0$.

Now if three or all four indices in the set $\{i,j,k,l\}$ are the same, such as $\{1,1,1,2\}$ or $\{1,1,1,1\}$, then the coefficient vectors $\vec{v}_{\rho\Delta}$ from $\phi^{\rho+}_{ab}$ in Eq. (2.25) and $\vec{u}_{\rho n}$ from $(\theta^{\rho+}_{ij}+\theta^{\rho+}_{kl})$ in Eq. (2.26) or (2.27) can never satisfy $\vec{v}_{\rho\Delta}\cdot\vec{u}_{\rho n} = -\pi$ for any $\{a,b\}$.

When only two indices are the same, we have to consider six cases since Eq. (2.26) and (2.27) reduce to different operator forms for different choices of the indices. Assume that $i = j$ and $k \neq l \neq i$ in the set $\{i,j,k,l\}$, for example $i = j = 1$, and $\{k,l\} = \{2,4\}$, and then $\{a,b\}$ must be chosen to have no common elements with $\{k,l\}$ (i.e. $\{a,b\}\cap\{k,l\} = 0$) in order to satisfy the condition $\vec{u}_{\rho\Delta}\cdot\vec{v}_{\rho n} = 0$, e.g. $\{a,b\} = \{1,3\}$ given the above choice of i,k and l. However, that will make $\vec{v}_{\sigma\Delta}\cdot\vec{u}_{\sigma n} \neq 0$ and therefore Eq. (2.25) is not compatible with Eq. (2.26) and (2.27) for $i = j$ and $k \neq l \neq i$.

Now assume $i = k$ and $j \neq l \neq i$. Since $a \neq b$, to make $\vec{u}_{\rho\Delta}\cdot\vec{v}_{\rho n} = 0$, we need $\{a,b\} = \{j,l\}$. Then we find that $\vec{u}_{\sigma\Delta}\cdot\vec{v}_{\sigma n} \neq 0$ from Eq. (2.25) and Eq. (2.26) and $\vec{v}_{\sigma\Delta}\cdot\vec{u}_{\sigma n} \neq 0$ from Eq. (2.25) and Eq. (2.27).

For $i = l$ and $j \neq k \neq i$, to make $\vec{u}_{\rho\Delta}\cdot\vec{v}_{\rho n} = 0$ true, we need to choose the indices so that $\{a,b\}\cap\{j,k\} = \varnothing$. For example, we can choose $i = l = 1$, $\{a,b\} = \{1,3\}$ and $\{j,k\} = \{2,4\}$. However, this condition $\{a,b\}\cap\{j,k\} = \varnothing$ will result in $\vec{v}_{\sigma\Delta}\cdot\vec{u}_{\sigma n} \neq 0$ from Eq. (2.25) and Eq. (2.26) and $\vec{u}_{\sigma\Delta}\cdot\vec{v}_{\sigma n} \neq 0$ from Eq. (2.25) and Eq. (2.27).

There are three more cases that we should consider. They are $j = k$, $j = l$ and $k = l$. In these cases, Eq. (2.26) and (2.27) actually reduce to three similar situations we have discussed above with some signs changed which don't effect the result. Thus, Eq. (2.25) is not compatible with Eq. (2.26) and (2.27) for the cases that only two indices are the same in the set $\{i,j,k,l\}$.

The last situations we have to consider are where $\{i,j,k,l\}$ are two pairs of indices. We first discuss the case $i = j$, $k = l$ and $i \neq k$. To satisfy the condition $\vec{v}_{\rho\Delta}\cdot\vec{u}_{\rho n} = -\pi$, only one index in the set $\{a,b\}$ should be chosen the same as one index in $\{i,k\}$, e.g. if $a = i$ then $b \neq k$. Then we find Eq. (2.25) and Eq. (2.26) or Eq. (2.27) will have $\vec{v}_{\sigma\Delta}\cdot\vec{u}_{\sigma n} \neq 0$.

In the case $i = k$, $j = l$ and $i \neq j$, similarly, only one of $\{a,b\}$ should be chosen the same as one of $\{i,k\}$ so as to have to have $\vec{v}_{\rho\Delta}\cdot\vec{u}_{\rho n} = -\pi$. Then $\vec{u}_{\rho\Delta}\cdot\vec{v}_{\rho n} \neq 0$ from Eq. (2.25) and either Eq. (2.26) or Eq. (2.27).

For $i = l$, $j = k$ and $i \neq j$, Eq. (2.26) reduces to the same form as that in the case for $i = j$, $k = l$ and $i \neq k$, which was already discussed. For Eq. (2.25) and Eq. (2.27), in order to have $\vec{v}_{\rho\Delta}\cdot\vec{u}_{\rho n} = -\pi$, only one of $\{a,b\}$ should be chosen the same as one of $\{i,k\}$. However, this will make $\vec{u}_{\sigma\Delta}\cdot\vec{v}_{\sigma n} \neq 0$ and therefore they are not compatible.

Now we want to ask further if *any* operator of non-zero charge can have a power-law decaying correlation function in a stripe phase. Inspired by the real space picture of stripes and the finite size spectrum analysis in the next section, we find that there is always some charge-four bipairing operator, which does so. The most general non-chiral bipairing operators are:

$$\psi_{Rs\alpha}\psi_{Lt\bar{\alpha}}\psi_{Ru\beta}\psi_{Lv\bar{\beta}} \sim e^{i\sqrt{\pi}[(\phi^{\rho+}_{st}+\phi^{\rho+}_{uv})+(\theta^{\rho-}_{st}+\theta^{\rho-}_{uv})\pm(\phi^{\sigma+}_{st}\pm\phi^{\sigma+}_{uv})\pm(\theta^{\sigma-}_{st}\pm\theta^{\sigma-}_{uv})]}. \tag{2.28}$$

Here s, t, u and v are arbitrary band indices. Although Eq. (2.28) are the possible bipairing operators in the most general sense, only when $s = t$ and $u = v$ or $s = v$ and $t = u$ does Eq. (2.28) carry zero momentum and have no real space modulation in the correlation functions. On the other hand, we have no reason to exclude the possibility that Eq. (2.28) does decay with a power law with an oscillating factor at this stage.

Following the previous discussion, now we will prove that any C1S0 phase with $4\bar{k}_F$ density oscillations, also has bipairing correlation. The conditions for bipairing and $4\bar{k}_F$ density operators to coexist are almost the same as Eq. (2.19)-(2.23) but now with $\vec{v}_{\rho,bi}\cdot\vec{u}_{\rho,n} = -2\pi$, where we use a subscript "bi" for bipairing operators. Now for simplicity, let's focus on the following two types of bipairing operators carrying zero momentum:

$$\psi_{Rs\alpha}\psi_{Ls\alpha}\psi_{Rt\bar{\alpha}}\psi_{Lt\bar{\alpha}} \sim e^{i\sqrt{4\pi}(\phi^{\rho+}_{st}\pm\phi^{\sigma-}_{st})}, \tag{2.29}$$

$$\psi_{Rs\alpha}\psi_{Ls\bar{\alpha}}\psi_{Rt\beta}\psi_{Lt\bar{\beta}} \sim e^{i\sqrt{4\pi}(\phi^{\rho+}_{st}\pm\theta^{\sigma\pm}_{st})}. \tag{2.30}$$

We find that Eq. (2.26), (2.27) and Eq. (2.29) can coexist if we choose $\{s,t\} = \{i,j\}$ or $\{k,l\}$. If we have $\alpha = \beta$ in Eq. (2.30), i.e. $\theta^{\sigma+}_{st}$ is present, then Eq. (2.26), (2.27) and Eq. (2.30) can coexist with the choice that $\{s,t\} = \{i,j\}$ or $\{k,l\}$. If we have $\alpha = \overline{\beta}$ in Eq. (2.30), then $\theta^{\sigma-}_{st}$ is present. Eq. (2.26) and (2.30) can coexist with the choice that $\{s,t\} = \{i,k\}$ or $\{j,l\}$. Eq. (2.27) and (2.30) can coexist if $\{s,t\} = \{i,l\}$ or $\{j,k\}$.

2.2 Gapless Field Is Not the Total Charge Mode

Now we should address the issue about the possibility of some pinned $\theta'_{i\rho}$ fields which are *not* orthogonal to $\Theta_{1\rho}$. In this case, $\Theta_{1\rho}$ can not be a basis field and thus the gapless charge mode won't be $\Theta_{1\rho}$ anymore. As we discussed at the beginning of this chapter, whether a $\theta'_{i\rho}$ field can be pinned or not depends on the renormalization of Fermi momenta. Fermi momenta are important regarding both translational symmetry and the interactions in the Hamiltonian. A certain $\theta'_{i\rho}$ field can be pinned if it's allowed by symmetry and there is a relevant interaction involving it in the Hamiltonian. The oscillating factors of four fermion interactions only involve the Fermi momentum combinations like $(k_{Fi} \pm k_{Fj} \pm k_{Fk} \pm k_{Fl})$ whereas any arbitrary combination can be considered from symmetry's point of view. Therefore, it will be much easier to discuss the possible pinned $\theta'_{i\rho}$ fields, not orthogonal to $\Theta_{1\rho}$, through the possible new interactions containing $\theta'_{i\rho}$ in the Hamiltonian.

In fact, we are only concerned about the question whether pairing and stripes can coexist when the gapless mode is not the total charge field. In the previous section, we saw that the correlation functions of two operators can decay with a power-law at the same time if and only if Eq. (2.19)-(2.23) are satisfied. When the gapless mode is not the total charge field, apparently Eq. (2.19), $\vec{v}_{\rho\Delta}\cdot\vec{u}_{\rho n}=-\pi$, is not correct. We just don't know the value for this inner product if we don't know what the gapless field is. Strictly speaking, the inner products, Eq. (2.20)-(2.23), between the coefficient vectors have to be zero after excluding the contribution from the gapless field. Mathematically, we mean $\vec{v}^{\perp}_{\rho A}\cdot\vec{u}^{\perp}_{\rho A}=0$, where $\vec{v}^{\perp}_{\rho A}=\vec{v}_{\rho A}-(\vec{v}_{\rho A}\cdot\vec{g})\vec{g}$ and $\vec{u}^{\perp}_{\rho A}=\vec{u}_{\rho A}-(\vec{u}_{\rho A}\cdot\vec{g})\vec{g}$ where the gapless charge mode is $\vec{g}\cdot\vec{\phi}_{\rho}$ ($\vec{g}$ is a unit vector). Take a two band system for example: the operator $O_A\sim e^{i\sqrt{2\pi}(\theta^{\rho}_1+\theta^{\rho}_2+\phi^{\rho}_1-\phi^{\rho}_2)}$ has the coefficient vectors $\vec{v}_{\rho A}=\sqrt{2\pi}(1,1)$ and $\vec{u}_{\rho A}=\sqrt{2\pi}(1,-1)$. It's easy to see that this operator satisfies the condition $\vec{v}_{\rho A}\cdot\vec{u}_{\rho A}=0$. If $(\theta^{\rho+}_{12},\phi^{\rho+}_{12})$ is the gapless charge mode, then $\vec{g}=(1,1)/\sqrt{2}$. Only θ fields contain the gapless mode. The gapless mode won't appear in the ϕ fields since in this case it's orthogonal to the ϕ field, $\phi^{\rho}_1-\phi^{\rho}_2$. Then there is no contribution to the inner product from the gapless mode and we have $\vec{v}^{\perp}_{\rho A}\cdot\vec{u}^{\perp}_{\rho A}=0$. This operator could have power-law decaying correlations. However, if $(\theta^{\rho}_1,\phi^{\rho}_1)$ is the gapless field, we have to exclude the part of the inner product due to the gapless field since the overlap between θ and ϕ fields is allowed for the gapless mode. Now $\vec{g}=(1,0)$, and we find the inner product $\vec{v}^{\perp}_{\rho A}\cdot\vec{u}^{\perp}_{\rho A}=-2\pi\neq 0$. Then the correlation function of this operator will decay exponentially since θ^{ρ}_2 and ϕ^{ρ}_2 can't be pinned at the same time. The conditions on the spin fields are still the same since they have nothing to do with the gapless charge mode. We will have to check the pair and $4k_F$ density operators for all possible gapless charge modes case by case.

In order to check through all the possible pinning patterns efficiently, our strategy is to start with one Fermi momentum renormalization condition so that the new interaction involving a $\theta'_{i\rho}$ field not orthogonal to $\Theta_{1\rho}$ is present in the Hamiltonian. Next, we will assume that interaction is relevant and $\theta'_{i\rho}$, as one of the basis fields, is indeed pinned. We further assume that the phase has pairing, that is, either Eq. (2.24) or (2.25) has power-law decaying correlations. So there will be two types of pairing to be discussed. Each type of pairing, will require that some boson fields get pinned. If another $\theta'_{i\rho}$ field needs to be pinned in order to have pairing, it's allowed but one more Fermi momentum renormalization condition must occur. For a phase with pairing, we will have a pinning pattern for some boson fields but the rest of it will still be undetermined. Then the question is if it's possible to have stripes by arbitrarily choosing the pinning pattern for the rest of the bosons. To answer it, we have to check the correlation functions of all $4k_F$ density operators carefully since some of them may correspond to stripes if additional Fermi momentum renormalization conditions are satisfied. After this is done, we repeat this procedure but start with a new $\theta'_{i\rho}$ field not orthogonal to $\Theta_{1\rho}$, that is, another Fermi momentum renormalization condition. When all the possible Fermi momentum conditions associated with the interactions are discussed, we will have completed the proof.

Recall that an interaction can appear in the Hamiltonian if its oscillating factor

becomes a constant, that is $\pm(k_{Fi} \pm k_{Fj} \pm k_{Fk} \pm k_{Fl}) = 0$ or 2π. Here i, j, k and l are arbitrary band indices (see the oscillating factor in Eq. (B.2) in Appendix B). These interactions contain charge fields like $\pm(\theta_{i\rho} \pm \theta_{j\rho} \pm \theta_{k\rho} \pm \theta_{l\rho})$ after bosonized. We have to consider the possible combination not orthogonal to the total charge mode $\Theta_{1\rho}$. If i, j, k and l are all different, we only need to consider $k_{Fi} + k_{Fj} + k_{Fk} - k_{Fl} = 0$ or 2π since $k_{Fi} + k_{Fj} + k_{Fk} + k_{Fl} = 2\pi n$ and $k_{Fi} + k_{Fj} - k_{Fk} - k_{Fl}$ doesn't result in the field not orthogonal to the total charge mode. If two indices are the same, say $i = l$, we need to consider $2k_{Fi} + k_{Fj} + k_{Fk} = 2\pi$ and $2k_{Fi} + k_{Fj} - k_{Fk} = 0$ or 2π where i, j and k are different. If three indices are the same, say $i = k = l$, we need to consider $3k_{Fi} + k_{Fj} = 2\pi$ and $3k_{Fi} - k_{Fj} = 0$ or 2π where $i \neq j$. If two pairs of indices are the same, then we need to consider $2k_{Fi} + 2k_{Fj} = 2\pi$ where $i \neq j$. When each of the above renormalization conditions is satisfied, there will be a new interaction containing a θ_ρ field not orthogonal to the total charge mode. In each case, we also allow other Fermi momentum renormalization conditions to occur so as to change the wave vector of density operators or pin some other θ_ρ field orthogonal to the total charge mode. We have to discuss the cases for $2k_{Fi} + 2k_{Fj} = 2\pi$ and $2k_{Fi} + k_{Fj} + k_{Fk} = 2\pi$ in details. As for other conditions, there will be a general argument.

In the following, we consider all possible four fermions interactions to determine the phases (or pinning patterns). We will show that pairing and stripes still can't coexist even if the gapless mode is not the total charge field.

2.2.1 New Interactions Due to $k_{Fp} + k_{Fq} = \pi$

We first consider when $k_{Fp} + k_{Fq} = \pi$ is satisfied where $p \neq q$. Then the oscillating factor of the interaction like $\psi^\dagger_{Rp\alpha}\psi^\dagger_{Rq\bar{\alpha}}\psi_{Lp\bar{\alpha}}\psi_{Lq\alpha}$ becomes one at each site. Therefore, $\theta^{\rho+}_{pq}$ may get pinned in this case. In order to reduce the confusion of indices, without loss of generality, we will choose explicitly $p = 1$ and $q = 2$. Now assume the new interaction is relevant and $\theta^{\rho+}_{12}$ is really pinned. Since the total charge field $\Theta_{1\rho}$ is always unpinned, this implies $\theta^{\rho+}_{34}$ is unpinned. However, this is not equivalent to say $\theta^{\rho+}_{34}$ is gapless yet. If either $\theta_{3\rho}$ or $\theta_{4\rho}$ is gapless, $\theta^{\rho+}_{34}$ is also unpinned. Say, $(\theta_{3\rho}, \phi_{3\rho})$ is gapless, then either $\theta_{4\rho}$ or $\phi_{4\rho}$ has to be pinned in a C1S0 phase. However, Eq. (2.6) and (2.3) states that $\theta_{4\rho}$ and $\phi_{4\rho}$ are not allowed to be pinned by symmetry if $k_{F4} \neq 0$. (See Sec. (2.3) for the case where $k_{F4} = 0$). Thus we conclude the gapless mode is $(\theta^{\rho+}_{34}, \phi^{\rho+}_{34})$ in this case. Now the basis in the charge channel could be given by the orthogonal rotation matrix

$$R_\rho = \begin{pmatrix} 0 & 0 & 1/\sqrt{2} & 1/\sqrt{2} \\ 0 & 0 & 1/\sqrt{2} & -1/\sqrt{2} \\ 1/\sqrt{2} & 1/\sqrt{2} & 0 & 0 \\ 1/\sqrt{2} & -1/\sqrt{2} & 0 & 0 \end{pmatrix}. \tag{2.31}$$

Note that at this stage, we only know for sure that $(\theta^{\rho+}_{34}, \phi^{\rho+}_{34})$ is gapless and the linear combination $\theta^{\rho+}_{12}$ is pinned. However, the basis could be chosen differently for the following reason. For example, assume that $\theta^{\rho-}_{12}$ is also pinned due to the interactions involving $\theta^{\rho-}_{12}$

with the extra condition $k_{F1} = k_{F2}$, then the orthogonal linear combinations $\theta_{12}^{\rho+}$ and $\theta_{12}^{\rho-}$ could be part of a new basis since the new fields are still orthogonal to the gapless mode. When the interaction involving $\theta_{34}^{\rho-}$ is also present, then there will be more choices of basis. Regardless of the consistency of these conditions on the Fermi momentum, we don't worry too much about different bases here for the following reasons. As we mentioned before, the inner product is invariant under orthogonal basis transformations. So if we find a conflict between pairing and stripes in one specific basis, the conflict still remains in any different basis which is related by an orthogonal transformation. Another important part of our proof is to argue that the wave-vectors of the $4k_F$ density operators won't correspond to that of stripes without causing inconsistency. That only depends on the band indices in Eq. (2.26), (2.27) and Fermi momentum renormalization conditions, which are all independent of the basis. For simplicity, we will use the R_ρ in Eq. (2.31) and keep in mind that the different choices of basis are possible.

Pairing Case I [Eq. (2.24)]

Now let's see what are the requirements we need in order to have pairing. Recall that we start with the condition $k_{F1} + k_{F2} = \pi$. The field $\theta_{12}^{\rho+}$ is pinned and $(\theta_{34}^{\rho+}, \phi_{34}^{\rho+})$ is the gapless field. To make the correlation function of the operator in Eq. (2.24) decay with a power-law, $\phi_{34}^{\rho-}$ and $\theta_{3\sigma}$ (or $\theta_{4\sigma}$) have to be pinned upon choosing $a = 3$ (or 4) in Eq. (2.24). So we conclude that $(\theta_{34}^{\rho+}, \phi_{34}^{\rho+})$ gapless, $\theta_{12}^{\rho+}$,$\phi_{34}^{\rho-}$ and $\theta_{3\sigma}$ (or $\theta_{4\sigma}$) pinned are the only possible pinning patterns for Eq. (2.24) to have pairing under the condition $k_{F1} + k_{F2} = \pi$. We will consider another possibility that the correlation function of the operator in Eq. (2.25) decay with a power-law later (in Pairing Case II). Now we should discuss whether it's possible to have stripes allowing arbitrary pinning patterns for the rest of the boson fields in this case.

Stripes are the density oscillation with wave-vector $2\pi n$, corresponding to $4\bar{k}_F$ density operators. However, a $4k_F$ density operator with wave-vector $k_{F1} + k_{F2} + 2k_{F3}$ could be identified as $4\bar{k}_F = 2\pi n$, if the renormalization of Fermi momentum $k_{F3} = k_{F4}$ happens. As we did before, we have to check all the possible $4k_F$ density operators that may correspond to $2\pi n$. The only difference now is that the gapless mode is $(\theta_{34}^{\rho+}, \phi_{34}^{\rho+})$. Eq. (2.26) and (2.27) are the most general $4k_F$ density operators. We have to consider four situations about the indices in Eq. (2.26) and (2.27), where the density operators reduce to different forms. These four situations are: (1) all the indices are different; (2) two indices are the same but different from the other two; (3) two pairs of indices are the same; (4) three indices are the same but different from the last one.

For case (1): When i, j, k and l are all different in Eq. (2.26) and (2.27), Eq. (2.24) can not coexist with both Eq. (2.24) since $\vec{u}_{\sigma\Delta} \cdot \vec{v}_{\sigma n} \neq 0$ due to the term $\theta_{a\sigma}$ in Eq. (2.24) and $(\phi_{ij}^{\sigma-} \pm \phi_{kl}^{\sigma-})$ in Eq. (2.26) or (2.27). As for Eq. (2.25), we need to choose $\{a, b\} = \{i, j\}$ or $\{k, l\}$ in order to satisfy $\vec{u}_{\sigma\Delta} \cdot \vec{v}_{\sigma n} = 0$ for the spin bosons. Then the inner product $\vec{u}_{\rho\Delta} \cdot \vec{v}_{\rho n}$ due to the term $\theta_{ab}^{\rho-}$ in Eq. (2.25) and $(\phi_{ij}^{\rho-} + \phi_{kl}^{\rho-})$ in Eq. (2.26) or (2.27) is nonzero. The inner product $\vec{v}_{\rho\Delta} \cdot \vec{u}_{\rho n}$ between the term $\phi_{ab}^{\rho+}$ in Eq.

(2.25) and $(\theta_{ij}^{\rho+}+\theta_{kl}^{\rho+})$ in Eq. (2.26) or (2.27) is also nonzero. We know that the inner product including the gapless mode can be nonzero but the part excluding the gapless mode $\vec{u}_{\rho\Delta}^{\perp}\cdot\vec{v}_{\rho n}^{\perp}$ and $\vec{v}_{\rho\Delta}^{\perp}\cdot\vec{u}_{\rho n}^{\perp}$ should be zero. That is to say, $\vec{u}_{\rho\Delta}\cdot\vec{v}_{\rho n}=\theta_{ab}^{\rho-}\cdot\phi_{ij}^{\rho-}$ and $\vec{v}_{\rho\Delta}\cdot\vec{u}_{\rho n}=\phi_{ab}^{\rho+}\cdot\theta_{ij}^{\rho+}$ should be both zero after the gapless mode is projected out. However, this is impossible since $\vec{u}_{\rho\Delta}\cdot\vec{v}_{\rho n}=\vec{v}_{\rho\Delta}\cdot\vec{u}_{\rho n}$ before the projection and $\theta_{ab}^{\rho-}$ is orthogonal to $\phi_{ab}^{\rho+}$. The above discussion is very general and doesn't assume anything about the gapless mode. The conclusion that these $4\bar{k}_F$ density operators and the pair operator Eq. (2.24) or (2.25) can't decay with a power-law at the same time holds for any gapless mode. In the later discussions, we don't have to worry about these $4\bar{k}_F$ density operators.

For case (2): We first assume only two indices are the same in Eq. (2.26) and (2.27). Then Eq. (2.26) and (2.27) will reduce to the operators with three band indices. We just have to work out all the operator forms when two out of four indices are the same in Eq. (2.26) and (2.27). The resultant operators have the general forms:

$$e^{-i\sqrt{\pi}[(\sqrt{2}\theta_{i\rho}+\theta_{jk}^{\rho+})+(\phi_{jk}^{\rho-})+(\sqrt{2}\theta_{i\sigma}\pm\theta_{jk}^{\sigma+})+(\phi_{jk}^{\sigma-})]}, \tag{2.32}$$

$$e^{-i\sqrt{\pi}[(\sqrt{2}\theta_{i\rho}+\theta_{jk}^{\rho+})+(\phi_{jk}^{\rho-})+(\theta_{jk}^{\sigma-})+(\sqrt{2}\phi_{i\sigma}-\phi_{jk}^{\sigma+})]}, \tag{2.33}$$

$$e^{-i\sqrt{\pi}[(\sqrt{2}\theta_{i\rho}+\theta_{jk}^{\rho+})+(\sqrt{2}\phi_{i\rho}-\phi_{jk}^{\rho+})+(\sqrt{2}\theta_{i\sigma}+\theta_{jk}^{\sigma+})+(\sqrt{2}\phi_{i\sigma}-\phi_{jk}^{\sigma+})]}, \tag{2.34}$$

$$e^{-i\sqrt{\pi}[(\sqrt{2}\theta_{i\rho}+\theta_{jk}^{\rho+})+(\sqrt{2}\phi_{i\rho}-\phi_{jk}^{\rho+})+(\theta_{jk}^{\sigma-})+(\phi_{jk}^{\sigma-})]}, \tag{2.35}$$

where i,j and k are all different. In fact, Eq. (2.32)-(2.35) don't cover all the possible operators forms. However, these other cases correspond to simply changing the signs in front of last three parentheses in Eq. (2.32)-(2.35). We only care about whether the inner products between coefficient vectors are zero or not. Therefore, we can ignore the signs. Let's focus on the charge channel of Eq. (2.34) and (2.35) and we will argue that their correlation functions decay exponentially when $(\theta_{34}^{\rho+},\phi_{34}^{\rho+})$ is the gapless mode. It's easy to see that $\{i,j,k\}\cap\{3,4\}\neq\varnothing$ because i,j and k are all different. The charge fields$\sqrt{2}\theta_{i\rho}+\theta_{jk}^{\rho+}$ and $\sqrt{2}\phi_{i\rho}-\phi_{jk}^{\rho+}$ in Eq. (2.34) and (2.35) will contain the gapless mode $\theta_{34}^{\rho+}$ and $\phi_{34}^{\rho+}$, respectively, for any $\{i,j,k\}$. When we rewrite Eq. (2.34) and (2.35) in terms of the pinning basis fields, after projecting out the gapless mode, the inner product between the coefficient vectors of θ and ϕ fields, $\vec{v}_{\rho A}^{\perp}\cdot\vec{u}_{\rho A}^{\perp}$, should be zero. If the inner product $\vec{v}_{\rho A}^{\perp}\cdot\vec{u}_{\rho A}^{\perp}$ is not zero, the correlation functions of Eq. (2.34) and (2.35) will decay exponentially. It's easy to check that for any choice of $\{i,j,k\}$ in Eq. (2.34) and (2.35), $\vec{v}_{\rho A}^{\perp}\cdot\vec{u}_{\rho A}^{\perp}\neq 0$. For example, for $i=1$, $j=2$ and $k=3$, the charge bosons in Eq. (2.34) and (2.35) can be written, in terms of the basis fields given by the orthogonal matrix Eq. (2.31), as $-\sqrt{\pi}(3\theta_{12}^{\rho+}+\theta_{12}^{\rho-}+\theta_{34}^{\rho+}+\theta_{34}^{\rho-})/2$ and $-\sqrt{\pi}(\phi_{12}^{\rho+}+3\phi_{12}^{\rho-}-\phi_{34}^{\rho+}-\phi_{34}^{\rho-})/2$. Excluding the gapless mode $(\theta_{34}^{\rho+},\phi_{34}^{\rho+})$ when calculate the inner product, the inner product $\vec{v}_{\rho A}^{\perp}\cdot\vec{u}_{\rho A}^{\perp}$ is $5\pi/4$. As we mentioned, this is independent of the basis as long as the gapless mode is the same. Then the operators in Eq. (2.34) and (2.35) have exponentially decaying correlations as long as $(\theta_{34}^{\rho+},\phi_{34}^{\rho+})$ is gapless. So we don't have to consider these two $4k_F$ density operators for the later discussion in this subsection.

So far we only require that $\theta_{12}^{\rho+}$,$\phi_{34}^{\rho-}$ and $\theta_{3\sigma}$ (or $\theta_{4\sigma}$) are pinned in order to have pairing and we have the choice of how to pin the other boson fields. Now look at the term $\phi_{jk}^{\rho-}$ in Eq. (2.32) and (2.33). We can only choose $\{j,k\} = \{3,4\}$ or $\{j,k\} = \{1,2\}$ when an additional boson $\phi_{12}^{\rho-}$ is pinned. If $\{j,k\} = \{1,2\}$, then i has to be either 3 or 4 in Eq. (2.32) or (2.33) and then the term $\sqrt{2}\theta_{i\rho}$ in the density operators will conflict with the assumption that $\phi_{34}^{\rho-}$ is pinned. If $\{j,k\} = \{3,4\}$, then the terms $\sqrt{2}\phi_{i\sigma} - \phi_{34}^{\sigma+}$ or $\phi_{34}^{\sigma-}$ in in Eq. (2.32) and (2.33) respectively will not be compatible with the requirement that $\theta_{3\sigma}$ (or $\theta_{4\sigma}$) is pinned.

For case (3): Next we discuss $4k_F$ density operators where two pairs of indices are the same in Eq. (2.26) and (2.27). Recall that we are considering the pinning pattern in which $(\theta_{34}^{\rho+}, \phi_{34}^{\rho+})$ is gapless and $\theta_{12}^{\rho+}$,$\phi_{34}^{\rho-}$ and $\theta_{3\sigma}$ (or $\theta_{4\sigma}$) are pinned. The $4k_F$ density operators reduce to the forms:

$$e^{-i\sqrt{4\pi}(\theta_{ij}^{\rho+} \pm \theta_{ij}^{\sigma\pm})}, \tag{2.36}$$

$$e^{-i\sqrt{4\pi}(\theta_{ij}^{\rho+} \pm \phi_{ij}^{\sigma-})}, \tag{2.37}$$

$$e^{-i\sqrt{4\pi}(\theta_{ij}^{\rho+} \pm \phi_{ij}^{\rho-} \pm \theta_{ij}^{\sigma+} \pm \phi_{ij}^{\sigma-})}, \tag{2.38}$$

$$e^{-i\sqrt{4\pi}(\theta_{ij}^{\rho+} \pm \phi_{ij}^{\rho-})}, \tag{2.39}$$

where $i \neq j$. If $\{i,j\} = \{3,4\}$, the correlation function of Eq. (2.37) and (2.38) decay exponentially since the term $\phi_{34}^{\sigma-}$ contains the dual of the pinned boson $\theta_{3\sigma}$ (or $\theta_{4\sigma}$). In this case, the correlation function of Eq. (2.36) can decay with a power-law and is actually compatible with the pairing. Furthermore, in this case the correlation function of Eq. (2.39) is a constant and the phase has a true long-ranged order. However, the wave-vector associated with the operators in Eq. (2.36) and (2.39) is $2(k_{F3} + k_{F4}) = 4\pi n - 2\pi$, which does not correspond to stripes.

If only one of $\{i,j\}$ belongs to $\{3,4\}$, say $\{i,j\} = \{1,3\}$, all the operators from Eq. (2.36) to (2.39) have exponentially decaying correlations since the term $\theta_{13}^{\rho+}$ conflicts with the pinned boson $\phi_{34}^{\rho-}$. If $\{i,j\} = \{1,2\}$, then their wave-vectors are $2(k_{F1} + k_{F2}) = 2\pi$, which doesn't correspond to that of stripes.

For case (4): When three indices are the same in Eq. (2.26) and (2.27), their correlation functions will decay exponentially since $\vec{u}_{\sigma n} \cdot \vec{v}_{\sigma n} = 0$ is never satisfied for those operators. This is in general true and independent of the pinning patterns. Thus in the following discussion, we don't have to consider this situation for $4k_F$ density operators.

Pairing Case II [Eq. (2.25)]

We have proven that under the Fermi momentum condition $k_{F1} + k_{F2} = \pi$, if the correlation function of the pair operator, Eq. (2.24) decays with a power-law, then $2\pi n$ density oscillations, i.e. stripes, don't occur. Recall that we start with the condition $k_{F1} + k_{F2} = \pi$. The field $\theta_{12}^{\rho+}$ is pinned and $(\theta_{34}^{\rho+}, \phi_{34}^{\rho+})$ is the gapless field. Now we need to consider the other possible situation that Eq. (2.25) has power decaying correlation. This is possible if $\theta_{34}^{\rho-}$, $\theta_{34}^{\sigma+}$ and $\phi_{34}^{\sigma-}$ are pinned, choosing $\{a,b\} = \{3,4\}$ in Eq. (2.25).

For $\{a,b\} \neq \{3,4\}$, the correlation function of Eq. (2.25) decays exponentially when $(\theta_{34}^{\rho+}, \phi_{34}^{\rho+})$ is gapless. However, to pin the boson $\theta_{34}^{\rho-}$ requires an additional condition $k_{F3} = k_{F4}$.

For this pairing phase, we have assumed that $(\theta_{34}^{\rho+}, \phi_{34}^{\rho+})$ is gapless and $\theta_{12}^{\rho+}$,$\theta_{34}^{\rho-}$, $\theta_{34}^{\sigma+}$ and $\phi_{34}^{\sigma-}$ are pinned. The momentum renormalization conditions are $k_{F1} + k_{F2} = \pi$ and $k_{F3} = k_{F4}$. Now we should investigate whether it can also be a stripe phase or not. There are four situations for Eqs. (2.26) and (2.27). As we discussed in the previous subsection, Pairing Case I, we don't have to worry about situations (1) and (4) but we still need to discuss (2) and (3)

For case (2): Following what we did before, we have to check all the $4k_F$ density operators. We first consider the $4k_F$ density operators when two indices are the same, that is, from Eq. (2.32) to (2.35). As we argued above, the correlation functions of Eq. (2.34) and (2.35) decay exponentially when the gapless mode is $(\theta_{34}^{\rho+}, \phi_{34}^{\rho+})$. To make the correlation functions of Eq. (2.32) to (2.33) decay with a power-law, regarding the charge bosons, we have to choose $\{j,k\} = \{1,2\}$ and assume that $\phi_{12}^{\rho-}$ is also pinned. However, in the spin channel, since the index i is either 3 or 4, the terms $(\sqrt{2}\theta_{i\sigma} \pm \theta_{12}^{\sigma+})$ and $(\sqrt{2}\phi_{i\sigma} - \phi_{12}^{\sigma+})$ are not compatible with the pinned bosons, $\phi_{34}^{\sigma-}$ and $\theta_{34}^{\sigma+}$, respectively.

For case (3): Now again start with the assumption that $(\theta_{34}^{\rho+}, \phi_{34}^{\rho+})$ is gapless and $\theta_{12}^{\rho+}$,$\theta_{34}^{\rho-}$, $\theta_{34}^{\sigma+}$ and $\phi_{34}^{\sigma-}$ are pinned. We consider the $4k_F$ density operators when two pairs of the indices are the same, i.e. Eq. (2.36)-(2.39). For $\{i,j\} = \{3,4\}$ or $\{i,j\} = \{1,2\}$, the wave-vector $2(k_{F3} + k_{F4})$ or $2(k_{F1} + k_{F2})$ doesn't correspond to that of stripes. If only one of $\{i,j\}$ belongs to $\{3,4\}$, for example $\{i,j\} = \{1,3\}$, the correlation functions of all operators decay exponentially since the terms $\phi_{13}^{\rho-}$, $\theta_{13}^{\sigma\pm}$ and $\phi_{13}^{\sigma-}$ involve the dual of pinned bosons $\theta_{34}^{\rho-}, \phi_{34}^{\sigma-}$ and $\theta_{34}^{\sigma+}$. For three indices are the same in Eq. (2.26) and (2.27), their correlation functions decay exponentially as discussed before.

At this point, we have completed the proof that pairing and stripes still can't coexist when the gapless mode is $(\theta_{34}^{\rho+}, \phi_{34}^{\rho+})$ and at least one Fermi momentum renormalization $2(k_{F1} + k_{F2}) = 2\pi$ occurs.

2.2.2 New Interactions Due to $2k_{Fp} + k_{Fq} + k_{Fr} = 2\pi$

Now we consider different renormalization conditions on Fermi momenta, $2k_{Fp} + k_{Fq} + k_{Fr} = 2\pi$, which can also result in the pinned charge field not orthogonal to the total charge mode. Without loss of generality, we choose $2k_{F1} + k_{F2} + k_{F3} = 2\pi$. In this case, for example, the interaction like $\psi_{R1\alpha}^\dagger \psi_{R2\bar{\alpha}}^\dagger \psi_{L1\alpha} \psi_{L3\bar{\alpha}}$ can be present in the Hamiltonian because its oscillating factor becomes a constant. If this new interaction is relevant, the charge field $(2\theta_{1\rho} + \theta_{2\rho} + \theta_{3\rho})/\sqrt{6}$, not orthogonal to the total charge mode, will get pinned. Assume it's really pinned and therefore $\Theta_{1\rho}$ can't be an element of the pinning basis anymore. What's the gapless mode in this case? We know that the field $\Theta_{1\rho}$ is never pinned even though the total charge field is not an element of the pinning basis. This implies that the combination like $\theta_{4\rho} - \theta_{1\rho}$ is also unpinned. If it's pinned, combining with the pinned field $(2\theta_{1\rho} + \theta_{2\rho} + \theta_{3\rho})/\sqrt{6}$, will imply that $\Theta_{1\rho}$ is pinned. One may

think that the field $(\theta_{4\rho}-\theta_{1\rho})/\sqrt{2}$ should be the gapless mode, yet it's not orthogonal to $(2\theta_{1\rho}+\theta_{2\rho}+\theta_{3\rho})/\sqrt{6}$, and can't be chosen as an element of the pinning basis. So what gapless field can let $\Theta_{1\rho}$ and $(\theta_{4\rho}-\theta_{1\rho})/\sqrt{2}$ both be unpinned? It could be either $(\theta_{1\rho},\phi_{1\rho})$ or $(\theta_{4\rho},\phi_{4\rho})$. However, any pinning basis field should be orthogonal to the pinning basis field $(2\theta_{1\rho}+\theta_{2\rho}+\theta_{3\rho})/\sqrt{6}$. Thus we conclude that $(\theta_{4\rho},\phi_{4\rho})$ is the gapless mode in this case. Besides $(2\theta_{1\rho}+\theta_{2\rho}+\theta_{3\rho})/\sqrt{6}$, the interaction $\psi^\dagger_{R1\alpha}\psi^\dagger_{R2\bar{\alpha}}\psi_{L1\alpha}\psi_{L3\bar{\alpha}}$ also contains another charge boson field $\phi^{\rho-}_{23}$. Then we should assume that $\phi^{\rho-}_{23}$ is also pinned by this relevant interaction. We find that orthogonal matrix representing the basis in the charge channel should be

$$R_\rho=\begin{pmatrix} 0 & 0 & 0 & 1\\ 2/\sqrt{6} & 1/\sqrt{6} & 1/\sqrt{6} & 0\\ 0 & 1/\sqrt{2} & -1/\sqrt{2} & 0\\ 1/\sqrt{3} & -1/\sqrt{3} & -1/\sqrt{3} & 0\end{pmatrix}. \tag{2.40}$$

With the condition that $(\theta_{4\rho},\phi_{4\rho})$ is gapless and $(2\theta_{1\rho}+\theta_{2\rho}+\theta_{3\rho})/\sqrt{6}$ and $\phi^{\rho-}_{23}$ are pinned, the only possible pairing operator that might have power-law correlations correspond to $a=4$ in Eq. (2.24). In addition we must assume that $\theta_{4\sigma}$ is also pinned. Now we should check the $4k_F$ density operators.

For case (2): We first consider the case when two indices in Eq. (2.26) and (2.27) are the same, giving Eq. (2.32)-(2.35). The correlation functions of Eq. (2.34) and (2.35) will decay exponentially because $(2\theta_{1\rho}+\theta_{2\rho}+\theta_{3\rho})/\sqrt{6}$ is pinned. Due to the $\phi^{\rho-}_{jk}$ term in Eq. (2.32) and (2.33), we can only choose $\{j,k\}=\{2,3\}$. The index i could be either 1 or 4. For $i=4$, the correlation functions of Eq. (2.32) and (2.33) could decay with a power-law if and only if $(\theta_{1\rho}-\theta_{2\rho}-\theta_{3\rho})/\sqrt{3}$ is also pinned, which requires an extra condition on the Fermi momenta but it's possible. The point here is that the corresponding wave-vector is $k_{F2}+k_{F3}+2k_{F4}$ and it only corresponds to $2\pi n$ if $k_{F1}=k_{F4}$. However, we started with the condition $2k_{F1}+k_{F2}+k_{F3}=2\pi$, which implies $k_{F1}-k_{F4}=2\pi-2\pi n\neq 0$. Therefore, there are no stripes in that case. For $i=1$, Eq. (2.32) and (2.33) correspond to the wave-vector $2k_{F1}+k_{F2}+k_{F3}=2\pi$, which doesn't correspond to that of stripes, either.

For case (3): Let's check the $4k_F$ density operator reducing to Eq. (2.36)-(2.39) with two pairs of indices the same. In order to have power-law decaying correlation functions, these operators should contain the gapless mode $(\theta_{4\rho},\phi_{4\rho})$, that is, one of $\{i,j\}$ should be 4. Then Eq. (2.37), (2.38) and (2.39) will have exponentially decaying correlations since they contain the dual of the pinned boson, $(2\theta_{1\rho}+\theta_{2\rho}+\theta_{3\rho})/\sqrt{6}$ or $\theta_{4\sigma}$. The correlation function of Eq. (2.36) with $\{i,j\}=\{1,4\}$ can decay with a power-law if $(\theta_{1\rho}-\theta_{2\rho}-\theta_{3\rho})/\sqrt{3}$ is pinned. So what's the interaction we need to pin the field $(\theta_{1\rho}-\theta_{2\rho}-\theta_{3\rho})/\sqrt{3}$? We started with the interaction $\psi^\dagger_{R1\alpha}\psi^\dagger_{R2\bar{\alpha}}\psi_{L1\alpha}\psi_{L3\bar{\alpha}}$ and $(2\theta_{1\rho}+\theta_{2\rho}+\theta_{3\rho})/\sqrt{6}$ and $\phi^{\rho-}_{23}$ are pinned. Is it possible that $(2\theta_{1\rho}+\theta_{2\rho}+\theta_{3\rho})/\sqrt{6}$,$\phi^{\rho-}_{23}$ and $(\theta_{1\rho}-\theta_{2\rho}-\theta_{3\rho})/\sqrt{3}$ are all pinned? It's possible if there is another relevant interaction involving the the fields $(\theta_{1\rho}-\theta_{2\rho}-\theta_{3\rho})/\sqrt{3}$ but not involving $\phi^{\rho-}_{23}$. This means that the θ field in that interaction must be orthogonal to $\phi^{\rho-}_{23}$ but not orthogonal to $(\theta_{1\rho}-\theta_{2\rho}-\theta_{3\rho})/\sqrt{3}$. The θ field in that

interaction also has to be orthogonal to the gapless mode $(\theta_{4\rho}, \phi_{4\rho})$. Then the interaction containing $\theta_{23}^{\rho+}$, such as $\psi_{R2\alpha}^{\dagger}\psi_{R2\bar{\alpha}}^{\dagger}\psi_{L3\bar{\alpha}}\psi_{L3\alpha}$, is what we need. This interaction can appear in the Hamiltonian if the condition $k_{F2} + k_{F3} = \pi$ is satisfied. However, the necessary condition that the $4k_F$ density operator with $\{i, j\} = \{1, 4\}$ can correspond to stripes is $\{k_{F1}, k_{F4}\} = \{k_{F2}, k_{F3}\}$. This will lead to the contradiction that $k_{F1}+k_{F2}+k_{F3}+k_{F4} = 2\pi \neq 2\pi n$. For the choices $\{i, j\} \neq \{1, 4\}$ in Eq. (2.36), the correlation functions of Eq. (2.36) will decay exponentially since $\phi_{23}^{\rho-}$ is pinned.

In this subsection, we have shown that pairing and stripes can't coexist when the gapless mode is $(\theta_{4\rho}, \phi_{4\rho})$ and at least one Fermi momentum condition $2k_{F1}+k_{F2}+k_{F3} = 2\pi$ is satisfied.

2.2.3 More Than One New Interaction

In the above discussion, although more than one Fermi momentum renormalization condition is allowed to occur, we always implicitly assume that the new interaction associated with the first Fermi momentum renormalization condition is the most relevant one. This assumption is related to how we determine the basis field. We always choose the basis fields guided by the interactions. For example, if the interaction $\psi_{R1\alpha}^{\dagger}\psi_{R1\bar{\alpha}}^{\dagger}\psi_{L2\bar{\alpha}}\psi_{L2\alpha}$ is relevant, then $\theta_{12}^{\rho+}$ will be pinned. Whether $\theta_{12}^{\rho+}$ is an element of the pinning basis is the issue here. If $\theta_{12}^{\rho+}$ is not a basis field, $\theta_{12}^{\rho+}$ should be expressed in terms of the combination of the pinning basis fields. If the interaction $\psi_{R1\alpha}^{\dagger}\psi_{R1\bar{\alpha}}^{\dagger}\psi_{L2\bar{\alpha}}\psi_{L2\alpha}$ is the most relevant interaction, there is no reason to write $\theta_{12}^{\rho+}$ in terms of other fields and we will choose $\theta_{12}^{\rho+}$ as an element of the pinning basis fields. However, what if the interactions such as $\psi_{R1\alpha}^{\dagger}\psi_{R1\bar{\alpha}}^{\dagger}\psi_{L2\bar{\alpha}}\psi_{L2\alpha}$ and $\psi_{R1\alpha}^{\dagger}\psi_{R1\bar{\alpha}}^{\dagger}\psi_{L3\bar{\alpha}}\psi_{L3\alpha}$ both appear in the Hamiltonian and are equally relevant? We know that $\theta_{12}^{\rho+}$ and $\theta_{13}^{\rho+}$ should be pinned but how do we choose the pinning basis? First of all, since $\Theta_{1\rho}$ is unpinned, then $\theta_{34}^{\rho+}$ and $\theta_{24}^{\rho+}$ are also unpinned. Then the gapless mode is $(\theta_{4\rho}, \phi_{4\rho})$ in this case. Now we can obtain the other three pinning basis fields by applying an orthogonal transformation to the band boson fields $\theta_{1\rho}$, $\theta_{2\rho}$ and $\theta_{3\rho}$. Rewrite $\theta_{12}^{\rho+}$ and $\theta_{13}^{\rho+}$ in terms of the pinning basis fields and see which pinning basis fields should be pinned. However, there are three basis fields but only two constraints ($\theta_{12}^{\rho+}$ and $\theta_{13}^{\rho+}$ are pinned). To get a C1S0 phase, we need another interaction. Is it possible to pin a ϕ field in this case? If such charge ϕ field exists, it has to be orthogonal to $\theta_{12}^{\rho+}$ and $\theta_{13}^{\rho+}$. Due to the charge conservation, any pinned charge ϕ field also has to be orthogonal to $\Phi_{1\rho}$. This is impossible for the ϕ field obtained from the linear combination of $\phi_{1\rho}, \phi_{2\rho}$ and $\phi_{3\rho}$. So the third pinned charge field is also a θ field.

Now comes the question: Is it possible that pairing and stripes can coexist under the condition when $(\theta_{4\rho}, \phi_{4\rho})$ is gapless and all three pinned charge boson are θ fields? The charge fields in the $4k_F$ density operators Eq. (2.36)-(2.37) are θ fields. The pair operator Eq. (2.24) with the choice $a = 4$, has no other θ dependent charge fields since the gapless mode $\phi_{4\rho}$ is the only charge field in Eq. (2.24). Then the correlation functions of Eq. (2.36)-(2.37) and Eq. (2.24) may decay with a power-law at the same time. Indeed, this is what happens. However, in order to pin three θ fields, three conditions on Fermi

momenta regarding the band indices $\{1,2,3\}$, such as $k_{F1}+k_{F2}=\pi$, $k_{F1}+k_{F3}=\pi$ and $k_{F2}=k_{F3}$, or $k_{F1}+k_{F2}=\pi$, $k_{F1}=k_{F3}$ and $k_{F2}=k_{F3}$ etc, need to be satisfied. Recall that $4\bar{k}_F=2\pi n$ is always satisfied. We also needs one additional Fermi momentum renormalization condition so that the wave-vectors of Eq. (2.36) and (2.37) correspond to $4\bar{k}_F$. There are five equations to solve four unknown Fermi momenta. We find there is no solution for all the possible cases. Thus pairing and stripes can't coexist in these situations.

2.2.4 New Interactions Due to Other Conditions

There are four more types of Fermi momentum renormalization conditions that can lead to the presence of new interactions that may pin the boson orthogonal to $\Theta_{1\rho}$. They are:

$$3k_{Fi}+k_{Fj} = 2\pi, \tag{2.41}$$
$$2k_{Fi}-k_{Fj}+k_{Fk} = 0 \text{ or } 2\pi, \tag{2.42}$$
$$3k_{Fi}-k_{Fj} = 0 \text{ or } 2\pi, \tag{2.43}$$
$$k_{Fi}+k_{Fj}+k_{Fk}-k_{Fl} = 0 \text{ or } 2\pi, \tag{2.44}$$

where the indices i,j,k and l are all different. Although these conditions will make some interactions non-oscillating, they can't be relevant since they will inevitably contain some charge boson and its dual at the same time, in other words, $\vec{u}_{\rho n}\cdot\vec{v}_{\rho n}\neq 0$ for these interactions.

This can be seen easily. According to our convention to define the boson fields, we know that the relation between chiral fermions and charge bosons are:

$$\varphi_{Ri\alpha} = \frac{1}{2\sqrt{2}}(\theta_{i\rho}+\phi_{i\rho}+\cdots), \tag{2.45}$$
$$\varphi_{Li\alpha} = \frac{1}{2\sqrt{2}}(\theta_{i\rho}-\phi_{i\rho}+\cdots). \tag{2.46}$$

When Eq. (2.41) is satisfied, the interaction like $\psi^\dagger_{Ri\alpha}\psi_{Li\alpha}\psi^\dagger_{Ri\bar{\alpha}}\psi_{Lj\bar{\alpha}}$ (or i and j exchanged) can appear in the Hamiltonian. However, this interaction contains $(-3\theta_{i\rho}+\theta_{j\rho})$ and $(-\phi_{i\rho}+\phi_{j\rho})$ which are not orthogonal to each other. Thus, it can not be relevant since a field and its dual can't be both pinned.

As for Eq. (2.42), (2.43) and (2.44), the corresponding interactions will have unequal numbers of right and left chiral fermions. For right moving fermions $\psi_{Ri\alpha}$, is associated with the Fermi momentum $+k_{Fi}$ while $-k_{Fi}$ is associated with the left moving fermions $\psi_{Li\alpha}$. Eq. (2.42), (2.43) and (2.44) are composed of three positive and one negative Fermi momentum. Therefore, the corresponding four fermion interactions with zero charge must contain three right and one left (or three left and one right) moving fermion fields. These interactions will inevitably result in $\vec{u}_{\rho n}\cdot\vec{v}_{\rho n}\neq 0$ and as a consequence they can't be relevant.

At this point, we have finally completed the proof that pairing and stripes can't coexist even if the gapless mode is not the total charge field, assuming all four bands are partially filled.

2.3 Completely Empty or Filled Bands

Another possible type of stripe phase has one or more of the bands completely empty (or completely filled). We now show that a standard treatment of these phases does not lead to any with coexisting pairing and stripes. Suppose that two bands are completely empty. Without loss of generality, we may choose then to be bands 3 and 4 so that all the electrons go into bands 1 and 2. It then follows from Eq. (1.7) that

$$k_{F1} + k_{F2} = 2\pi n = 2\pi(1-\delta). \tag{2.47}$$

So stripes, i.e. Friedel oscillations at wave-vector $2\pi n$, corresponds to $2k_F$ oscillations in the effective 2-band model. There are two cases to consider:

$$\psi^\dagger_{Li\alpha}\psi_{Ri\alpha} \sim e^{i\sqrt{2\pi}(\theta^\rho_i \pm \theta^\sigma_i)} \tag{2.48}$$

$$\psi^\dagger_{Li\alpha}\psi_{Rj\alpha} \sim e^{i\sqrt{\pi}\left(\theta^{\rho+}_{ij} - \phi^{\rho-}_{ij} \pm \theta^{\sigma+}_{ij} \mp \phi^{\sigma-}_{ij}\right)}. \tag{2.49}$$

For the above situation, we have $\{i,j\} = \{1,2\}$ in Eq. (2.48) and (2.49). Following the similar method, we can prove the incompatibility of pairing and $2k_F$ oscillations. If instead bands 3 and 4 are completely filled, Eq. (1.7) now implies:

$$k_{F1} + k_{F2} + 2\pi = 2\pi n, \tag{2.50}$$

but this is equivalent to the case of the two bands being empty since $\exp(2\pi i n x) = \exp[2\pi i(n-1)x]$ for any lattice site, x. If only one band (4) is empty (or filled) then stripes would correspond to oscillations at wave-vector $k_{F1} + k_{F2} + k_{F3}$ which can never occur since any operator which occurs in the continuum representation of the density operator must contain an even number of fermion fields. Similarly stripes could not occur in a phase with 3 empty (or filled) bands since this would require oscillations at k_{F1}.

2.4 Conclusion

Therefore, for the C1S0 phases with stripes, there is no pairing but bipairing occurs. In Sec. V we will discuss the case of small $t_{\perp,2}$, $V_{\perp,2}$ and the analogy with a 2-leg bosonic ladder. The bipairing correlation in the four-band fermion system may correspond to the boson pair superfluid (BPSF) phase in Ref. [84].

Now we would like to generalize this argument a little bit further. What about any other generalized charge two operators such as

$$\psi_{Ra\alpha}\psi_{Lb\bar{\alpha}}\psi^\dagger_{Li\alpha}\psi_{Rj\alpha} \sim e^{i\sqrt{\pi}[(\theta^{\rho-}_{ab}+\theta^{\rho+}_{ij})+(\phi^{\rho+}_{ab}-\phi^{\rho-}_{ij})\pm(\theta^{\sigma+}_{ab}+\theta^{\sigma+}_{ij})\pm(\phi^{\sigma-}_{ab}-\phi^{\sigma-}_{ij})]}? \tag{2.51}$$

Although the correlation amplitude should be smaller compared to the usual pairing operators, still, is it possible that such generalized pairing operators after renormalized by some density-like (charge neutral) operators can coexist with stripes? There will be a lot more such charge two operators since Eq. (2.24), (2.25) and other unconventional pair operators can be combined with any charge neutral operator, as long as in the end we have a non-chiral, spin zero and charge two operator. So far we have checked up to charge two operators composed of six fermions and concluded none of them can coexist with stripes as expected. But what about charge two operators composed of more fermions? This endless question may require another approach for its resolution. Instead, we will study the finite size spectrum of a C1S0 phase, from which a connection between charge operator and the lowest density oscillation is established.

Chapter 3

Finite Size Spectrum

In this Chapter, we relate the charge excitations and the smallest allowed density oscillation wave-vector by investigating the finite size spectrum. The low energy effective Hamiltonian in a C1S0 phase is simply that of a free boson.

$$H - \mu N_e = \frac{v_{1\rho}}{2} \int dx \left[K_{1\rho} (\partial_x \Phi_{1\rho})^2 + \frac{1}{K_{1\rho}} (\partial_x \Theta_{1\rho})^2 \right]. \tag{3.1}$$

In the rest of this subsection we only discuss the boson $\Phi_{1\rho}$ (and its conjugate boson $\Theta_{1\rho}$) so, for convenience, in this section we drop the superscript ρ and the subscript 1. Here $v\partial_x \Theta = K \partial_t \Phi = \Pi$, where Π is the canonical momentum variable conjugate to Φ. It is natural to regard Φ as a periodic variable. Consider first a pairing phase where a charge two operator:

$$\Delta(x) \sim e^{i\sqrt{\frac{\pi}{2}}\Phi}, \tag{3.2}$$

has power law decay. Only keeping operators in the low energy Hilbert space which exhibit power-law decay , we expect that all such operators will have even charge, involving only the exponential of integer multiples of $i\sqrt{\frac{\pi}{2}}\Phi$. It is then natural to assume that we should make the periodic identification:

$$\Phi \leftrightarrow \Phi + 2\sqrt{2\pi}. \tag{3.3}$$

That is to say, we regard $\sqrt{\pi/2}\Phi$ as an angular variable. We now wish to argue that consistent quantization of the free boson requires that Θ also be regarded as a periodic variable with:

$$\Theta \leftrightarrow \Theta + \sqrt{\frac{\pi}{2}}. \tag{3.4}$$

As we shall see, this, in turn implies that the minimum Friedel oscillation wavevector is $8\bar{k}_F$. Alternatively, in a bipairing phase, the lowest dimension charge operators is $\exp[i\sqrt{2\pi}\Phi_1^\rho]$ and it is now natural to identify

$$\Phi \leftrightarrow \Phi + \sqrt{2\pi}. \tag{3.5}$$

We then will argue that consistent quantization requires:

$$\Theta \leftrightarrow \Theta + \sqrt{2\pi}, \tag{3.6}$$

which we will show implies that the minimum Friedel oscillation wavevector is $4\bar{k}_F$. This approach confirms the conclusions arrive at by more pedestrian means in the previous

sub-section. As a biproduct of this discussion, we will derive the finite size spectrum, with both periodic and open BCs, in both pairing and bipairing (stripe) phases.

First consider a C1S0 pairing phase. We place the system in a box of size L with periodic boundary conditions. The mode expansion for $\Phi(t,x)$ takes the form:

$$\begin{aligned}\Phi(t,x) &= \Phi_0 + 2\sqrt{2\pi}m\frac{x}{L} + \sqrt{\frac{\pi}{2}}\frac{p}{K}\frac{vt}{L} + \\ &\sum_{k=1}^{\infty}\sqrt{\frac{1}{4\pi kK}}\left(a_{Rk}e^{-i(2\pi k/L)(vt-x)} + a_{Lk}e^{-i(2\pi k/L)(vt+x)} + h.c.\right). \qquad (3.7)\end{aligned}$$

Here m and p are arbitrary integers; a_{Rk} and a_{Lk} are bosonic annihilation operators for right and left movers. The normalization of the mx/L term in the expansion is determined by the periodic BCs and the identification Eq. (3.3). i.e. $\Phi(L) = \Phi(0) + 2\sqrt{2\pi}m$ is equivalent to PBC using Eq. (3.3). The (very important) normalization of the vt/L term requires more explanation. We may think of this term as being proportional to a zero mode conjugate momentum operator $\hat{\Pi}_0$, which is canonically conjugate to $\hat{\Phi}_0$:

$$[\Phi_0, \Pi_0] = i, \qquad (3.8)$$

$$\Phi(t,x) = \Phi_0 + \frac{\hat{\Pi}_0 vt}{KL} + \ldots \qquad (3.9)$$

$\hat{\Pi}_0$ is the zero momentum Fourier mode of the conjugate momentum field $\Pi(x)$:

$$\hat{\Pi}_0 \equiv \int_0^L \Pi(x). \qquad (3.10)$$

The $\hat{\Pi}_0 vt/(KL)$ term in the mode expansion for Φ is necessary in order that the canonical commutation relations are obeyed:

$$[\Phi(x), \partial_t\Phi(y)] = \frac{i}{KL}\sum_{k=-\infty}^{\infty} e^{i(2\pi k/L)(x-y)} = \frac{i}{K}\delta_P(x-y), \qquad (3.11)$$

where $\delta_P(x-y)$ is the periodic Dirac δ-function. The $k=0$ term in this Fourier expansion of the δ-function comes from the commutator in Eq. (3.8). Comparing the mode expansion in Eq. (3.7) to (3.9), we see that the eigenvalues of the canonical momentum operator, $\hat{\Pi}_0$ are:

$$\Pi_0 = \sqrt{\frac{\pi}{2}}p, \qquad (3.12)$$

for integer p. That these are the correctly normalized eigenvalues follows from the fact that the wave-functionals contain factors of the form:

$$\Psi(\Phi_0) = e^{i\Pi_0\Phi_0} = e^{i\sqrt{\frac{\pi}{2}}p\Phi_0}. \qquad (3.13)$$

These wave-functions are single-valued under the identification of Eq. (3.3). The eigenvalues of $\hat{\Pi}_0$, i.e. the normalization of the vt/L term in the mode expansion of Eq. (3.7) determines the charge quantum numbers of all low-lying states in the spectrum with periodic boundary conditions. This follows from observing that the total electron number operator is:

$$\hat{N}_e = \frac{2K}{v}\sqrt{\frac{2}{\pi}}\int_0^L dx \partial_t \Phi. \tag{3.14}$$

This in turn can be checked by confirming that:

$$[\hat{N}_e, \Delta] = 2\Delta, \tag{3.15}$$

where Δ is the charge-2 operator in Eq. (3.2). The mode expansion of Eq. (3.7) then implies that the charges of all states in the low energy spectrum are:

$$N_e = 2p, \tag{3.16}$$

even integers. This is an example of the general one-to-one correspondence between operators and states in the finite size spectrum with PBC in a conformal field theory. In a phase in which all operators have even charge, all states in the spectrum also have even charge.

We can go further and deduce the Friedel oscillation wavevector from the normalization of the vt/L term in Eq. (3.7). This can be done by using $K\partial_t\Phi = v\partial_x\Theta$, $\partial_t\Theta = vK\partial_x\Phi$, to deduce the mode expansion for the field $\Theta(t,x)$:

$$\begin{aligned}\Theta(t,x) &= \Theta_0 + \sqrt{\frac{\pi}{2}}p\frac{x}{L} + 2\sqrt{2\pi}Km\frac{vt}{L} \\ &\quad + \sum_{k=1}^{\infty}\sqrt{\frac{K}{4\pi k}}\left(-a_{Rk}e^{-i(2\pi k/L)(vt-x)} + a_{Lk}e^{-i(2\pi k/L)(vt+x)} + h.c.\right). \end{aligned}\tag{3.17}$$

From this mode expansion we see that Θ is periodically identified as in Eq. (3.4). Insert Eq. (3.7) and (3.17) into the Hamiltonian (3.1), we obtain the finite size spectrum of a pairing phase with PBC:

$$E - 2\mu p = \frac{2\pi v}{L}\left[2Km^2 + \frac{p^2}{8K} + \sum_{k=1}^{\infty}k(n_{Lk} + n_{Rk})\right], \tag{3.18}$$

where n_{Lk} and n_{Rk} are the occupation numbers for the left and right moving states of momentum $\pm 2\pi k/L$.

Now consider the Friedel oscillations. Oscillations at wave-vector of the form $2n\bar{k}_F$ (actually a sum of any $2n$ of the k_{Fi}'s) can only occur if some operator of the form $(\psi_R^\dagger\psi_L)^n$ has power law decay. Upon bosonizing, all such operators are expressed as $\exp\left(i\sqrt{\pi/2}n\Theta_1^\rho\right)$ multiplied by an exponential involving only pinned boson fields. However, not all such operators can occur in the low energy spectrum since they must respect

the periodic identification in Eq. (3.4). The lowest dimension operator allowed by this identification has $n = 4$ corresponding to $8\bar{k}_F$ oscillations. Again we are effectively using the relationship between the finite size spectrum and the operator content. The $n = 4$ operator corresponds to the $p = 1$ state in the mode expansion of Eq. (3.17).

Now consider a bipairing phase where there are no charge 2 operators in the low energy spectrum, the lowest charge being 4, corresponding to the operator $\exp[i\sqrt{2\pi}\Phi]$, leading to the periodicity condition on Φ in Eq. (3.5). The mode expansion for Φ is therefore altered to:

$$\begin{aligned}\Phi(t,x) &= \Phi_0 + \sqrt{2\pi}m\frac{x}{L} + \sqrt{2\pi}\frac{p}{K}\frac{vt}{L} \\ &\quad + \sum_{k=1}^{\infty}\sqrt{\frac{1}{4\pi kK}}\left(a_{Rk}e^{-i(2\pi k/L)(vt-x)} + a_{Lk}e^{-i(2\pi k/L)(vt+x)} + h.c.\right). \quad (3.19)\end{aligned}$$

The coefficient of vt/L gets multiplied by a factor of 2 since the wave-functional $\exp[i\Pi_0\Phi_0]$ must now be invariant under the shift of Eq. (3.5), requiring the conjugate momentum, $\hat{\Pi}_0$ to have eigenvalues $\sqrt{2\pi}p$. Correspondingly the mode expansion for Θ becomes:

$$\begin{aligned}\Theta(t,x) &= \Theta_0 + \sqrt{2\pi}p\frac{x}{L} + \sqrt{2\pi}Km\frac{vt}{L} \\ &\quad + \sum_{k=1}^{\infty}\sqrt{\frac{K}{4\pi k}}\left(-a_{Rk}e^{-i(2\pi k/L)(vt-x)} + a_{Lk}e^{-i(2\pi k/L)(vt+x)} + h.c.\right), \quad (3.20)\end{aligned}$$

implying the periodic identification of Eq. (3.6). Now the lowest dimension Friedel oscillation operator with power law decay is $\exp(i\sqrt{2\pi}\Theta_1^\rho)$, which is a $4\bar{k}_F$ operator. The finite size spectrum of a bipairing phase with PBC is:

$$E - 4\mu p = \frac{2\pi v}{L}\left[\frac{K}{2}m^2 + \frac{p^2}{2K} + \sum_{k=1}^{\infty}k(n_{Lk} + n_{Rk})\right]. \quad (3.21)$$

These arguments show, based only on plausible assumptions about regarding the fields Φ_1^ρ and Θ_1^ρ as periodic variables, that C1S0 phases with pairing have $8\bar{k}_F$ oscillations (and hence no stripes) but phases with bipairing have $4\bar{k}_F$ oscillations, corresponding to stripes.

With OBC, the boundary conditions:

$$\Theta(0) = \text{constant}, \quad \Theta(L) = \text{constant}, \quad (3.22)$$

are applied. This sets the quantum number $m = 0$ and $a_{Rk} = a_{Lk}$ in the mode expansion of Eq. (3.17) and (3.20). Setting $Q = 2p$ for the pairing phase and $Q = 4p$ for the biparing phase, the finite size spectrum implied by these mode expansions and the Hamiltonian of Eq. (3.1) is:

$$E - \mu Q = \frac{\pi v}{L}\left[\frac{Q^2}{16K} + \sum_{k=1}^{\infty}kn_{Lk}\right], \quad (3.23)$$

where the charge, Q (measured from a reference point like half-filling) is restricted to all even integers in a pairing phase but is restricted to integer multiples of 4 in a bipairing phase. For even Q, in a bipairing phase, there is a gap Δ_E, to states with $Q/2$ odd, so we may write, for any even Q in a bipairing phase:

$$E - \mu Q = \Delta_E \frac{[1 - (-1)^{Q/2}]}{2} + O(\frac{1}{L}). \tag{3.24}$$

The parameters v, K, μ and Δ_E all vary with density. Nonetheless, this zigzag pattern of energies for even Q should allow unambiguous detection of a biparing phase for large enough L.

Chapter 4

RG For Doped 4-Leg Ladders

The combination of weak-coupling RG and bosonization is one standard tool to study the phase diagram of N-leg systems [85, 86, 87, 88, 89, 90]. The results for doped 4-leg ladder are mostly within the context of the Hubbard model [89, 90]. Here we will show that the stripe phase can be found in the special solution of RG equations. This phase doesn't have pairing but bipairing, which is consistent with our bosonization argument.

The first step is to determine the relevant couplings according to the RG flow since they will control which boson fields will get "pinned" and therefore will allow us to map out the phase diagram in terms of bare interactions and doping. However, to analyze the RG flow is a tricky task for there are 32 coupled nonlinear differential equations. It seems that RG ultimately flows onto a special set of solutions, corresponding to some direction in the multi-dimensional coupling constant space. These special solutions are called "fixed rays" and different rays usually indicate different phases [89]. Some fixed-ray solutions may correspond to phases with higher symmetry than the original Hamiltonian. Two-leg ladders at half-filling provide one example of such symmetry enhancement in the low energy limit [91]. Later on, some subleading corrections were found which make the RG flow deviate from the fixed ray. However, these subleading terms don't grow fast enough to really spoil the fixed ray in the undoped case but give some anomalous corrections to the gap functions, vanishing in the weak coupling limit [92, 93]. Things become dramatically different in the doped systems. Now these subleading terms are relevant perturbations for the fragile gapless modes. They will generate gaps although these may be much smaller compared to those driven by the "fixed ray". For example, the weak coupling RG phase diagram for doped two-leg ladders is modified after taking these terms into consideration [93]. Recently, a hidden potential structure of RG equations in ladder systems was discovered. Everything can be understood better within the framework of this "RG potential" which allows the RG flow to be viewed as the trajectory of a particle finding a minimum in the coupling constant space [92, 94]. Then the fixed ray is just like a "valley/ridge" in the "mountains" of the RG potential. The topography near the vicinity of such a "valley/ridge" will determine the stability of the fixed ray and give the exponents governing the subleading terms.

4.1 RG Potential and Its Implications

The method we discuss is very general but we mainly focus on $N = 4$. As the conventional starting point, we first diagonalize the hopping terms in Eq. (1.8) and obtain 4 bands.

Next we linearize each band around different Fermi points in the low energy limit, and introduce $SU(2)$ scalar and vector current operators

$$J_{ij}^{L/R} = \frac{1}{2}\,\psi_{L/Ri\alpha}^{\dagger}\,\psi_{L/Rj\alpha}\,, \quad \boldsymbol{J}_{ij}^{L/R} = \frac{1}{2}\,\psi_{L/Ri}^{\alpha\dagger}\,\vec{\sigma}_{\alpha}^{\beta}\,\psi_{L/Rj\beta}\,. \tag{4.1}$$

(Note the unconventional factor of 1/2 in the scalar operators, introduced for later convenience.) We can rewrite the interactions in Eq. (1.9) in terms of the current operators in Eq. (4.1):

$$\begin{aligned} H_{int} \;=\; & \tilde{c}_{ij}^{\rho} J_{ij}^{R} J_{ij}^{L} - \tilde{c}_{ij}^{\sigma} \boldsymbol{J}_{ij}^{R} \cdot \boldsymbol{J}_{ij}^{L} \\ & + \tilde{f}_{ij}^{\rho} J_{ii}^{R} J_{jj}^{L} - \tilde{f}_{ij}^{\sigma} \boldsymbol{J}_{ii}^{R} \cdot \boldsymbol{J}_{jj}^{L}, \end{aligned} \tag{4.2}$$

where $\tilde{f}_{ij}$ and $\tilde{c}_{ij}$ denote the forward and Cooper scattering amplitudes, respectively, between bands i and j. Many repeated indices appear in this section, such as i and j in Eq. (4.2) and they are always implicitly summed over. In Eq. (4.2), we only keep the Lorentz invariant interactions involving the product of a left current and a right current. The LL and RR terms don't contribute to the RG equations at second order and are expected to only shift the velocities of the various modes. Note that $\tilde{c}_{ii}$ and $\tilde{f}_{ii}$ describe the same vertex and we set $\tilde{f}_{ii} = 0$. Also, symmetries imply $\tilde{c}_{ij} = \tilde{c}_{ji}$ and $\tilde{f}_{ij} = \tilde{f}_{ji}$ [89]. That's how we get 32 different couplings in doped 4-leg ladders. Then one can derive RG equations by the operator product expansions of these $SU(2)$ scalar and vector current operators.

Provided that the RG equations are known [89], how to analyze the RG flow is still non-trivial since all the interactions in Eq. (4.2) are marginal at first glance. If one numbers all the couplings $\tilde{f}_{ij}$ and $\tilde{c}_{ij}$ and rename them as $\tilde{g}_i$ (i from 1 to 32), within the one-loop calculations, the coupled non-linear RG equations can be written in the concise form:

$$\frac{d\tilde{g}_i}{dl} = \tilde{M}_i^{jk}\,\tilde{g}_j\tilde{g}_k, \tag{4.3}$$

where g_i is some coupling and the coefficient matrices $\tilde{M}_i^{jk} = \tilde{M}_i^{kj}$ are symmetric in indices j and k by construction. [l is the logarithm of the ratio of a characteristic length scale to the lattice scale, $l \equiv \ln(L/a)$.] Recently, an unexpected potential structure of Eq. (4.3) was proven [92, 94]. After a proper rescaling to new couplings $g_i = \alpha_i\tilde{g}_i$, where α_i are constants, Eq. (4.3) can be reduced to

$$\frac{dg_i}{dl} = M_i^{jk}\,g_j g_k = -\frac{\partial V(\vec{g})}{\partial g_i}. \tag{4.4}$$

where M_i^{jk} is totally symmetric in indices i, j and k and $V(\vec{g})$ is the so called RG potential [92]. The scaling constants α_i and the explicit RG potential form can be found in Appendix B. It now provides a geometric picture for the RG flows of Eq. (4.4), which can be regarded as the trajectory of an overdamped particle searching for a potential minimum in the multi-dimensional coupling space. Thus, the ultimate fate of the flow

would either rest on the fixed points or flow along some directions as the "valleys/ridges" of the potential profile but there is only a trivial fixed point (all $\tilde{g}_i = 0$) within one-loop order.

Precisely, these directions are special sets of analytic solutions of Eq. (4.4):

$$g_i(l) = \frac{G_i}{l_d - l}, \tag{4.5}$$

if the constants G_i satisfy the algebraic constraint,

$$G_i = M_i^{jk} G_j G_k. \tag{4.6}$$

Eq. (4.5) is only valid for $l < l_d = \ln \xi/a$ where ξ is a characteristic length scale where the coupling constants become large. These special analytic solutions are referred to as "fixed rays" because they grow under RG with the fixed ratios. Sometimes, the specific ratios of the fixed ray reflect extra symmetry in the Hamiltonian and the fixed ray is called a "symmetric ray" [91].

In general, it's very unlikely that the bare values of $g_i(0)$ are proportional to the constants G_i. Then we have to check whether these fixed rays are stable against deviations [92]. As long as the deviations grow slower than Eq. (4.5), then the fixed ray is stable. Within the RG potential picture, the stability of each fixed ray is determined by the local topography along the direction.

In the vicinity of a fixed ray, there may be some small deviations away from it

$$g_i(l) = \frac{G_i}{l_d - l} + \Delta g_i(l), \tag{4.7}$$

where $\Delta g_i(l) \ll g_i(l)$. The equations which describe the deviations Δg_i are

$$\frac{d}{dl}(\Delta g_i) = \frac{B_{ij}}{l_d - l} \Delta g_j , \tag{4.8}$$

where $B_{ij} = 2M_{jk}^i G_k$. Since M_{jk}^i is totally symmetric in i, j and k, the matrix B_{ij} is symmetric in i and j. B_{ij} can be diagonalized by an orthogonal matrix O_{nm} so that Eq. (4.8) will decouple into independent equations,

$$\frac{d}{dl}(\delta g_n) = \frac{\lambda_n}{l_d - l} \delta g_n , \tag{4.9}$$

where $\delta g_n = O_{ni} \Delta g_i$, are the couplings after the linear transformation and λ_n are the eigenvalues of the matrix B_{ij}. If the initial bare couplings $\delta g_n(0) \ll G_n/l_d$, then the solutions of Eq. (4.9) are

$$\delta g_n(l) = \delta g_n(0) \left(\frac{l_d}{l_d - l}\right)^{\lambda_n} \sim \frac{G'_n}{(l_d - l)^{\lambda_n}}, \tag{4.10}$$

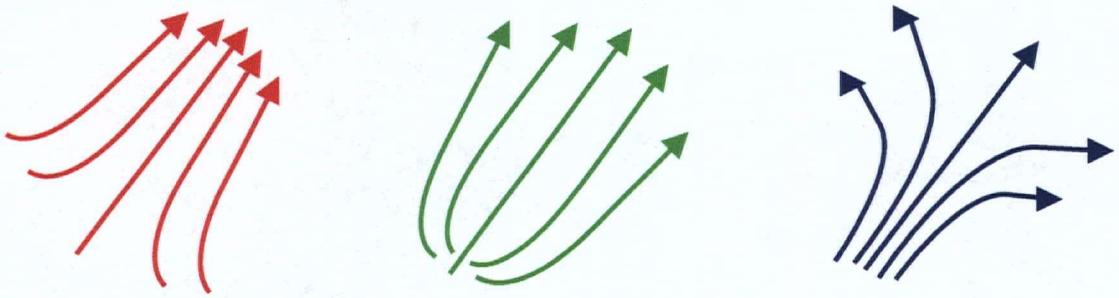

Figure 4.1: The topography of RG flows near the fixed ray with $\lambda \leq 0$, $0 < \lambda \leq 1$ and $\lambda > 1$. It's clear that the deviation is irrelevant for $\lambda \leq 0$ and relevant for $\lambda > 1$. The analysis of RG flow is more subtle for $0 < \lambda \leq 1$. In this case, although the deviation from fixed ray is growing, the fixed ratios still remain. Therefore, RG still flows onto the fixed ray but the phase is not only determined by the fixed ray couplings.

where $G'_n \sim O((U/t)^{1-\lambda_n})$ is generally non-universal depending on the initial couplings. Therefore, the appropriate ansatz for the RG flows should be

$$g_i(l) \simeq \frac{G_i}{l_d - l} + \frac{O_{in} G'_n}{(l_d - l)^{\lambda_n}}, \tag{4.11}$$

$$\simeq \frac{G_i}{l_d - l} + \frac{G''_i}{(l_d - l)^{\lambda_i^{\max}}} + \cdots, \tag{4.12}$$

where $\lambda_i^{\max}$ in Eq. (4.12) is the largest one among the λ_n's with nonzero coefficients $O_{in} G'_n \equiv G''_i$ and the divergent behavior is dominated by $\lambda_i^{\max}$. Although Eq. (4.12) is derived from the stability analysis near the fixed ray, it turns out to be the general behavior of the RG flow but the values of some $\lambda_i^{\max}$ may vary from the eigenvalues of B_{ij} when away from the fixed ray. In fact, such power-law divergent solutions were suggested before [88, 89] but the analysis only focused on the most relevant terms with exponent one, i.e. $G_i \neq 0$ terms . Note that Eq. (4.12) is still not the exact solutions of RG equations but it captures the divergent part correctly and is enough to determine the phase diagram.

For $\lambda_i^{\max} < 0$, these deviations are irrelevant whereas if $\lambda_i^{\max} > 1$, the deviations grow faster than the fixed ray, so that the phase associated with the fixed ray is fragile. For $0 < \lambda_i^{\max} \leq 1$, the deviations actually grow although not strongly enough to spoil the asymptotic fixed ray, as illustrated in Fig. (4.1). Nevertheless, it doesn't mean they won't affect anything since they are also relevant couplings in the conventional classification but just less relevant than the fixed ray ones.

The effects of these subleading divergent terms on the RG flow of a particular coupling g_i are dramatically different depending on whether $G_i = 0$ or not. We can separate the effective Hamiltonian at the cutoff length scale into the most relevant fixed ray part and the subleading deviations as a perturbation. For $G_i \neq 0$, g_i is relevant and it will lead to a gap. The subleading perturbations will not destroy the original ground state but only modify the gap function by giving rise to anomalous scaling [92]. On the other hand, if $G_i = 0$, the subleading perturbations become important if $0 < \lambda_i^{\max}$ and will generate a small but non-zero gap for some of the initial gapless modes. Note that only when initial deviations away from the fixed ray are small, are $\lambda_i^{\max}$ universal and can they be obtained from the eigenvalues of $B_{ij} = 2M^i_{jk}G_k$.

In fact, we can numerically solve the RG equations using the standard solver in Mathematica. However, from numerical solutions of the RG equations we find that interaction couplings always diverge with the power law behavior like Eq. (4.12) even though $\lambda_i^{\max}$ is not the same as an eigenvalue of B_{ij}. We can extract $\lambda_i^{\max}$ directly from the numerical solution of the RG equations for those terms with $G_i = 0$ and thus determine the phase diagram from these relevant interactions. Surprisingly, as we will see in the following sub-sections, the fixed ray and subleading terms with universal $\lambda_i^{\max}$ from B_{ij} already are sufficient to determine the pinned bosons uniquely within bosonization.

To recap, even in the weak-coupling RG analysis, there are different energy scales. The fixed ray only represents the most relevant couplings. The subleading couplings should be treated as perturbations to the effective Hamlitonian corresponding to the fixed ray and they are relevant enough to drive the effective Hamiltonian into a phase in which the fragile gapless modes become gapped but these gaps are small compared to those driven by the fixed ray couplings.

4.2 The Stripe Phase

Now we know the ultimate fate of weak coupling RG must be a fixed ray due to the existence of RG potential [92, 94]. The fixed ray indicates a direction in which the interactions will be renormalized in the strong coupling region. If one can survey all the fixed ray solutions in Eq. (4.6) and the corresponding subleading terms determined by the topography, then in principle all the phases in the weak coupling RG are obtained. Following this idea, here we try to find the fixed ray whose corresponding phase gives the stripe density oscillations. It turns out that following fixed ray will do so:

$$\begin{aligned}
\sqrt{2}c^{\rho}_{11} &= \sqrt{2}c^{\rho}_{44} = -\frac{c^{\rho}_{14}}{2} = \frac{c^{\sigma}_{14}}{2\sqrt{3}} = -f^{\rho}_{14} = \frac{f^{\sigma}_{14}}{2\sqrt{3}} = \\
\sqrt{2}c^{\rho}_{22} &= \sqrt{2}c^{\rho}_{33} = -\frac{c^{\rho}_{23}}{2} = \frac{c^{\sigma}_{23}}{2\sqrt{3}} = -f^{\rho}_{23} = \frac{f^{\sigma}_{23}}{2\sqrt{3}} = -\frac{1}{16(l_d - l)}.
\end{aligned} \tag{4.13}$$

Eq. (4.13) will be the solution of Eq. (4.6) if $v_1 = v_4$ and $v_2 = v_3$. So if RG really flows onto this fixed ray from some initial set of bare couplings, the interpretation is the fermi

velocities get renormalized in the corresponding phase [91]. The upper and lower line in Eq. (4.13) correspond to the CDW fixed ray on effective 2-leg systems composed of band pairs (1,4) and (2,3), respectively. In principle, the fixed ray as the permutation of band indices in Eq. (4.13) also exists. The reason why we favor Eq. (4.13) is motivated by the fixed ray Eq. (4.19), found in the Hubbard model as we will see in the later sections.

Now we know that the fixed ray solution isn't the whole story for the RG flow. The phase should be determined by all the relevant interactions, including the subleading divergent ones. As long as G_i is given by the Eq. (4.13) and with the known RG matrix M_i^{jk}, then the largest divergent exponent $\lambda_i^{\max}$ can be deduced analytically from the eigenvalues and eigenvectors of the matrix $B_{ij} = 2M_{jk}^i G_k$ in the vicinity of the fixed ray. There are two 5/8, four 1/2, four 1/8, four $-1/2$, two $-3/8$, and 0s for the eigenvalues λ_n of B_{ij}. The couplings are divergent for $\lambda_n > 0$ even though they are small compared to the fixed ray in the critical region. We should take more care about the terms with eigenvalues 5/8, 1/2 and 1/8. To see what's their influence, we have to know the direction corresponding to δg_n, Eq. (4.10), in the multi-dimensional space expanded in the coupling basis Δg_i. The eigenvectors of B_{ij} give this information. The subleading terms δg_n corresponding to two $\lambda_n = 5/8$ eigenvectors are in the directions having non-zero projection on $c_{12}^\rho, c_{13}^\rho, c_{24}^\rho, c_{34}^\rho, c_{12}^\sigma, c_{13}^\sigma, c_{24}^\sigma$, and c_{34}^σ. The eigenvectors of those corresponding to four $\lambda_n = 1/2$ have components on $c_{11}^\rho, c_{22}^\rho, c_{33}^\rho, c_{44}^\rho, c_{14}^\rho, c_{23}^\rho, c_{11}^\sigma, c_{22}^\sigma, c_{33}^\sigma, c_{44}^\sigma, c_{14}^\sigma, c_{23}^\sigma, f_{14}^\rho, f_{23}^\rho, f_{14}^\sigma$ and f_{23}^σ. The terms with $\lambda_n = 1/8$ have components on $c_{12}^\rho, c_{13}^\rho, c_{24}^\rho, c_{34}^\rho, c_{12}^\sigma, c_{13}^\sigma, c_{24}^\sigma$, and c_{34}^σ. Provided with this information, we know the largest divergent exponent for each coupling, that is, $\lambda_i^{\max}$ for the non-fixed ray couplings. Table (4.1) summarizes λ_n and the projections of corresponding δg_n in terms of coupling basis g_i.

	nonzero component
5/8	$c_{12}^\rho, c_{13}^\rho, c_{24}^\rho, c_{34}^\rho, c_{12}^\sigma, c_{34}^\sigma$
5/8	$c_{12}^\rho, c_{13}^\rho, c_{24}^\rho, c_{34}^\rho, c_{13}^\sigma, c_{24}^\sigma$
1/2	$c_{11}^\rho, c_{44}^\rho, c_{14}^\rho, c_{11}^\sigma, c_{44}^\sigma, f_{14}^\rho, f_{14}^\sigma$
1/2	$c_{22}^\rho, c_{33}^\rho, c_{23}^\rho, c_{22}^\sigma, c_{33}^\sigma, f_{23}^\rho, f_{23}^\sigma$
1/2	$c_{14}^\rho, c_{11}^\sigma, c_{44}^\sigma, c_{14}^\sigma$
1/2	$c_{23}^\rho, c_{22}^\sigma, c_{33}^\sigma, c_{23}^\sigma$
1/8	c_{12}^ρ, c_{34}^ρ
1/8	c_{13}^ρ, c_{24}^ρ
1/8	$c_{12}^\sigma, c_{34}^\sigma$
1/8	$c_{13}^\sigma, c_{24}^\sigma$

Table 4.1: This table summarizes the topography in the vicinity of the fixed ray Eq.(4.13). It shows the eigenvalues $\lambda_n > 0$ of the matrix B_{ij} and their corresponding eigen-direction in terms of the RG couplings.

Now we would like to check numerically whether the RG will really flow onto this fixed ray Eq. (4.13). It's very illuminating to plot $\log[|g_i(l)|]$ v.s. $\log[(l_d - l)]$ from the numerical solution of the RG equations, where the absolute value makes sure there won't

be problems for those with $G_i < 0$. In the scaling region, if Eq. (4.12) is correct, then we should see a straight line for each coupling $g_i(l)$, whose slope indicates the exponent controlling the divergence. The slopes will be negative one for the fixed ray, $-\lambda_i^{\max}$ for the subleading terms and zero for irrelevant terms.

If we choose the initial bare couplings with the ratios in Eq. (4.13) and with Fermi velocities $v_1 = v_4$ and $v_2 = v_3$, we do find all the couplings grow with the fixed ratios under RG flow toward the fixed ray Eq. (4.13). In order to see the subleading terms, we add some small deviations to the initial bare couplings and Fermi velocity. The log-log plot of each coupling agrees very well with the predicted slopes in Table (4.1). A few selected examples are shown in Fig.(4.2).

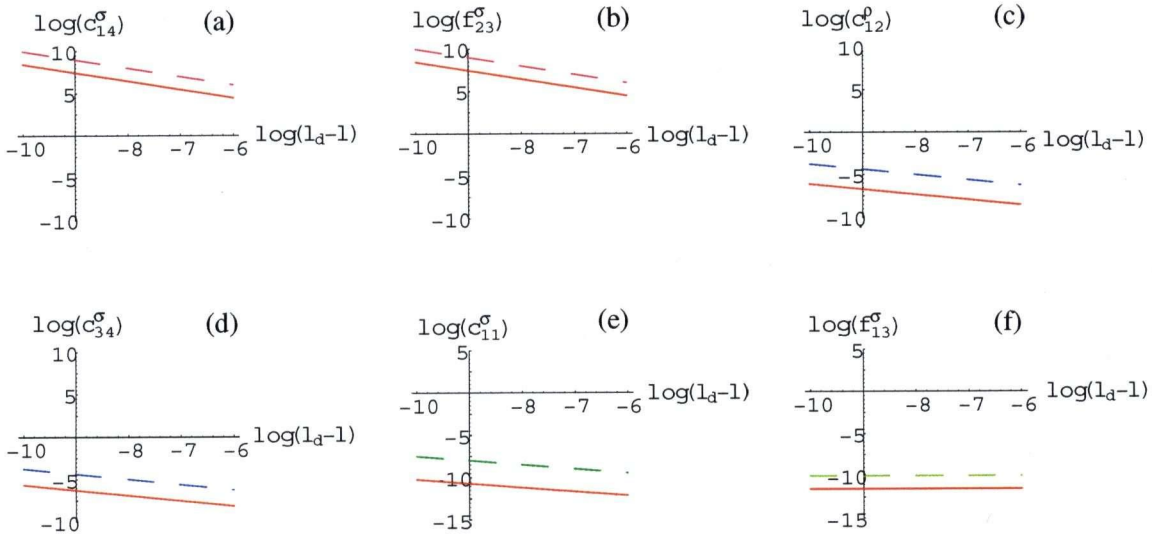

Figure 4.2: This is the $\log[|g_i(l)|]$ v.s. $\log[(l_d - l)]$ plot for several typical couplings of stripe fixed ray Eq. (4.13). The slopes give us the divergent exponent for each coupling. The solid (red) lines are the numerical solutions for the RG equations. The dashed lines are pure straight lines as reference with the predicted $\lambda_i^{\max}$: 1 (pink: c_{14}^{σ} (a), f_{23}^{σ} (b)), 5/8 (blue: b_{12}^{ρ} (c), c_{34}^{σ} (d)), 1/2 (green: c_{11}^{σ} (e)), and 0 (yellow: f_{13}^{σ} (f)), respectively. In this case, the numerical solutions agree very well with the prediction for all the couplings.

Although the subleading terms are also divergent for $0 < \lambda_i^{\max} < 1$, they are still small compared to the fixed ray couplings. Therefore, we treat the subleading couplings as the perturbations to the effective Hamiltonian corresponding to Eq. (4.13) in the bosonization method.

We bosonize the relevant couplings to determine the phase diagram. The fully bosonized form of Eq. (4.2) is

$$H_{int} = \frac{1}{4}\sum_i \tilde{c}_{ii}^{\sigma} \cos(\sqrt{8\pi}\theta_{i\sigma})$$

$$+\frac{1}{4}\sum_{i\neq j}[(\tilde{c}^{\rho}_{ij}+\tilde{c}^{\sigma}_{ij})\cos\sqrt{4\pi}\phi^{\rho-}_{ij}\cos\sqrt{4\pi}\theta^{\sigma-}_{ij}+2\tilde{c}^{\sigma}_{ij}\cos\sqrt{4\pi}\phi^{\rho-}_{ij}\cos\sqrt{4\pi}\theta^{\sigma+}_{ij}$$
$$+(\tilde{c}^{\rho}_{ij}-\tilde{c}^{\sigma}_{ij})\cos\sqrt{4\pi}\phi^{\rho-}_{ij}\cos\sqrt{4\pi}\phi^{\sigma-}_{ij}-2\tilde{f}^{\sigma}_{ij}\cos\sqrt{4\pi}\phi^{\sigma-}_{ij}\cos\sqrt{4\pi}\theta^{\sigma+}_{ij}], \quad (4.14)$$

where these bosons fields are defined in Eq. (1.26). Since $\tilde{c}^{\rho}_{ii}$ and $\tilde{f}^{\rho}_{ij}$ only contribute to the gradient terms, they are not important here. The reason we express the Hamiltonian by the tilded interactions $\tilde{c}$, $\tilde{f}$ and Eq.(1.26) is only for convenience of notation. We emphasize that the basis of boson fields should be determined by the hierarchy of relevant interactions. In other words, the relevant interactions should not only tell us what boson fields are pinned but also the basis in terms of which they are pinned.

At some intermediate length scale, the most relevant interactions, those in Eq. (4.13), are large but the others, including the subleading terms, are still small compared to them. In order to minimize Eq. (4.14), the most relevant couplings in Eq. (4.13) will pin the values of $\phi^{\rho-}_{14}, \phi^{\rho-}_{23}, \theta^{\sigma+}_{14}, \theta^{\sigma+}_{23}, \phi^{\sigma-}_{14}$ and $\phi^{\sigma-}_{23}$. These pinned bosons for θ or ϕ, immediately suggest a basis. In the spin channel, since there are already four mutually orthogonal combinations of band bosons getting pinned, it's natural to choose R_σ corresponding to the pinned combinations. So the basis for spin fields is fixed. As for the charge channel, there are two combinations of band bosons which get pinned and we also know symmetry requires the gapless mode to be total charge field $(\Phi_{1\rho}, \Theta_{1\rho})$ since there is no interaction involving boson fields not orthogonal to it here. These three fields and the orthonormal condition will uniquely fix the only unknown basis field,

$$\Phi_{2\rho}=\frac{1}{2}(\phi_{1\rho}-\phi_{2\rho}-\phi_{3\rho}+\phi_{4\rho}), \quad (4.15)$$

similarly for $\Theta_{2\rho}$ if replace ϕ by θ. In this case, the relevant interactions suggest the basis we should adopt is:

$$R_\rho=\begin{pmatrix} 1/2 & 1/2 & 1/2 & 1/2 \\ 1/\sqrt{2} & 0 & 0 & -1/\sqrt{2} \\ 0 & 1/\sqrt{2} & -1/\sqrt{2} & 0 \\ 1/2 & -1/2 & -1/2 & 1/2 \end{pmatrix}, R_\sigma=\begin{pmatrix} 1/\sqrt{2} & 0 & 0 & 1/\sqrt{2} \\ 1/\sqrt{2} & 0 & 0 & -1/\sqrt{2} \\ 0 & 1/\sqrt{2} & 1/\sqrt{2} & 0 \\ 0 & 1/\sqrt{2} & -1/\sqrt{2} & 0 \end{pmatrix}.$$

Now we will rewrite the interactions Eq. (4.14) in terms of the new basis given by R_ρ and R_σ. So far we get six pinned bosons only by considering the fixed ray interactions. At lower energy scale, the subleading terms also become large, yet still small compared with the fixed ray. Replacing the pinned bosons by their pinned values, we get a C2S0 effective Hamiltonian and the subleading terms will be treated as the perturbations. $\Phi_{1\rho}$ is absent in Eq. (4.14) and it will remain gapless as we expected. The question is about whether $\Phi_{2\rho}$ will get pinned due to the perturbation involving it, such as $c^{\rho}_{12}, c^{\rho}_{13}, c^{\rho}_{24}, c^{\rho}_{34}, c^{\sigma}_{12}, c^{\sigma}_{13}, c^{\sigma}_{24}$ and c^{σ}_{34}. At first glance, one may conclude the gapless bosons $\Phi_{2\rho}$ won't get pinned since all the subleading perturbations also contain the dual of pinned spin boson $\phi^{\sigma-}_{14}$ and $\phi^{\sigma-}_{23}$. In other words, these subleading interactions should be irrelevant and $\Phi_{2\rho}$ can't be pinned. It's true for this analysis. But the common wisdom tells us that the gapless mode is usually fragile unless protected by some symmetry or incommensurability. In

fact, there are always some other higher order interactions which can be generated in the continuum limit as long as they are allowed by symmetry. We usually don't pay attention to these higher order terms for they should be much smaller and less relevant than the interactions in Eq. (4.2). However, the scaling dimension of these higher order interactions can be changed due to the existence of some other interactions [95, 96]. For example, consider a 4^{th} order term in perturbation theory:

$$\delta H \propto (c_{12}^{\rho})^2 c_{11}^{\sigma} c_{22}^{\sigma} [\cos\sqrt{4\pi}\phi_{12}^{\rho-} \cos\sqrt{2\pi}(\theta_{1\sigma}+\theta_{2\sigma})]^2 \cos\sqrt{8\pi}\theta_{1\sigma} \cos\sqrt{8\pi}\theta_{2\sigma} \qquad (4.16)$$

Using the operator product expansion, we can replace all factors involving $\theta_{1\sigma}$ and $\theta_{2\sigma}$ by a constant. The remaining operator contains a term:

$$\delta H \propto \cos\sqrt{8\pi}(\phi_{1\rho}-\phi_{2\rho}) = \cos\sqrt{4\pi}(\sqrt{2}\Phi_{2\rho}+\phi_{14}^{\rho-}-\phi_{23}^{\rho-}) \to \cos\sqrt{8\pi}\Phi_{2\rho}, \qquad (4.17)$$

where we have used R_ρ to obtain the second expression and replaced $\phi_{14}^{\rho-}$ and $\phi_{23}^{\rho-}$ by their expectation values in the third. This operator doesn't depend on spin fields anymore and we have an effective sine-Gordon Hamilatonian for $(\Phi_{2\rho}, \Theta_{2\rho})$. The cosine interaction has a scaling dimension of $2/K_{2\rho}$. If the renormalized value of the Luttinger parameter for the $\Phi_{2\rho}$ boson, $K_{2\rho} > 1$, then Eq. (4.17) is relevant. In general, it's highly nontrivial to determine the renormalized value $K_{2\rho}$ after integrating out the gapped modes. However, we can calculate the renormalization of $K_{2\rho}$ due to the gradient terms of interactions:

$$K_{2\rho} = \sqrt{\frac{\pi\overline{v}-\overline{c}+\overline{f}}{\pi\overline{v}+\overline{c}-\overline{f}}}, \qquad (4.18)$$

where

$$\begin{aligned} \overline{v} &= (v_1+v_2+v_3+v_4)/4, \\ \overline{c} &= \tilde{c}_{11}^{\rho}+\tilde{c}_{22}^{\rho}+\tilde{c}_{33}^{\rho}+\tilde{c}_{44}^{\rho}, \\ \overline{f} &= \tilde{f}_{12}^{\rho}+\tilde{f}_{13}^{\rho}-\tilde{f}_{14}^{\rho}-\tilde{f}_{23}^{\rho}+\tilde{f}_{24}^{\rho}+\tilde{f}_{34}^{\rho}. \end{aligned}$$

According to the ratios in Eq. (4.13), we find that $K_{2\rho} > 1$. Therefore, $\Phi_{2\rho}$ should also be pinned with this sine-Gordon type interactions. We conclude the final phase should be C1S0 and the pinned bosons are $\Phi_{2\rho}, \phi_{14}^{\rho-}, \phi_{23}^{\rho-}, \theta_{14}^{\sigma+}, \theta_{23}^{\sigma+}, \phi_{14}^{\sigma-}$ and $\phi_{23}^{\sigma-}$. For this pinning pattern, the correlation functions of the $4\bar{k}_F$ density operators Eq. (2.26) and (2.27) with $\{i,j\} = \{1,4\}$ and $\{k,l\} = \{2,3\}$, decay with a power-law. Also, with $\{s,t\} = \{1,4\}$ or $\{2,3\}$, the correlation functions of the bipairing operators Eq. (2.29) and the term with $\theta_{st}^{\sigma+}$ in Eq. (2.30) decay with a power-law. All the pairing operators Eq. (2.24) and (2.25) decay exponentially. This phase has stripes and bipairing correlations. The result is also consistent with FSS.

The only question left is how to find the proper initial couplings so that the RG will flow to the fixed ray. The initial bare couplings are determined by the interactions in the model. As long as one includes enough short ranged interactions in the Hamiltonian,

the initial bare couplings can be tuned near the ratios in Eq. (4.13). The point is that the fixed ray should indicate some phase in the strong coupling regions. Thus, to find the proper initial bare couplings that RG will flow to this fixed ray may not be the most important issue for our purpose.

The fact that we need $v_1 \simeq v_4$ and $v_2 \simeq v_3$ in order to see the stripe phase in RG resembles the situation in the decoupled 2-leg ladders limit we study in section V. It seems to suggest that the stripe phase should be related to the renormalization of Fermi velocities from both limits we study.

4.3 The Repulsive Hubbard Model

In the previous section, we found the fixed ray corresponding to the stripe phase without knowing the exact underlying model. Now we would like to switch gears and study the fixed rays corresponding to parameters of the Hubbard model in Eq. (1.8) and (1.9).

In the four-band region, the RG flows to the following fixed ray [89],

$$\sqrt{2}c^{\rho}_{11} = \sqrt{2}c^{\rho}_{44} = -\frac{c^{\rho}_{14}}{2} = \sqrt{\frac{2}{3}}\frac{c^{\sigma}_{11}}{2} = \sqrt{\frac{2}{3}}\frac{c^{\sigma}_{44}}{2} = -\frac{c^{\sigma}_{14}}{2\sqrt{3}} = -f^{\rho}_{14} = -\frac{1}{16(l_d - l)}. \quad (4.19)$$

It seems that only the interactions between band 1 and 4 are relevant and band 2 and 3 are totally decoupled from the system. Also, the fixed ratios in Eq. (4.19) are the same as those of the C1S0 phase in a doped 2-leg ladder if band 1 and 4 are regarded as an effective 2-leg system. So the final phase was referred to as C1S0 + C2S2 = C3S2. Notice that the RG equations, in the g_i basis of Eq. (4.4), are invariant under the permutations of indices but the bare values, $g_i(0)$, favor the phase in which the couplings involving bands 1 and 4 get large. This can be seen from the factors of $1/v_i$ relating the g_i's to the $\tilde{g}_i$'s in Eq. (B.9)-(B.12).

However, now we know that the fixed ray solution isn't the whole story for the RG flow. Bands 2 and 3 are never really decoupled since there are subleading coupling constants that involve these bands. Once again, we will plot $\log[|g_i(l)|]$ v.s. $\log[(l_d - l)]$ from the numerical solution of the RG equations and we see nice straight lines in the scaling region. The slopes will be compared with $-\lambda_i^{\max}$, which can be deduced from the eigenvalues λ_n and eigenvectors of the matrix $B_{ij} = 2M^i_{jk}G_k$.

With the G_i given by Eq. (4.19), there are two $-1/2$, six $-1/16$, two $1/2$, two $15/16$, a 1 and other 0s for λ_n. Terms corresponding to $-1/2$ and $-1/16$ are irrelevant and not harmful to anything. We should carefully look at the terms with $1/2$, $15/16$, and 1. The effects on the phase diagram depend on whether they have components on the couplings with $G_i = 0$. This information is given by their corresponding eigenvectors. One may think in general $\lambda_n = 1$ means the fixed ray is unstable. This is true if the deviations δg_n have non-zero components on the couplings besides the fixed ray ones. Fortunately, here the eigenvector for $\lambda_n = 1$ only has two components with negative c^{σ}_{11} and positive c^{σ}_{44} in

terms of the original coupling basis. It will shift the values of fixed ratios regarding c^{σ}_{11} and c^{σ}_{44} in Eq. (4.19) a little bit but it won't change the fact that those seven couplings are the most relevant ones. This only reflects that the fixed ray Eq. (4.5), is just a special set of the solutions and not the most general one. Table (4.2) summarizes λ_n and their projections in terms of coupling basis g_i.

	nonzero component
1/2	$c^{\rho}_{14}, c^{\sigma}_{14}, f^{\sigma}_{14}$
1/2	$c^{\rho}_{11}, c^{\rho}_{44}, c^{\rho}_{14}, c^{\sigma}_{11}, c^{\sigma}_{44}, c^{\sigma}_{14}, f^{\rho}_{14}$
15/16	$c^{\rho}_{13}, c^{\rho}_{34}, c^{\sigma}_{13}, c^{\sigma}_{34}$
15/16	$c^{\rho}_{12}, c^{\rho}_{24}, c^{\sigma}_{12}, c^{\sigma}_{24}$
1	$c^{\sigma}_{11}, c^{\sigma}_{44}$

Table 4.2: This table summarizes the topography in the vicinity of the fixed ray Eq.(4.19). It shows the eigenvalues $\lambda_n = 1$ of the matrix B_{ij} and their corresponding eigen-direction in terms of the RG couplings.

This result can be checked by plotting $\log[|g_i(l)|]$ v.s. $\log[(l_d - l)]$ for the numerical solutions of RG equations. As a test, we can artificially tune the ratios of initial conditions based on Eq. (4.19), such that the RG flow will be really in the vicinity of the fixed ray. In this case, the slope of each coupling agrees perfectly with the prediction given above.

Now using the initial conditions as shown in Appendix B, determined by physical parameters on-site interaction U and the doping δ, we can do the same analysis. Even in the region where the RG flow is still controlled by the fixed ray Eq. (4.19), we now find that not all the slopes agree with the prediction. Some couplings with predicted $\lambda_i^{\max} = 0$, actually have non-zero slopes in the log-log plot and those slopes may vary according to the initial conditions. They are new subleading terms besides those given by the stability check near the fixed ray. However, we don't find notable changes of the slopes for those couplings with $\lambda_i^{\max} = 5/16, 1/2$ or 1, as long as the RG flow is still dominated by the same fixed ray. That is, the universal analytic prediction in the vicinity of the fixed ray is still correct to some extent.

A few selected typical examples are shown in Fig. (4.3). The failure to predict all $\lambda_i^{\max}$ correctly for each couplings doesn't mean we can't determine the phase diagram. The point is that we should treat all the divergent terms with the exponent $0 < \lambda_i^{\max} \leq 1$ as the perturbations to the effective Hamiltonian corresponding to the fixed ray in the bosonization scheme.

In order to minimize Eq. (4.14), the most relevant couplings in Eq. (4.19) will pin the values of $\phi^{\rho-}_{14}, \theta^{\sigma+}_{14}$, and $\theta^{\sigma-}_{14}$. The fixed ray interactions and the symmetry imply we should choose $\Phi^{\rho}_2, \phi^{\rho-}_{14}, \theta^{\sigma+}_{14}$, and $\theta^{\sigma-}_{14}$ for the new basis of bosons. Unlike the previous case of stripe fixed ray, here there are still two undetermined fields in charge and spin channel each. So the choices of the basis is not unique anymore. Any two charge (or spin) fields orthogonal to Φ^{ρ}_2 and $\phi^{\rho-}_{14}$ (or $\theta^{\sigma+}_{14}$, and $\theta^{\sigma-}_{14}$) can be used. For example, the simplest choice would be the same as R_ρ and R_σ used in the previous section.

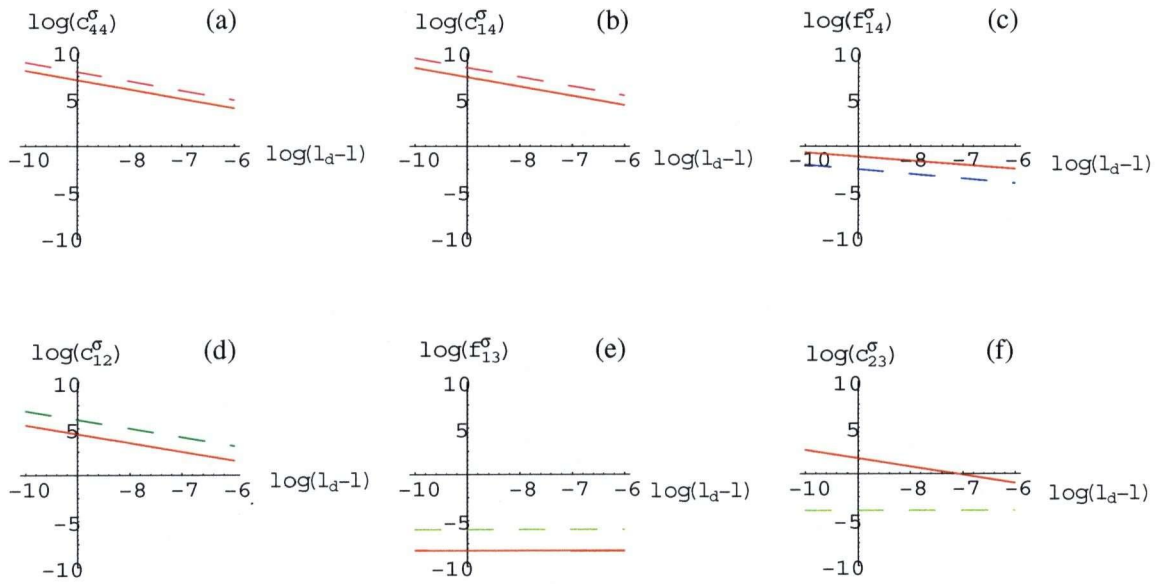

Figure 4.3: $\log[|g_i(l)|]$ v.s. $\log[(l_d - l)]$ plot for several typical couplings. The parameters are chosen as $t = t_{i,\perp} = 1$, $U = 0.01$ and the hole doping is 0.135. The slope gives us the divergent exponent for each coupling. The solid (red) lines are the numerical solutions for the RG equations. The dashed lines are pure straight lines as reference with the predicted slopes 1 (pink: c^{σ}_{44} (a), c^{σ}_{14} (b)), 1/2 (blue: f^{σ}_{14} (c)), 15/16 (green: c^{σ}_{12} (d)), and 0 (yellow: f^{σ}_{13} (e), c^{σ}_{23} (f)), respectively. As one can see, the numerical solution of c^{σ}_{23} (f) doesn't agree with its predicted exponent. The number of couplings, whose slopes don't agree with the stability analysis, depends on the initial conditions. With the initial conditions used here, there are total 11 couplings, predicted with zero slope near the fixed ray, but have nonzero slopes in the numerical solution. However, these new term don't change the pinned bosons and the final phase is the same as that when these terms are irrelevant.

We then follow the hierarchy of these subleading terms in repulsive Hubbard model. Pick the largest one among them and rewrite it in terms of the new fields according to R_ρ and R_σ. After replace $\phi^{\rho-}_{14}, \theta^{\sigma+}_{14}$, and $\theta^{\sigma-}_{14}$ by constants, The largest subleading term $(c^{\rho}_{12} + c^{\sigma}_{12})$ in Eq. (4.14) becomes:

$$\begin{aligned} & \cos\sqrt{4\pi}\phi^{\rho-}_{12} \cos\sqrt{4\pi}\theta^{\sigma-}_{12} \\ = \; & \cos\sqrt{\pi}(\sqrt{2}\Phi_{2\rho} + \phi^{\rho-}_{14} - \phi^{\rho-}_{23}) \cos\sqrt{\pi}(\theta^{\sigma+}_{14} + \theta^{\sigma-}_{14} - \theta^{\sigma+}_{23} - \theta^{\sigma-}_{23}) \\ \to \; & \cos(\sqrt{2\pi}\Phi^{\rho}_{2} - \sqrt{\pi}\phi^{\rho-}_{23}) \cos\sqrt{\pi}(\theta^{\sigma+}_{23} + \theta^{\sigma-}_{23}). \end{aligned} \tag{4.20}$$

Similarly, next largest term $(c^{\rho}_{13} + c^{\sigma}_{13})$ becomes:

$$\begin{aligned} & \cos\sqrt{4\pi}\phi^{\rho-}_{13} \cos\sqrt{4\pi}\theta^{\sigma-}_{13} \\ \to \; & \cos(\sqrt{2\pi}\Phi^{\rho}_{2} + \sqrt{\pi}\phi^{\rho-}_{23}) \cos\sqrt{\pi}(\theta^{\sigma+}_{23} - \theta^{\sigma-}_{23}). \end{aligned} \tag{4.21}$$

With the perturbations like Eq. (4.20) and (4.21), four more boson fields $\Phi_2^\rho, \phi_{23}^{\rho-}, \theta_{23}^{\sigma+}$ and $\theta_{23}^{\sigma-}$ will get pinned. Thus, as long as the RG flow is dominated by Eq. (4.19), the final phase should be C1S0 and the pinned bosons are $\Phi_2^\rho, \phi_{14}^{\rho-}, \phi_{23}^{\rho-}, \theta_{14}^{\sigma+}, \theta_{14}^{\sigma-}, \theta_{23}^{\sigma+}$ and $\theta_{23}^{\sigma-}$. This pinning pattern will make the pair operator Eq. (2.24) decay with a power law and $4k_F$ density operators Eq. (2.26) and (2.27) decay exponentially. So it's a pairing phase with no stripes. Since in this phase the pinned charge or spin bosons are all ϕ or θ fields, respectively, we can use other choices for R_ρ and R_σ and the result will be the same.

Chapter 5

Limit of 2 Decoupled 2-Leg Ladders

5.1 Mapping to the 2-Leg Bosonic Model

One interesting limit in which it is relatively easy to understand the stripe phase is the limit of two 2-leg ladders weakly coupled by electron hopping and density-density interactions. Essentially this limit was discussed in Ref. [89], sub-section (VII-B-1) in the context of a 2-dimensional array of 2-leg ladders. As we discuss below, the low energy effective Hamiltonian in this limit is the same one describing the 2-leg *bosonic* ladder which was discussed in Ref. [84] based on the "bosonization" for 1D bosons [97]. See Fig. (5.1) for illustration.

This limit corresponds to $t_{2,\perp}$ and $V_{2,\perp}$ very small, in the following Hamiltonian:

$$H_0 = -\sum_{\alpha=\pm}\left[\sum_{x=1}^{L-1}\sum_{a=1}^{N} t c^{\dagger}_{a,\alpha}(x)c_{a,\alpha}(x+1) + \sum_{x=1}^{L}\sum_{a=1}^{N-1} t_{a,\perp} c^{\dagger}_{a,\alpha}(x)c_{a+1,\alpha}(x)\right] + h.c. \qquad (5.1)$$

and

$$H_{int} = U\sum_{x=1}^{N}\sum_{a=1}^{L} n_{a,\uparrow}(x)n_{a,\downarrow}(x) + \sum_{\alpha=\pm}\sum_{x=1}^{L}\frac{V_{2,\perp}}{2} n_{2,\alpha}(x)n_{3,\alpha}(x). \qquad (5.2)$$

We set $t_{1,\perp} = t_{3,\perp} = t$ for simplicity, but this is not essential. Thus we may begin by considering the behavior of 2 decoupled 2-leg Hubbard ladders. Over a wide range of parameters, the 2-leg Hubbbard ladder is expected to be in a C1S0 phase [23, 85, 86, 87]. Introducing band bosons, $\phi^U_{1\nu}$, $\phi^U_{2\nu}$ for the upper 2-leg ladder (on legs 1 and 2 and $\nu = \rho$ or σ) and then changing variables to

$$\phi^U_{\pm\nu} \equiv (\phi^U_{1\nu} \pm \phi^U_{2\nu})/\sqrt{2}, \qquad (5.3)$$

this phase is expected to have $\phi^U_{-\rho}$ and $\theta^U_{\pm\sigma}$ pinned. The lowest Friedel oscillation wavevector is $4\bar{k}_F$, corresponding to the 2-leg version of stripes, namely equally spaced pairs of holes (1 on each leg) forming a "quasi charge density wave" near the boundary. The $\phi^U_{+\rho}$ boson is, of course, gapless. Let Δ be the minimum gap for the other three bosons. In the limit $U << t$, we expect $\Delta \propto t\exp[-\text{const} \times t/U]$. For $U \geq t$ we expect Δ to be $O(t)$ or larger. Of course the lower 2 legs have a gapless boson $\phi^L_{+\rho}$.

We now turn on small $t_{2\perp}$ and $V_{2\perp}$, coupling together the two 2-leg ladders. Both interactions involve duals of pinned bosons, $\theta^{U/L}_{-\rho}$ and $\phi^{U/L}_{\pm\sigma}$ and hence are ultimately irrelevant. On the other hand, a pair-hopping term, with amplitude $t' \propto t^2_{2,\perp}$ and an

interaction between the $4\bar{k}_F$ density operators in the two 2-leg ladders, of strength $V' \propto V_{2,\perp}$ are generated perturbatively. [This linear dependence of V' on $V_{2,\perp}$ follows since, by analogy with the calculation in Appendix A), the $4\bar{k}_F$ term in the density operators for each 2-leg ladder is $O(U)$. Here we disagree slightly with Ref. [89] which found this interaction to be $\propto (V_{2,\perp})^2$.] Neither of these interactions involves the dual of any pinned bosons. For sufficiently weak $t_{2,\perp}$ and $V_{2,\perp}$ we may analyze the low energy theory by simply replacing all pinned bosons from the two 2-leg ladders by their expectation values and writing an effective Hamiltonian for $\phi^U_{+\rho}$ and $\phi^L_{+\rho}$. The effective Hamiltonian describes the physics at energy scales $\ll \Delta$ and for it to be valid the energy scales characterizing the pair hopping and $4\bar{k}_F - 4\bar{k}_F$ density interactions must also be $\ll \Delta$. It is now convenient to change boson variables to:

$$\phi_\pm \equiv [\phi^U_{+\rho} \pm \phi^L_{+\rho}]/\sqrt{2}, \tag{5.4}$$

since the pair hopping and $4\bar{k}_F$-$4\bar{k}_F$ density interactions only involve ϕ_- and its dual, θ_-. The effective Hamiltonian at energy scales $\ll \Delta$ can be written:

$$\begin{aligned} H_{eff} &= \int dx \{ \frac{v_+}{2}[K_+(\partial_x \phi_+)^2 + \frac{1}{K_+}(\partial_x \theta_+)^2] \\ &+ \frac{v_-}{2}[K_-(\partial_x \phi_-)^2 + \frac{1}{K_-}(\partial_x \Theta^\rho_-)^2] \\ &+ t' \cos(\sqrt{2\pi}\phi_-) + V' \cos(\sqrt{8\pi}\theta_-)\}. \end{aligned} \tag{5.5}$$

Here, to lowest order in $t_{2,\perp}$ and $V_{2,\perp}$, $K_+ = K_-$ is simple the Luttinger parameter of the $\phi^{U/L}_{+\rho}$ bosons on the upper and lower 2-leg ladders and likewise $v_+ = v_-$ is the corresponding velocity. The Luttinger parameter of the 2-leg ladder is expected to approach 1 at half-filling and to decrease as the density moves away from half-filling.

We observe that the connection between $\phi_\pm$ and the fields Φ^ρ_A, in Eq. (2.2) is not so straightforward, even in the limit $t_{2,\perp} \to 0$. Ignoring for the moment all interactions, when $t_{2,\perp}$ is strictly zero the bands come in two identical pairs, one member of each pair from the upper 2 legs and one from the lower 2 legs. However, as soon as $t_{2,\perp} \neq 0$, these bands are mixed. This band-mixing is not taken into account in the present approach in which bosonization fields are introduced separately for the bands on the upper 2 and lower 2 legs. The present approach should be the correct one in the limit considered of very small $t_{2,\perp}$, but it is non-trivial to connect the results with those obtained from the standard weak coupling approach. We note that a very analogous situation occurs even in the much simpler and well-studied 2-leg spinless fermion model. If the inter-chain hopping is sufficiently weak one normally bosonizes the fermions on each leg, whereas in the weak coupling limit, bosons are introduced for each band. Because of the exponentials entering the bosonization formulas the relationship between the "leg boson" and "band bosons" is very non-linear. Nonetheless, it appears that the same phase diagram can be obtained using either approach. This can be seen by comparing the various features of the phases obtained using either method [85, 86].

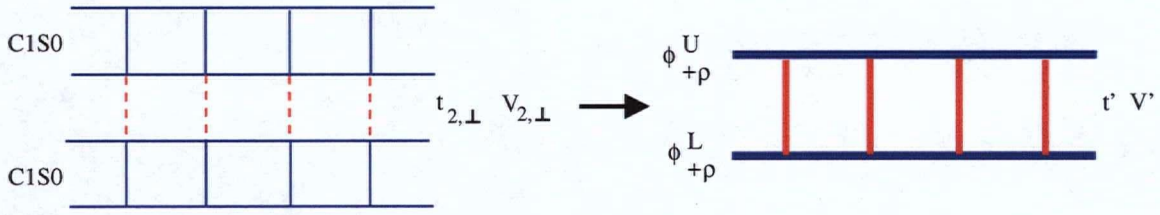

Figure 5.1: In the limit that $t_{2,\perp}$ and $V_{2,\perp}$ are much smaller than the minimum gap of the bosons, Δ, each 2-leg ladder is well-described by the C1S0 phase, which has pairing and $4\bar{k}_F$ density oscillation. The direct electron hopping $t_{2,\perp}$ becomes an irrelevant process yet pair hopping, t', generated by the higher order process will appear and $4\bar{k}_F - 4\bar{k}_F$ component, V', is the lowest order relevant term in the interaction $V_{2,\perp}$. The phase is determined by the competition between t' and V'. If t' dominates, the system has pairing (boson superfluid) and $8\bar{k}_F$ ($4\pi\rho_0$) density oscillation in fermion (boson) language, where ρ_0 is the average boson density. If V' dominates, the system has bipairing (boson pair superfluid) and $4\bar{k}_F$ ($2\pi\rho_0$) density.

It is not so straightforward to estimate the conditions on $t_{2,\perp}$ and $V_{2,\perp}$ for this effective Hamiltonian to be valid. Fortunately, this is not important for our purposes. Normalizing the operators in Eq. (5.5) so that:

$$\begin{aligned} < e^{i\sqrt{2\pi}\phi_-(x)} e^{-i\sqrt{2\pi}\phi_-(y)} > &= \frac{1}{|x-y|^{1/K_-}} \\ < e^{i\sqrt{8\pi}\theta_-(x)} e^{-i\sqrt{8\pi}\theta_-(y)} > &= \frac{1}{|x-y|^{4K_-}}, \end{aligned} \tag{5.6}$$

we see that t' has a scaling dimension of (energy)$^{2-1/(2K_-)}$ and V' has a scaling dimension of (energy)$^{2-2K_-}$ (after setting $v_- = 1$). These energies scales must be much less than the cut-off scale, Δ, i.e.

$$\begin{aligned} t' &\ll \Delta^{2-1/(2K_-)} \\ V' &\ll \Delta^{2-2K_-}. \end{aligned} \tag{5.7}$$

Here we assume $1/4 < K_- < 1$, which is certainly true near half-filling. As mentioned above, $t' \propto t_{2,\perp}^2$ and $V' \propto V_{2,\perp}$. A more complete estimate of these parameters is more difficult to make and could be quite different depending on whether the 2-leg ladders are in the weak or strong coupling domain.

The phase diagram of the model in Eq. (5.5) has been discussed in Ref. [89] in the context of a 2D array of 2-leg ladders. Precisely the same model also arises from a treatment of a 2-leg ladder of spinless *bosons* in Ref. [84]. The boson annihilation operators on the upper and lower legs are represented as:

$$\Psi^{U/L} \propto e^{-i\sqrt{\pi}\phi^{U/L}_{+\rho}} + \ldots, \tag{5.8}$$

and the boson density operators as:

$$\Psi^{U/L\dagger}(x)\Psi^{U/L}(x) \propto n_b + \frac{1}{\sqrt{\pi}}\partial_x\theta_{+\rho}^{U/L} + \text{constant} \times \{\exp[i2\pi n_b x + i\sqrt{4\pi}\theta_{+\rho}^{U/L}] + h.c.\} + \ldots. \tag{5.9}$$

Here n_b is the density of bosons on each leg. Of course, it is hardly surprising that this low energy Hamiltonian describes a 2-leg bosonic ladder; in our low energy approximation, the fermionic degrees of freedom on each 2-leg ladder have been discarded keeping only the spinless pairs, corresponding to bosons. t' represents (single) boson hopping between the chains and V' represents inter-chain boson back-scattering. It follows from Eq. (5.7) that both t' and V' are relevant for $1/4 < K_- < 1$ (and in general at least one of them is relevant for all K_-). Thus one of ϕ_- and θ_- boson is always gapped, yielding a C1S0 phase. There are two possible phases in which either ϕ_- or θ_- is pinned [84]. These two phases have evident physical interpretations in the various underlying models from which H_{eff} arises. In the 2-leg boson model, the phase in which t' is relevant and ϕ_- is pinned corresponds to a standard 1D superfluid phase in which the boson creation operator has a power-law decaying correlation function but the term in the boson density operator oscillating at wave-vector $2\pi n_b$ decays exponentially. On the other hand, the phase in which θ_- is pinned corresponds to a boson pairing phase. Now the boson creation operator has an exponentially decaying correlation function. There is a corresponding gap to create a single boson. The 2-boson creation operator $\Psi(x)\Psi(x)$ has a power law decaying correlation function as does the term in the boson density operator oscillating at wave-vector $2\pi n_b$. In the 2D array of 2-leg fermionic ladders, discussed in Ref. [89], the phase in which ϕ_- is pinned is a conventional 2D superconducting phase and the one phase in which θ_- is pinned is an incommensurate charge density wave phase. (The power-law decay in the single or double 2-leg ladder system is expected to become true long range order in the 2D system.) The physical interpretation of these phases in our model of 2 weakly coupled 2-leg (fermionic) ladders is now also clear. The phase in which ϕ_- is pinned is a conventional pairing phase. Note that the density of bosons (average number of bosons per site in the 2-leg bosonic ladder) should be identified with the density of electrons (average number of electrons per site in the 4-leg ladder). This follows since there are half as many sites per unit length in the bosonic 2-leg ladder as in the fermionic 4-leg ladder. Equivalently, we may identify the boson density with the fermion density measured from half-filling

$$n_b = \delta = 1 - n. \tag{5.10}$$

Thus we see that there are no density oscillations at $2\pi\delta$ or equivalently $4\bar{k}_F$ in the pairing phase. The phase in which θ_- is pinned is a bipairing phase with stripes.

Which phase occurs depends on K_- and also the relative size of t' and V'. When K_- is in the range $1/4 < K_- < 1$, where both t' and V' are relevant, we may estimate the phase boundary by the condition that the corresponding energy scales, determined from Eq. (5.7) are equal. Thus we expect the stripe phase to occur, for this range of K_-

where:

$$V' > (t')^{[2-2K_-]/[2-1/(2K_-)]}. \tag{5.11}$$

Decreasing K_- favors the stripe phase. Noting that we expect K_- to decrease from 1 as we dope away from half-filling, it is natural to expect that, for large enough V'/t', the pairing phase will occur close to half-filling and the stripe phase at larger doping, which is consistent with the DMRG result [17].

At this point it is appropriate to point out that much of the same physics was discussed in two other earlier papers. In Ref. [74] an effective 2-leg bosonic model was also discussed as an approximation to the 4-leg fermionic ladder. In that case the derivation was more heuristic than what appears here. A somewhat longer range interaction was chosen in the 2-leg bosonic model (up to separations of 3 lattice sites along the chain direction) in order to partially match the numerical results on the 4-leg fermionic ladder with those on the 2-leg bosonic ladder. In particular, the Friedel oscillations were compared in the 2 models and shown to exhibit stripes in both models at higher doping. The advantage of considering 2 nearly decoupled 2-leg fermionic ladders ($t_{2,\perp}$, $V_{2,\perp}$ small) is that we can make this mapping more rigorous. In Ref. [90] the limit of very small δ is studied, for fixed U. It was argued that, starting with half-filling, at small δ, 2 of the bands remain in a gapped state with an average filling of $1/2$ while the other band pair is doped. At higher doping, both band pairs are doped. It was assumed that each of these doped band pairs yields fermion pairs. At somewhat higher doping they argue that these pairs form 4-hole clusters. Friedel oscillations were not discussed. Although both of these papers discuss 4-hole clusters, as does the earlier DMRG work of Ref. [17], none of them discuss the implications of such 4-hole clusters that follow from 1D field theory considerations: exponentially decaying pair correlations and a gap to add a single pair of holes to the system. In particular, it seems likely that the effective 2-leg bosonic ladder model studied in Ref. [74] was in the boson pairing phase, with a gap to add a single boson and exponential decay of the boson creation operator correlation function, but this point was not commented on. In this regard, Figures (16) and (17) of Ref. [74] are very interesting. Fig. (16) appears to be a plot of $E(N_b) - E(N_b - 1)$ versus $(N_b - 1/2)/2L$ where N_b is the number of bosons in the 2-leg bosonic ladder. In a boson pairing phase, we expect:

$$E(N_b) \to \mu N_b + \frac{\Delta_b}{2}(-1)^{N_b} + O(1/L), \tag{5.12}$$

where 2μ is the chemical potential for boson pairs and Δ_b is the single boson gap. Thus:

$$E(N_b) - E(N_b - 1) \to \mu + (-1)^{N_b}\Delta_b + O(1/L). \tag{5.13}$$

Both μ and Δ_b will evolve smoothly with density but this zig-zag structure of $E(N_b) - E(N_b - 1)$ is the signal of a boson gap, i.e. of boson pairing. Such a zig-zag is seen for the last three points in Fig. (16), implying that $E_8 + E_{10} < 2E_9$ (for $L = 23$) and a corresponding boson gap at $\delta \approx .2$ of $\Delta_b \approx .05t$. A zig-zag is not seen in Fig. (16) at smaller N_b, despite the fact that the change in Friedel oscillations to stripes appears to

occur at $\delta_c \approx .125$. Possibly this is because the boson gap is too small relative to the finite size gap to be observable for δ closer to δ_c. Fig. (17) shows the analogous quantity for the 4-leg fermionic ladder, $E(N_h) - E(N_h - 2)$ plotted versus $(N_h - 1)/(4L)$ for even N_h. In this case no clear zig-zag is seen, which would indicate a gap to add a single fermionic pair, up to $\delta = .2$. Possibly the problem is again that the gap is too small relative to the finite size gap. This may indicate that the heuristic mapping is not working in great detail since the bosonic gap appears to be significantly larger than the fermionic pair gap. Clearly more numerical work on both 2-leg bosonic and 4-leg fermionic models would be interesting, either or larger L or for a different choice of interaction parameters, to clarify whether or not a bosonic gap (and corresponding fermionic pair gap) exists in the stripe phase, $\delta > \delta_c$.

5.2 Concluding Remarks on 4-Leg Stripes

We have taken a number of different approaches to the 4-leg generalized Hubbard ladder based on bosonization and RG. We gave general arguments about possible phases based on possible ways of pinning bosons and the finite size spectrum. We studied particular phases from solving the weak coupling RG equations. We determined the phases which occur in the limit of two weakly coupled 2-leg ladders, using the connection with a 2-leg bosonic ladder. All of these approaches led to the same conclusion. It is not possible to find any C1S0 phases that have both stripes and pairing. On the other hand, it *is* entirely possible to find phases in which stripes coexist with bipairing. Whether or not 4 leg ladders, for physically reasonable and numerically accessible ranges of parameters have such a phase remains an open question. DMRG results have suggested a phase with stripes, but have, so far, found no evidence for bipairing. We can see three resolutions of this paradox.

- Our methods are based on certain approximations: either weak coupling, or weakly coupled pairs of 2-leg ladders. It is entirely possible that other phases may exist for these systems which are inaccessible to these methods. Possibly these phases include ones with coexisting stripes and pairing. We remark, however, that these field theory methods have been remarkably successful in the past at describing many types of 1D strongly correlated systems, including, for example, 2-leg ladders [23, 85, 86, 87]. It would be an important discovery that they break down for the 4-leg ladder.

- Possibly these systems *do not* really have a stripe phase in the sense that we are using. We have given a precise meaning to "stripes" in the limit of a very long 4-leg ladder. We mean Friedel oscillations at a dominant wave-vector of $4\bar{k}_F = 2\pi n$ where n can be taken to be the hole density. Existing DMRG results certainly suggest this but it is possible that careful extrapolation to larger systems might not confirm this result.

- Possibly the stripe phase apparently observed with DMRG *is* a bipairing phase. We remind the reader that we define bipairing precisely to be a phase in which correlation functions of all pair operators decay exponentially but correlation functions of some charge 4 operators exhibit power law decay. Furthermore, such a phase has a gap to add one or two particles, but no gap for four particles. The limited published DMRG results have suggested that the decay of the pair correlation function may be power law and have not seen a gap to add two particles. Possibly the correlation length for the exponential decay is too large, and the corresponding gap to add two particles too small, to be observed so far. Further DMRG calculations could clarify this point. One could either study larger systems or else change the parameters of the model in an attempt to make the correlation length and inverse gap smaller. In this regard, numerical work on 2-leg bosonic ladders would also be useful to confirm that, as expected from field theory arguments, a boson pairing phase occurs in a wide range of parameters. As has been emphasized before, it may be crucial to include long range Coulomb interactions to understand stripe phases in real materials.

We encourage further DMRG and analytical work to decide which of these possibilities is correct. Confirming any of them would be an important advance.

Assuming, for the moment, that 4 leg ladders *do* exhibit stripes and bipairing, we speculate on the implications for the 2-dimensional Hubbard model. One might think that if 2-hole clusters form on 2-leg ladders and 4-hole clusters form on 4-leg ladders then perhaps, extrapolating to an infinite number of legs would simply give an incommensurate charge density wave. Such a state is perhaps not conducive to superconductivity. Stripes have also been observed in 6 leg ladders [19, 20]. In this case, it appears that the number of holes per rung is 4, rather than 6, as might have been expected. This is suggestive of more exotic behavior than a simple CDW, closer to ideas about fluctuating 1D conducting wires, that have been proposed for stripe phases in 2D. Developing a field theory description of this stripe phase in 6-leg ladders is an important open problem.

Chapter 6

Impurity Entanglement Entropy

6.1 Introduction to Entanglement Entropy and the Impurity Model

Quantum mechanics has been highly successful in producing correct experimental predictions. However, its very fundamental property, entanglement, is still not fully understood. First of all, what do we mean by an entangled state? Consider two noninteracting systems A and B, with respective Hilbert spaces H_A and H_B. The composite system is $H_A \otimes H_B$. If the system A is in the state $\mid \psi\rangle_A$ and B is in the state $\mid \phi\rangle_B$, then the composite system is in the state $\mid \psi\rangle_A \otimes \mid \phi\rangle_B$. States of the composite system which can be represented in this form are called *separable states*, or product states. If a state is not separable, it is called an *entangled state*. The singlet state of two 1/2 spins is one simple example.

The so called entanglement entropy is one way to quantify the entanglement property of a quantum state. If we have an entangled state $\mid \Psi_{AB}\rangle$ of systems A and B, which is a pure state, then the pure density matrix (or operator) is $\rho = \mid \Psi_{AB}\rangle\langle\Psi_{AB} \mid$. We can get the reduced density matrix $\rho_{A(B)}$ for subsystem A (B) by tracing out the degrees of freedom for the rest part B (A), $\rho_{A(B)} = \mathrm{Tr}_{B(A)}\rho$. Then the entanglement entropy, sometimes called von Neumann entropy of the reduced density matrix for either subsystem, is:

$$S = -\mathrm{Tr}_A \rho_A \ln \rho_A = -\mathrm{Tr}_B \rho_B \ln \rho_B. \tag{6.1}$$

One interesting feature of Eq. (6.1) is that two subsystems A and B share the same value of entanglement entropy. This is the original motivation to propose entanglement entropy as a measure of entanglement since two subsystem should share the same amount of entanglement between each other. Here we take a two-spins system for example. Consider a general wave function,

$$\mid \Psi_{12}\rangle = \cos\theta \mid\uparrow\downarrow\rangle + \sin\theta \mid\downarrow\uparrow\rangle. \tag{6.2}$$

Now we trace over spin 1 to get the reduced density matrix of spin 2,

$$\begin{aligned} \rho_2 &= \mathrm{Tr}_1 \mid \Psi_{12}\rangle\langle\Psi_{12} \mid = \langle\uparrow\mid \Psi_{12}\rangle\langle\Psi_{12} \mid\uparrow\rangle + \langle\downarrow\mid \Psi_{12}\rangle\langle\Psi_{12} \mid\downarrow\rangle \\ &= \cos^2\theta \mid\uparrow\rangle\langle\uparrow\mid + \sin^2\theta \mid\downarrow\rangle\langle\downarrow\mid . \end{aligned} \tag{6.3}$$

Then entanglement entropy between spin 1 and 2 is

$$\begin{aligned} S &= -\mathrm{Tr}\rho_2 \ln \rho_2 \\ &= -\cos^2\theta \ln\cos^2\theta - \sin^2\theta \ln\sin^2\theta. \end{aligned} \tag{6.4}$$

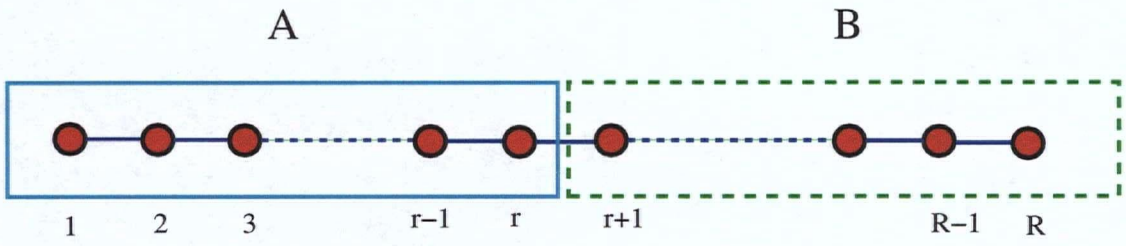

Figure 6.1: The total system size is R. The subsystem A is from site 0 to r and region B, from site $r+1$ to R, is traced out in the density matrix

It's clear to see that S is maximal at ln2 when $\theta = -3\pi/4$ or $\pi/2$, that is, when two spins form a singlet or triplet. Loosely speaking, we can regard entanglement entropy as a kind of measurement of how many degrees of freedoms are shared between two subsystems. A singlet and a triplet state have different parity. Through this simple example, we actually see that entanglement entropy may not be sensitive to the symmetry property of a quantum state.

The first connection between entanglement properties and quantum phase transitions was observed in Ref. [98]. Later on, Eq. (6.1) was applied to many body quantum states in 1D systems [25]. These authors showed that entanglement entropy scales universally with logarithmic dependence on subsystem size at quantum critical points. This logarithmic scaling behavior can be obtained by conformal field theory (CFT) methods [26, 27]. For a 1D spin chain with open boundary conditions and total system size R, the entanglement entropy between the subsystem A:$[0, r]$ and the rest, region B: $[r+1, R]$ (see Fig. (6.1)) has a universal scaling:

$$S(r) = -\mathrm{Tr}_r \rho(r) \ln \rho(r) = \frac{c}{6} \ln[\frac{2R}{\pi} \sin(\frac{\pi r}{R})] + \ln g + \frac{s_1}{2}, \tag{6.5}$$

in the limit $R, r \gg 1$. The constant c is the central charge of the associated CFT, $\ln g$ is the boundary entropy introduced in Ref. [99] and s_1 is a non universal constant related to the ultra-violet cut-off. The nearest neighbor Heisenberg spin chain can be described by a $c = 1$ CFT plus a marginally irrelevant operator [100]. In order to avoid the logarithmic corrections due to this marginally irrelevant operator, we can add the next nearest neighbor coupling J_2, tuned to the critical $J_{2c} \approx .2412$ [101].

When we study the nearest neighbor and critical $J_1 - J_2$ Heisenberg spin chain with open boundary conditions, we find that on top of Eq. (6.5), there are some even-odd alternating corrections [2]. This even-odd alternation is related to the antiferromagnetic nature of the ground state. Motivated by the valence bond picture of entanglement entropy proposed in Ref. [102], we find that the alternating correction to the entanglement entropy is proportional to the alternating part of the energy density (or equivalent to dimerization induced by the boundary) [2]. Moreover, the proportional constant is related to the spin velocity. A derivation for the dimerization is in Appendix C.

How the impurity effects the entanglement is an interesting subject [103, 104, 105]. We study the critical $J_1 - J_2$ Heisenberg spin chain with an extra impurity spin on the boundary, as shown in Fig. (6.2), where $J'_K < J_1 = 1$. For $J_2 = J_{2c} \approx .2412$, the low energy theory of the Hamiltonian Eq. (6.6) is analogous to the Kondo problem [101].

$$H = J'_K \left(\vec{S}_1 \cdot \vec{S}_2 + J_2 \vec{S}_1 \cdot \vec{S}_3 \right) + J_1 \sum_{r=2}^{R-1} \vec{S}_r \cdot \vec{S}_{r+1} + J_2 \sum_{r=2}^{R-2} \vec{S}_r \cdot \vec{S}_{r+2}, \tag{6.6}$$

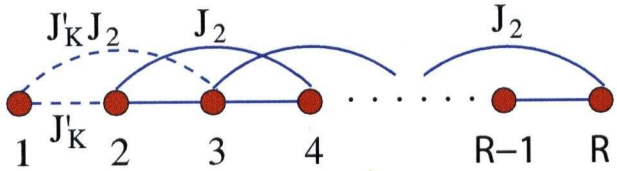

Figure 6.2: Schematic picture for the $J_1 - J_2$ spin chain model (6.6) with an impurity located at the left boundary and coupled with J'_K.

The impurity interaction J'_K is marginally relevant and becomes stronger and stronger toward the lower energy scale [106]. The Kondo temperature T_K is the energy scale when the effective coupling reaches order one. When energy is of order or lower than T_K, the perturbation theory breaks down since the effective coupling is large. At zero temperature, the effective coupling becomes infinity. The impurity will be screened and form a singlet with its neighbour. Then the Kondo length scale

$$\xi_K = \frac{v_s}{T_K} \tag{6.7}$$

can be regarded as the typical size of this screening cloud, where v_s is the spin wave velocity. Many physical quantities of the impurity are shown to be universal scaling functions of R/ξ_K and T/T_K [107, 108, 109, 110, 111]. We would like to define the "impurity entanglement entropy" as

$$S_{imp} = S(\text{with impurity}) - S(\text{no impurity}). \tag{6.8}$$

However, as we mentioned before, besides the uniform part S_U, there is an alternating part S_A in the entanglement entropy,

$$S(r, R) = S_U(J'_K, r, R) + (-1)^r S_A(J'_K, r, R), \tag{6.9}$$

where $S_U(J'_K = 0, r, R)$ is just Eq. (6.5). We *do not* define $S(\text{no impurity})$ as S with $J'_K = 0$ since for $J'_K = 0$ the impurity spin can have a non-trivial entanglement with the rest of the chain due to the degeneracy when R is even. It then follows that the complete impurity contribution to the entanglement entropy cannot be obtained by subtracting

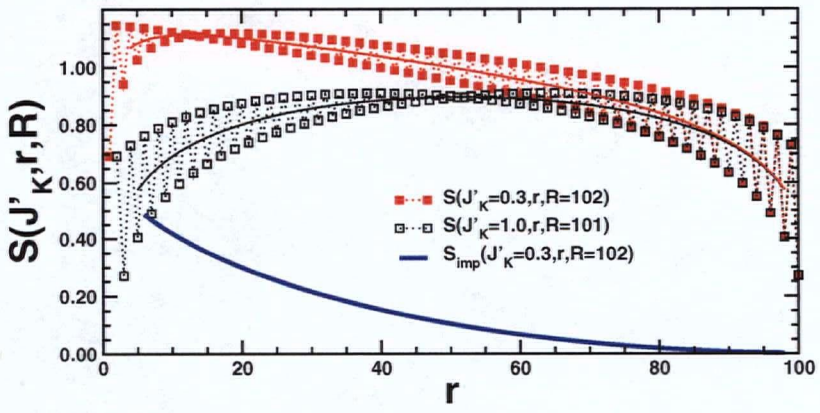

Figure 6.3: Total entanglement entropy, $S(J'_K, r, R)$ for a 102 site spin chain at J_2^c, with a $J'_K = 0.3$ Kondo impurity along with $S(J'_K = 1, r-1, R-1)$ (no impurity). Uniform parts (solid lines) and the resulting S_{imp}.

results for a system with $J'_K = 0$. We thus define the uniform part of the impurity entanglement entropy precisely as

$$S_{imp}(J'_K, r, R) \equiv S_U(J'_K, r, R) - S_U(1, r-1, R-1), \tag{6.10}$$

where $r > 1$. The typical DMRG result is shown in Fig. (6.3).

In general, Eq. (6.10) is a function of all three variables J'_K, r and R. However, similarly to many other impurity quantities, we find that the impurity entanglement entropy is indeed a universal scaling function,

$$S_{imp} = S_{imp}(r/\xi_K, r/R), \tag{6.11}$$

as shown in Fig. (6.4). When R is finite, the ground state has total spin 0 and 1/2 for even and odd R, respectively. In the limit $R \to \infty$ we expect that $S(r/\xi_K, r/R)$ will become the same for 0 or 1/2 total spin, and will be qualitatively similar to the spin-0 case for finite R, approaching $\ln 2$ at $r/\xi_K \to 0$, reflecting the fact that the impurity is screened in region B. On the other hand, for total spin 1/2 (and R finite), S_{imp} must vanish as $r/\xi_K \to 0$ since $\xi_K \to \infty$ corresponds to $J'_K = 0$. In this limit, for 1/2 total spin, the Fermi sea of conduction electrons has spin zero and the impurity is unscreened, hence contributing nothing to S. Screening only becomes probable when $\xi_K \leq R$, or equivalently $T_K \geq v_s/R$, the finite size gap for s-wave excitations. Hence, for total spin 1/2 and fixed r/R the maximum of S_{imp} as a function of r/ξ_K occurs at $r/\xi_K \approx r/R$.

In the next section, we will calculate this function in the limit $r >> \xi_K$ by CFT methods based on Nozières' Fermi liquid theory [112, 113, 114, 115].

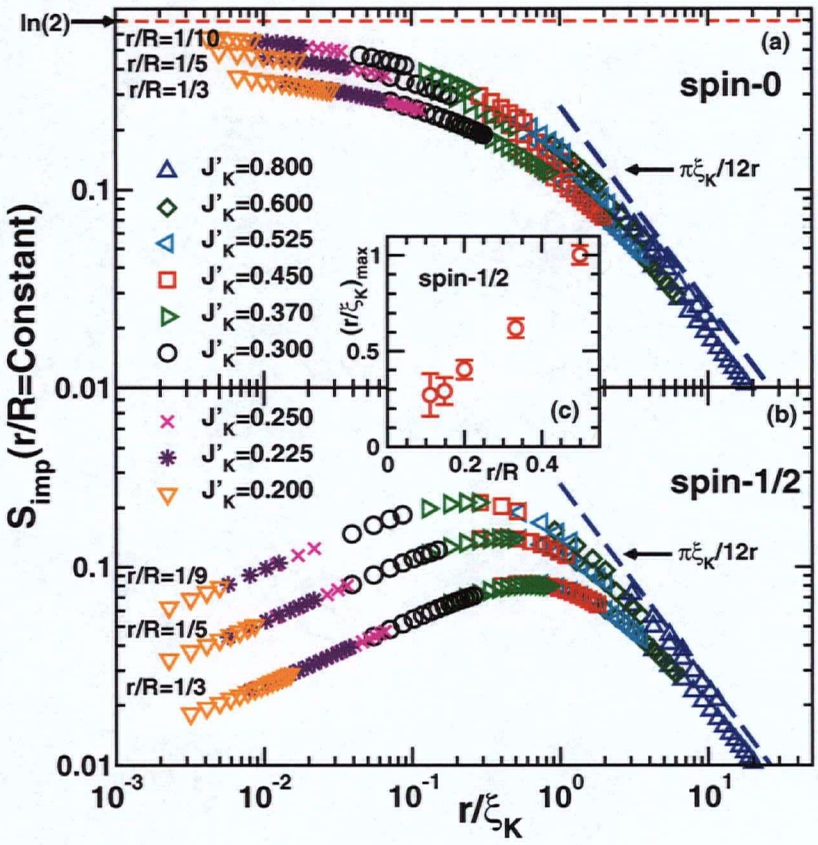

Figure 6.4: Universal scaling plot of $S_{\rm imp}$ for fixed r/R, (a) for $R \leq 102$ *even*, (b) for $R \leq 101$ *odd*. DMRG results for the $J_1 - J_2$ chain at J_2^c for various couplings J_K'. The lines marked $\pi\xi_K/(12r)$ are the FLT prediction, Eq. (6.40). c) the location of the maximum, $(r/\xi_K)_{\rm max}$, of S_{imp} for odd R, plotted versus r/R.

6.2 Fermi Liquid Theory

We will start with the low energy effective theory of Eq. (6.6) with $J_K' = 0$. One standard way is to transform spins to spinless fermions via Jordan-Wigner transformation and then apply the Abelian bosonization, as we introduced in Chapter 1, to spinless fermions. In the end, we will get a free boson Hamiltonian, up to irrelevant operators [81]. However, in this approach, the SU(2) symmetry is not preserved anymore. Another well known method to obtain the low energy effective theory of a spin chain is by non-Abelian bosonization. It turns out the spin chain can be described by the spin sector of 1D spinful fermions at half filling [116]. Then the low energy theory of a spin chain with an impurity on the boundary is equivalent to the spin sector in the Kondo problem [101].

6.2.1 Spin Chain with an Impurity and the Kondo Model

Here we first briefly review the theory of the Kondo model based on the treatment in [113, 114]. The Kondo model is used to describe 3D free electrons interacting with a magnetic spin 1/2 impurity at the origin. The 3D Hamiltonian is

$$H = \int d^3r[\psi^\dagger_\alpha(\frac{-\nabla^2}{2m})\psi_\alpha + J_K\delta^3(\vec{r})\psi^\dagger_\alpha(\frac{\vec{\sigma}_{\alpha\beta}}{2})\psi_\beta \cdot \vec{S}], \tag{6.12}$$

where $\vec{\sigma}$ are Pauli matrices and α, β are the spin indices. If one expands the electron operators in spherical harmonics, due to the δ-function form of the Kondo interaction J_K, only the s-wave harmonic interacts with the impurity [113, 114]. Similar to how we deal with the ladder systems in Chapter 1, assuming a weak Kondo coupling, we may linearize the dispersion relation near the Fermi momentum, k_F, yielding the 1D low energy effective Hamiltonian in terms of chiral fermions:

$$\begin{aligned} H &= (v_F/2\pi)\int_0^\infty dx \left[i\psi^\dagger_{L\alpha}\frac{d}{dx}\psi_{L\alpha} - i\psi^\dagger_{R\alpha}\frac{d}{dx}\psi_{R\alpha}\right] \\ &+\frac{v_F\lambda_K}{4}(\psi^\dagger_{L\alpha}(0)+\psi^\dagger_{R\alpha}(0))\frac{\vec{\sigma}_{\alpha\beta}}{2}(\psi_{L\beta}(0)+\psi_{R\beta}(0))\cdot\vec{S}. \end{aligned} \tag{6.13}$$

Note that $0 < x < \infty$ means the distance from the fermions to the origin and $\lambda_K = \nu J_K$ where $\nu = k_F m/(2\pi^2)$ is the density of states (per spin per band). As we also discussed in Chapter 1, due to the OBC, the boundary condition for the fermion operators at the origin is:

$$\psi_{L\alpha}(x=0) = -\psi_{R\alpha}(x=0), \tag{6.14}$$

and we can regard the right moving fermions as the analytic continuation of the left moving ones to the negative axis:

$$\psi_{L\alpha}(-x) \equiv -\psi_{R\alpha}(x), \quad (x>0). \tag{6.15}$$

Then the Hamiltonian, written in terms of only left-movers but now living on the line from $-\infty$ to ∞, becomes:

$$H = (v_F/2\pi)\int_{-\infty}^\infty dx \left[i\psi^\dagger_{L\alpha}\frac{d}{dx}\psi_{L\alpha}\right] + v_F\lambda_K\psi^\dagger_{L\alpha}(0)\frac{\vec{\sigma}_{\alpha\beta}}{2}\psi_{L\beta}(0)\cdot\vec{S}. \tag{6.16}$$

We can bosonize the left-movers by Eq. (1.16) but the SU(2) symmetry is not preserved. An alternative method is to describe the system by the charge and spin current operators, similar to Eq. (4.1) with one band index:

$$J_L(x) \equiv \psi^\dagger_{L\alpha}(x)\psi_{L\alpha}(x), \quad \vec{J}_L(x) \equiv \psi^\dagger_{L\alpha}\frac{\vec{\sigma}_{\alpha\beta}}{2}\psi_{L\beta}(x). \tag{6.17}$$

Then Eq. (6.16) becomes [113, 114]:

$$\begin{aligned} H &= (v_F/2\pi)\int_{-\infty}^{\infty} dx \left[\frac{1}{4} : J_L J_L(x) : + \frac{1}{3}\vec{J}_L \cdot \vec{J}_L\right] \\ &\quad + v_F \lambda_K \vec{J}_L(0) \cdot \vec{S}. \end{aligned} \tag{6.18}$$

In Eq. (6.18), the impurity spin $\vec{S}$ only couples to the spin current operator $\vec{J}_L$ and the charge part of the Hamiltonian is not effected by the impurity. We can regard the spin and charge currents as some spin and charge boson fields, respectively.

Now consider the spin chain model Eq. (6.6) with OBC. Without the impurity, the low energy theory of the $J_1 - J_2$ Heisenberg spin chain is equivalent to the spin part of the 1D fermion model [101]:

$$H_0 = (v_s/2\pi)\int_{-\infty}^{\infty} dx \frac{1}{3}\vec{J}_L \cdot \vec{J}_L, \tag{6.19}$$

where v_s is the spin-wave velocity. Although nontrivial to prove, Eq. (6.19) is actually a $c = 1$ CFT since the Hamiltonian is nothing but a free spin boson field [116].

We can represent the spin operator at site j as

$$\vec{S}_j \approx [\vec{J}_L(j) + \vec{J}_R(j)] + (-1)^j \text{constant} \cdot \vec{n}(j). \tag{6.20}$$

The alternating part of the spin operators, $\vec{n}(j)$, can be written in terms of the spin boson field in a non-linear way. At the end of the chain, due to the open boundary condition, we find that $\vec{n}(0) \to$ constant $\times\, \vec{J}_L(0)$ and therefore:

$$\vec{S}_2 + J_2 \vec{S}_3 \approx C\vec{J}_L(0), \tag{6.21}$$

where C is a non-universal constant, depending on the second neighbor coupling, J_2 in the Hamiltonian. (C has dimensions of inverse length, and is proportional to the inverse lattice spacing.)

Now including a weak coupling, J'_K to the first spin, the low energy effective Hamiltonian becomes:

$$H = (v_s/2\pi)\int_{-\infty}^{\infty} dx \frac{1}{3}\vec{J}_L \cdot \vec{J}_L + CJ'_K \vec{J}_L(0) \cdot \vec{S}. \tag{6.22}$$

Comparing the low energy effective Hamiltonian for the spin chain model, (6.22) to the low energy effective Hamiltonian for the Kondo model, (6.18), we see that they are equivalent, apart from the extra charge degrees of freedom in the Kondo model, which anyway are non-interacting and decouple from the spin degrees of freedom. Thus, dropping the charge bosons and replacing:

$$v_F \to v_s, \quad v_F \lambda_K \to CJ'_K, \tag{6.23}$$

the two low energy effective Hamiltonian become the same. The constant can be extracted by studying the end-to-end spin correlation function in the chain without the weakly coupled spin, yielding:

$$J'_K \approx 1.3807 \lambda_K. \tag{6.24}$$

6.2.2 Fermi Liquid Theory for the Kondo Problem

Since the impurity interaction J'_K is marginally relevant, it becomes larger when we lower the energy scale [106]. At high temperatures, one can do perturbation directly because the effective coupling strength is still small. At low energies and long length scales, the effective Kondo coupling becomes large, and the effective Hamiltonian flows to the strong coupling fixed point. In the electron version of the Kondo model we may think of this fixed point as one where the impurity spin is "screened", i.e. it forms a singlet with a conduction electron. The remaining electrons behave, at low energies and long length scales, as if they were non-interacting, except that they obey a modified boundary condition reflecting the fact that they cannot break up the singlet by occupying the same orbital as the screening electron. This modified boundary condition corresponds to a $\pi/2$ phase shift. Correspondingly in the spin chain Kondo model, the impurity spin gets "adsorbed into the chain" and no longer behaves like a paramagnetic spin at low energies and long distances. The leading corrections to this low energy long distance picture are described by lowest order perturbation theory in the leading irrelevant operator at the strong coupling fixed point. This is an interaction between the remaining conduction electrons, near the screened impurity. (It doesn't involve the impurity itself since it is screened and doesn't appear in the low energy effective Hamiltonian.)

This leading irrelevant operator is $\vec{J}_L(0) \cdot \vec{J}_L(0)$ [112, 113], which is proportional to Eq. (6.19). It is the entire energy density in the low energy effective Hamiltonian for the spin chain. The energy density has dimensions of (energy)/(length) so the corresponding coupling constant in the effective Hamiltonian must have dimensions of length. On general scaling grounds we expect it to be proportional to ξ_K. The precise constant of proportionality simple corresponds to giving a precise definition of what we mean by ξ_K. We adopt the convention:

$$H_{int} = -(\pi\xi_K)\mathcal{H}_{s,L}(0). \tag{6.25}$$

Here the subscripts s and L are a reminder that this is the spin only part of the energy density for left movers when compare to the Kondo model. Note that if we start with a system of length R (with left and right movers), then we can map into a system of length $2R$ with left movers only. For the purpose of doing first order perturbation theory in H_{int} for quantities like the susceptibility, specific heat or ground state energy, which are translationally invariant in 0^{th} order, we may replace [113] H_{int} by:

$$H_{int} \to -[\pi\xi_K/(2R)] \int_{-R}^{R} \mathcal{H}_{s,L}(x). \tag{6.26}$$

This is equivalent to a length dependent reduction of the velocity:

$$v_s \to v_s[1 - \frac{\pi\xi_K}{2R}]. \tag{6.27}$$

This then implies that the susceptibility, which is $R/(2\pi v_s)$ in the absence of the Kondo

impurity becomes:

$$\begin{aligned}\chi &\rightarrow \frac{R}{2\pi v_s}[1-\frac{\pi\xi_K}{2R}] \\ &\approx R/(2\pi v_s)+\xi_K/(4v_s) = R/(2\pi v_s)+1/(4T_K). \end{aligned} \tag{6.28}$$

Thus the zero temperature impurity susceptibility is $1/(4T_K)$ It is this form of the impurity susceptibility, simply related to the high temperature, free spin behavior, $1/(4T)$, which motivates the definition of ξ_K (and hence $T_K = v_s/\xi_K$) implied by (6.25). We note that this interaction H_{int} is present even in the absence of an impurity, for free fermions but then the coupling constant is of order a lattice constant. Similarly it is also present for the spin chain with no impurity (i.e. $J_K' = 1$) with a coupling constant of order a lattice constant. The effect of a weak Kondo coupling is to make this coupling constant large. We emphasize that this precise choice of definition of T_K has no physical consequences. The power of Fermi liquid theory is to predict not only the form of low energy quantities but also ratios of various low energy quantities such as impurity susceptibility, impurity specific heat, resistivity, etc., corresponding to various generalized Wilson ratios.

6.2.3 Fermi Liquid Theory for S_{imp}

In the limit $\xi_K \ll r$, within the FLT as discussed before, we can calculate the universal scaling S_{imp} by treating H_{int} in Eq. (6.25) in lowest order perturbation theory. We first would like to review the CFT method to calculate the bulk entanglement entropy in Ref. [27]. Consider a conformally invariant system, such as the spin chain model without an impurity, Eq. (6.19), when the total system size is R and the subsystem A is from 0 to r. We trace out the degrees of freedom outside the subsystem from r to R and obtain the reduced density matrix $\rho(r)$. The entanglement entropy S is then $-\mathrm{Tr}_r\rho(r)\ln\rho(r)$. It's very difficult to calculate this quantity directly. We can detour around it by means of the replica trick. If $\mathrm{Tr}\rho(r)^n$ is known, then

$$S = -\lim_{n\rightarrow 1}\frac{d}{dn}[\mathrm{Tr}\rho(r)^n], \tag{6.29}$$

where we omit the subscript r for Tr without the confusion. In the path integral representation of Euclidean space-time,

$$\mathrm{Tr}\rho(r)^n = \frac{Z_n(r)}{Z^n}, \tag{6.30}$$

where $Z_n(r)$ is the partition function on an n-sheeted Riemann surface $\mathcal{R}_n$, with the sheets joined at the cut extending from r to R [26, 27]. Z^n is the n^{th} power of the usual the partition function without the cut. This factor makes sure that $\mathrm{Tr}\rho(r) = 1$, as expected for the density operator. Now the original problem has been transformed into the calculation of the partition function with a nontrivial geometry. It is well known that the partition functions of conformal invariant systems have some universal scaling

behaviors [117, 118]. Here we have the similar situation yet the partition function are defined on an n-sheeted Riemann surface $\mathcal{R}_n$.

We use the approach where the Hamiltonian, such as Eq. (6.19), is written in terms of left movers only, obeying PBC on an interval of length $2R$. In the critical region, the system is conformally invariant and CFT methods are applicable. Now the cut is from the branch point $v = -ir$ to the branch point $u = ir$ on each sheet. Starting with zero temperature and R infinity, the n-sheeted Riemann surface, $\mathcal{R}_n$, can be mapped to the usual complex plane $\mathcal{C}$ [27] by the transformation

$$w \to z = (\frac{w-u}{w-v})^{\frac{1}{n}}, \tag{6.31}$$

where w and z are the variable on $\mathcal{R}_n$ and $\mathcal{C}$, respectively. The energy momentum tensor T is transformed by

$$T(w) = (\frac{dz}{dw})^2 T(z) + \frac{c}{12}\{z, w\}, \tag{6.32}$$

where c is the central charge and $\{z, w\}$ is the Schwartzian derivative $(z'''z' - \frac{3}{2}(z'')^2)/(z')^2$. Since on the complex plane $\langle T(z)\rangle_{\mathcal{C}} = 0$ due to the rotational symmetry, the expectation value of the energy momentum tensor T on $\mathcal{R}_n$ is simply given by Schwartzian derivative:

$$\langle T(w)\rangle_{\mathcal{R}_n} = \frac{\Delta_n (u-v)^2}{(w-u)^2(w-v)^2}, \tag{6.33}$$

where $\Delta_n = (c/24)(1 - (1/n)^2)$.

Imaging that there are two primary operator $\Phi_n(u)$ and $\Phi_{-n}(v)$ sitting on the branch points with the scaling dimension $\Delta_n = (c/24)(1-(1/n)^2)$. Then the three point function on the complex plane $\mathcal{C}$ can be calculated by the Ward identity:

$$\begin{aligned} & \langle T(w)\Phi_n(u)\Phi_{-n}(v)\rangle_{\mathcal{C}} \\ = & \left(\frac{\Delta_n}{(w-u)^2} + \frac{\Delta_n}{(w-v)^2} + \frac{1}{w-u}\frac{\partial}{\partial u} + \frac{1}{w-v}\frac{\partial}{\partial v}\right)\langle \Phi_n(u)\Phi_{-n}(v)\rangle_{\mathcal{C}} \\ = & \frac{\Delta_n}{(w-u)^2(w-v)^2(u-v)^{2\Delta_n - 2}}, \end{aligned} \tag{6.34}$$

where $\langle \Phi_n(u)\Phi_{-n}(v)\rangle_{\mathcal{C}} = (u-v)^{2\Delta_n}$. Then Calabrese and Cardy observed its important connection to Eq. (6.33):

$$\langle T(w)\rangle_{\mathcal{R}_n} \equiv \frac{\int [d\phi] T(w) e^{-S_E(\mathcal{R}_n)}}{\int [d\phi] e^{-S_E(\mathcal{R}_n)}} = \frac{\langle T(w)\Phi_n(u)\Phi_{-n}(v)\rangle_{\mathcal{C}}}{\langle \Phi_n(u)\Phi_{-n}(v)\rangle_{\mathcal{C}}}. \tag{6.35}$$

Since Eq. (6.35) is ensured by the Ward identity, they concluded that any conformal transformation on the the n-sheeted Riemann surface $\mathcal{R}_n$ is equivalent to that on the two point functions on each sheet. In other words, $\mathrm{Tr}\rho^n = Z_n/Z^n$ behave identically to the n-th power of $\langle \Phi_n(ir)\Phi_{-n}(-ir)\rangle_{\mathcal{C}}$ under the conformal mappings or explicitly,

$$\mathrm{Tr}\rho^n \cong \tilde{c}_n (2r/a)^{(c/12)(n-1/n)}. \tag{6.36}$$

Applying the replica trick and $\tilde{c}_1 = 1$, the entanglement entropy is $S \sim (c/6)\ln(2r)$, which is consistent with Eq. (6.5) in the limit $R \gg r$. Then they extended the result to finite system size R at zero temperature or infinite system size at finite temperature $T = 1/\beta$ by applying the corresponding conformal mapping to $\langle \Phi_n(ir)\Phi_{-n}(-ir)\rangle_C$ [27].

Since $\Phi_{\pm n}$ are primary fields, under a conformal mapping from z to $w(z)$, the two point function transforms according to

$$\langle \Phi_n(w_1)\Phi_{-n}(w_2)\rangle = \left(\frac{\partial z}{\partial w}\right)^{\Delta_n}_{w=w_1} \left(\frac{\partial z}{\partial w}\right)^{\Delta_n}_{w=w2} \langle \Phi_n(z_1)\Phi_{-n}(z_2)\rangle \,. \tag{6.37}$$

From the complex plane z to a finite strip w with size $2R$, the transformation is $w = \frac{R}{\pi}\ln z$. So we obtain that the entanglement entropy for the total size R with OBC at zero temperature is Eq. (6.5). From the complex plane z to a cylinder w with circumference β, the transformation is $iw = \frac{\beta v_s}{2\pi}\ln z$. Then the entanglement entropy for the infinite total size with OBC at finite temperature β is

$$S_U(r) = \frac{c}{6}\ln[\frac{\beta v_s}{\pi}\sinh(\frac{2\pi r}{\beta v_s})] + \ln g + \frac{s_1}{2}. \tag{6.38}$$

In the high temperature limit $r \gg \beta v_s$, Eq. (6.38) recovers the well-known 1D thermal entropy $\pi c r/3\beta v_s$ [117, 118]. In the opposite limit $\beta v_s \gg r$, Eq. (6.38) becomes $(c/6)\ln(2r)$.

Now we should consider the system with an impurity in the Fermi liquid theory region, that is, the system is described by the Hamiltonian Eq. (6.19) plus the local irrelevant interaction Eq. (6.25). With the presence of this local operator, we should calculate perturbatively the correction to the partition function Z_n in order to get the impurity entanglement entropy S_{imp}. Luckily, the irrelevant interaction is just the energy momentum tensor itself and its expectation value on the n-sheeted Riemann surface is just Eq. (6.33). The correction to Z_n of first order in ξ_K is:

$$\begin{aligned} -\delta Z_n &= -(\xi_K \pi) n \int_{-\infty}^{\infty} d\tau \langle \mathcal{H}_{s,L}(\tau, 0)\rangle_{\mathcal{R}_n} \\ &= -(\frac{\xi_K}{2}) n \int_{-\infty}^{\infty} \frac{\Delta_n (2ir)^2}{(\tau - ir)^2(\tau + ir)^2}, \end{aligned} \tag{6.39}$$

$\mathcal{H}_{s,L} = T/(2\pi)$ where $T(\tau, x)$ is the conventionally normalized energy-momentum tensor for the $c = 1$ and $\langle T\rangle_{\mathcal{R}_n}$ is given by Eq. (6.33). After doing the simple integral and taking the replica limit, for $R \to \infty$, we get

$$S_{imp} = \frac{\pi \xi_K}{12r}. \tag{6.40}$$

In Fig. (6.4), for $R \to \infty$, the FLT is applicable and $S_{imp}(r/\xi_K) \to \pi\xi_K/12r$, no matter R is even or odd as we expected.

In principle, in order to extend the FLT calculation to finite R, we will need the conformal mapping from a infinite n-sheeted Riemann surface to a finite one, which we

don't know. On the other hand, we can also try to exploit Eq. (6.35) following the similar idea in Ref. [27] by applying the standard finite size conformal mapping to $\langle \Phi_n \Phi_{-n} \rangle_c$ and Eq. (6.34), $\langle T\Phi_n \Phi_{-n} \rangle_c$.The three point function $\langle T(w)\Phi_n(w_1)\Phi_{-n}(w_2)\rangle$ for the system with a finite size R at zero temperature is:

$$\frac{(\pi/2R)^{2\Delta_n+2}}{\left[2\sinh\frac{\pi(w-w_1)}{2R}\right]^2\left[2\sinh\frac{\pi(w-w_2)}{2R}\right]^2\left[2\sinh\frac{\pi(w_1-w_2)}{2R}\right]^{2\Delta_n-2}}, \tag{6.41}$$

where $w = v_s\tau$, $w_1 = ir$ and $w_2 = -ir$. The terms proportional to $1/R^2$ is the disconnected part and will be cancelled by the denominator Z^n. Then, in the first order perturbation,

$$-\delta(\frac{Z_n}{Z^n}) = -(\frac{\xi_K}{2})n \times \int_{-\infty}^{\infty} d\tau[(\frac{\pi}{2R})\frac{\sinh[i\pi r/R]}{\sinh[\frac{\pi(v\tau-ir)}{2R}]\sinh[\frac{\pi(v\tau+ir)}{2R}]}]^2. \tag{6.42}$$

We use the integral

$$\int_0^{\infty} \frac{dx}{\cosh ax - \cos t} = \frac{t}{a}\csc t, \tag{6.43}$$

from Ref. [119] and differentiate Eq. (6.43) with respect to t on the both sides. Applying this result and the product-to-sum hyperbolic identity to Eq. (6.42), we can complete the integral and after the replica limit we get:

$$S_{imp} = \frac{\pi\xi_K}{12R}[1 + \pi(1 - \frac{r}{R})\cot(\frac{\pi r}{R})]. \tag{6.44}$$

Of course, Eq. (6.44) reduces to Eq. (6.40) for $R \gg r$ and both of them agree with the scaling form of S_{imp}. Interestingly, Eq. (6.44) can be regarded as the first order Taylor expansion in ξ_K/r and ξ_K/R of $S_U = (1/6)\ln[R\sin\pi r/R]$ with r and R both shifted by $\pi\xi_K/2$. Consistently, Eq. (6.40) can be also obtained from expanding $(1/6)\ln(r+\pi\xi_K/2)$. In fact, many other quantities such as impurity susceptibility, specific heat and ground state energy correction can be also obtained in this fashion by shafting total system R to $R + \pi\xi_K/2$.

Within CFT methods, we can also calculate S_{imp} for infinite R but at finite temperature βv_s. We apply the standard finite temperature conformal mapping to $\langle T\Phi_n\Phi_{-n}\rangle_c$ and $\langle \Phi_n\Phi_{-n}\rangle_c$. The result for first order perturbation is just to replace $2R$ by β and sinh by sin in Eq. (6.42) with the integral from $-\beta/2$ to $\beta/2$. Completing the straightforward integral yields

$$S_{imp} = \frac{\pi^2\xi_K T}{6v_s}\coth(\frac{2\pi r T}{v_s}). \tag{6.45}$$

In the high temperature limit, $rT \gg v_s$, Eq. (6.45) approaches the thermodynamic impurity entropy, $S_{imp} \to \pi^2\xi_K T/(6v_s) = \pi^2 T/(6T_K)$ [113]. In the low temperature limit $v_s \gg rT$, it becomes Eq. (6.40), $\pi\xi_K/(12r)$. As we discussed above, this is consistent with the observation in Ref. [27] that bulk entanglement entropy at finite temperature approaches the thermal entropy and that of infinite size at zero temperature in both limits.

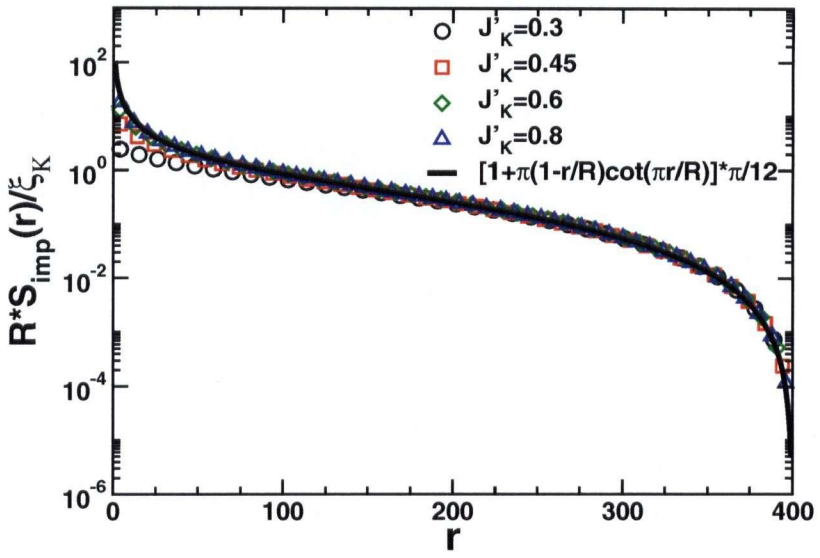

Figure 6.5: (a) DMRG results for $RS_{\rm imp}/\xi_K$ versus r, with $R = 400$, for the spin chain at J_2^c and various values of J_K' in the Fermi liquid regime. The black curve is the FLT prediction, Eq. (6.44).

6.3 The Comparison with DMRG

Now we compare the FLT calculation with the DMRG data. It's important to note that the FLT result only works in the strong effective coupling region, i.e. $r, R \gg \xi_K$. The first step is thus to obtain ξ_K. However, there is no unique way to determine the Kondo length scale ξ_K. We can use Eq. (6.11) to make the data of impurity entanglement entropy collapse on a universal scaling curve by rescaling ξ_K. When R is finite, the ground state has total spin 0 and 1/2 for even and odd R, respectively. ξ_K for even and odd R are listed in table (6.1).

J_K'	0.8	0.6	0.525	0.45	0.41	0.37	0.30	0.25	0.225	0.20
ξ_K (R even)	1.89	5.58	9.30	17.40	25.65	40.5	111	299	~565	~1196
ξ_K (R odd)	1.65	5.45	9.30	17.40	25.65	39.2	127	411	~ 870	~ 2200

Table 6.1: The numerically determined values for $\xi_K(J_K')$ using naive rescaling of $S_{imp}(J_K', r, R)$ at fixed r/R for $J_2 = J_2^c$. For R odd system sizes of $R = 19 \ldots 101$ have been used and for R even $R = 18 \ldots 102$. The estimates become unreliable once $\xi_K \gg R$.

For $R = 400$, the comparison between the uniform part of the entanglement entropy, Eq. (6.44) and DMRG data is shown in Fig. (6.5). They agree very well for $J_K' < 1$, i.e. the region $r, R \gg \xi_K$. In fact, one can also estimate ξ_K by means of Eq. (6.44). The

result is shown in table (6.2) and it's consistent with those in table (6.1). More details and other methods to obtain ξ_K can be found in Ref. [3, 4].

J_K'	1.00	0.80	0.60	0.525	0.45	0.41	0.37	0.30
ξ_K	0.65	1.97	5.93	9.84	17.83	25.65	38.29	83.79

Table 6.2: $\xi_K(J_K')$ as determined from $S_{imp}(J_K', r, R)$ for $R = 400$ using the FLT prediction, Eq. (6.44). The estimates become unreliable once ξ_K becomes comparable to R.

The presence of impurities will clearly affect the entanglement and we have here defined the impurity contribution to the entanglement entropy, S_{imp}. Using the equivalence of the electronic Kondo model and the $J_1 - J_2$ spin chain model in the regime $J_2 < J_2^c$ we have shown numerical evidence that S_{imp} follows a scaling form $S_{imp}(r/\xi_K, r/R)$ demonstrating the presence of the length scale ξ_K associated with screening of the impurity. We have provided rather strong arguments in favor of this scaling and analytical results based on a Fermi liquid approach valid for $r \gg \xi_K$. Finally, we have argued that at finite temperatures the entanglement entropy for a sub-system A of size r, $S(T)$, will approach the thermal entropy, $S_{th}(T)$, for $T \gg v_s/r$. In light of the generality of our model we expect our results to be quite widely applicable. The study of quantum impurity entanglement as it occurs in more complex models with many body ground-states displaying non-trivial order would clearly be of considerable interest.

References

[1] M.-S. Chang and I. Affleck. *Phys. Rev. B*, 76:054521, 2007.

[2] N. Laflorencie, E. S. Sørensen, M.-S. Chang, and I. Affleck. *Phys. Rev. Lett.*, 96: 100603, 2006.

[3] E. S. Sørensen, M.-S. Chang, N. Laflorencie, and I. Affleck. *J. Stat. Mech.*, page L01001, 2007.

[4] E. S. Sørensen, M.-S. Chang, N. Laflorencie, and I. Affleck. *J. Stat. Mech.*, page 08003, 2007.

[5] H.J. Schulz. *Phys. Rev. B*, 34:6372, 1986.

[6] E. Dagotto and T.M. Rice. *Science*, 271:618, 1996.

[7] S. Gopalan T.M. Rice and M. Sigrist. *Europhysics Letters*, 23:445, 1993.

[8] R.M. Noack-D.J. Scalapino C.A. Hayward, D. Poilblanc and W. Hanke. *Phys. Rev. Lett.*, 75:926, 1995.

[9] S.R. White. *Phys. Rev. Lett.*, 77:3633, 1997.

[10] D.P. Goshorn D.C. Johnston, J.W. Johnson and A.J. Jacobson. *Phys. Rev. B*, 35: 219, 1987.

[11] M. Takano-K. Ishida M. Azuma, Z. Hiroi and Y. Kitaoka. *Phys. Rev. Lett.*, 73: 3463, 1994.

[12] J. Akimitsu-H. Takahashi N. Mori M. Uehara, T. Nagata and K. Kinoshita. *J. Phys. Soc. Jpn.*, 65:2764, 1994.

[13] H. Eisaki T. Osafune, N. Motoyama and S. Uchida. *Phys. Rev. Lett.*, 78:1980, 1996.

[14] S.R. White R. Noack and D.J. Scalapino. *Phys. Rev. Lett.*, 73:882, 1994.

[15] S.R. White and D.J. Scalapino. *Phys. Rev. Lett.*, 80:1272, 1998.

[16] S.R. White and D.J. Scalapino. *Phys. Rev. B*, 57:3031, 1998.

[17] S.R. White and D.J. Scalapino. *Phys. Rev. B*, 55:R14706, 1997.

[18] S.R. White and D.J. Scalapino. *Phys. Rev. B*, 60:R753, 1999.

[19] S.R. White and D.J. Scalapino. *Phys. Rev. Lett.*, 91:136403, 2003.

[20] E. Jeckelmann G. Hager, G. Wellein and H. Fehske. *Phys. Rev. B*, 71:075108, 2005.

[21] J.D. Axe-Y. Nakamura J.M. Tranquada, B.J. Sternlieb and S. Uchida. *Nature*, 375: 561, 1995.

[22] T.G. Perring-H. Goka G.D. Gu G. Xu M. Fujita J.M. Tranquada, H. Woo and K. Yamada. *Nature*, 429:534, 2004.

[23] I. Affleck S.R.White and D.J. Scalapino. *Phys. Rev. B*, 65:165122, 2002.

[24] C. H. Bennett, H. J. Bernstein, S. Popescu, and B. Schumacher. *Phys. Rev. A*, 53: 2046, 1996.

[25] G. Vidal, J. I. Latorre, E. Rico, and A. Kitaev. *Phys. Rev. Lett.*, 90:227902, 2003.

[26] C. Holzhey, F. Larsen, and F. Wilczek. *Nucl. Phys. B*, 424:443, 1994.

[27] P. Calabrese and J. Cardy. *J. Stat. Mech.*, page 06002, 2004.

[28] S.A. Kivelson E.W. Carlson, V.J. Emery and D. Orgad. *Concepts in High Temperature Superconductivity, review chapter in The Physics of Conventional and Unconventional Superconductors.* Springer-Verlag, Germany, first edition, 2003.

[29] J.R. Schrieffer. *Theory of Superconductivity, Frontiers in Physics.* Addison-Wesley, U.S.A., first edition, 1988.

[30] J.B. Bednorz and K.A. Muller. *Z. Phys. B*, 64:189, 1986.

[31] V.J. Emery and S.A. Kivelson. *Phys. Rev. Lett.*, 74:3253, 1995.

[32] P.W. Anderson. *Science*, 256:1526, 1987.

[33] P.A. Lee. *Physica C*, 317-318:194, 1999.

[34] T. Timusk and B. Statt. *Rep. Prog. Phys.*, 62:61, 1999.

[35] B.O. Wells D.M. King W.E. Spicer A.J. Arko D. Marshall-L.W. Lombardo A. Kapitulnik P. Dickinson S. Doniach J. DiCarlo T. Loeser Z.-X. Shen, D.S. Dessau and C.H. Park. *Phys. Rev. Lett.*, 70:1553, 1993.

[36] J.C. Campuzano T. Takahashi M. Randeria M.R. Norman T. Mochiku K. Kadowaki H. Ding, T. Yokoya and J. Giapintzakis. *Nature*, 382:51, 1996.

[37] S.A. Kellar T. Noda H. Eisaki S. Uchida Z. Hussain Z.-X. Shen X.J. Zhou, P. Bogdanov. *Science*, 286:268, 1999.

[38] C. Renner S. Ono M. Kugler, O. Fischer and Y. Ando. *Phys. Rev. Lett.*, 86:4911, 2001.

[39] H.L. Kao J. Kwo R.J. Cava J.J. Krajewski H. Takagi, B. Batlogg and W. F. Peck Jr. *Phys. Rev. Lett.*, 69:2975, 1992.

[40] J.L. Tallon and J.W. Loram. *Physica C*, 349:53, 2001.

[41] Jr. D.J. Scalapino, E. Loh and J.E. Hirsch. *Phys. Rev. B*, 34:8190, 1986.

[42] D.C. Morgan Ruixing Liang W.N. Hardy, D.A. Bonn and Kuan Zhang. *Phys. Rev. Lett.*, 70:3999, 1993.

[43] W.C. Lee D.M. Ginsberg D.A. Wollman, D.J. Van Harlingen and A.J. Leggett. *Phys. Rev. Lett.*, 71:2134, 1993.

[44] C.C. Chi L.S. Yu-Jahnes A. Gupta T. Shaw J.Z. Sun C.C. Tsuei, J.R. Kirtley and M.B. Ketchen. *Phys. Rev. Lett.*, 73:593, 1994.

[45] S. Sachdev. *Science*, 288:475, 2000.

[46] G. Gruner. *Density Waves in Solids.* Perseus Books Group, U.S.A., first edition, 2000.

[47] J. Zaanen and O. Gunnarsson. *Phys. Rev. B*, 40:7391, 1989.

[48] H.J. Schulz. *Phys. Rev. Lett.*, 64:1445, 1990.

[49] J.M. Tranquada. *Physica B*, 241-243:745, 1998.

[50] S.A. Kivelson V.J. Emery and J.M. Tranquada. *Proc. Natl/ Acad. Sci.*, 96:8814, 1999.

[51] T.E. Mason H. Mook S.M. Hayden P.C. Canfield Z. Fisk-K.N. Clausen S-W. Cheong, G. Aeppli and J.L. Martinez. *Phys. Rev. Lett.*, 67:1791, 1991.

[52] E.M. McCarron W.E. Farneth J.D. Axe H. Chou M.K. Crawford, R.L. Harlow and Q. Huang. *Phys. Rev. B*, 44:7749, 1991.

[53] K. Yamada M. Fujita, H. Goka and M. Matsuda. *Phys. Rev. Lett.*, 88:167008, 2002.

[54] K.M. Lang V. Modhavan H. Eisaki S. Uchida J.E. Hoffman, E.W. Hudson and J.C. Davis. *Science*, 295:466, 2002.

[55] N. Kaneko M. Greven C. Howald, H. Eisaki and A. Kapitulnik. *Phys. Rev. B*, 67: 14533, 2003.

[56] K. Hirota Y. Endoh K. Yamada G. Shirane Y.S. Lee M.A. Kastner H. Kimura, H. Matsushita and R.J. Birgeneau. *Phys. Rev. B*, 61:14366, 2000.

[57] K. Kurahashi J. Wada S. Wakimoto S. Ueki H. Kimura Y. Endoh S. Hosoya G. Shirane R.J. Birgeneau M. Greven M.A. Kastner K. Yamada, C.H. Lee and Y.J. Kim. *Phys. Rev. B*, 57:6165, 1998.

[58] M.A. Kastner Y. Endoh S. Wakimoto K. Yamada R.W. Erwin S.-H. Lee G. Shirane Y.S. Lee, R.J. Birgeneau. *Phys. Rev. B*, 60:3643, 1999.

[59] Pengcheng Dai H.A. Mook and F. Dogan. *Phys. Rev. Lett.*, 88:097004, 2002.

[60] S. Trugman. *Phys. Rev. B*, 37:1597, 1988.

[61] J.E. Hirsch. *Phys. Rev. Lett.*, 59:228, 1987.

[62] S.A. Kivelson V.J. Emery and H.Q. Lin. *Phys. Rev. Lett.*, 64:475, 1990.

[63] A.R. Bishop A. H. Castro Neto B.P. Stojkovi, Z.G. Yu and N. Gronbech-Jensen. *Phys. Rev. Lett.*, 82:4679, 1999.

[64] A.H. Castro Neto. *Phys. Rev. B*, 51:3254, 1995.

[65] M. Seul and D. Andelman. *Science*, 267:476, 1995.

[66] F. Becca C. Gazza L. Capriotti A. Parola S. Sorella, G.B. Martins and E. Dagotto. *Phys. Rev. Lett.*, 88:117002, 2002.

[67] E. Fradkin S.A. Kivelson and V.J. Emery. *Nature*, 393:550, 1998.

[68] E.W. Carlson V.J. Emery X.J. Zhou D. Orgad, S.A. Kivelson and Z.-X. Shen. *Phys. Rev. Lett.*, 86:4362, 2001.

[69] S.A. Kivelson E.W. Carlson, D. Orgad and V.J. Emery. *Phys. Rev. B*, 62:3422, 2000.

[70] A. Rusydi A. Gozar P.G. Evans T. Siegrist L.Venema H. Eisaki-E.D. Isaacs P. Abbamonte, G. Blumberg and G.A. Sawatzky. *Nature*, 431:1078, 2004.

[71] M. Fabrizio and A. Gogolin. *Phys. Rev. B*, 51:17827, 1995.

[72] S. Eggert and I. Affleck. *Phys. Rev. Lett.*, 75:934, 1995.

[73] R. Egger and H. Grabertr. *Phys. Rev. Lett.*, 75:3505, 1995.

[74] T.M. Rice T. Siller, M. Troyer and S.R. White. *Phys. Rev. B*, 65:205109, 2002.

[75] S. Capponi and D. Poilblanc. *Phys. Rev. B*, 66:R180503, 2002.

[76] M. Oshikawa M. Yamanaka and I. Affleck. *Phys. Rev. Lett.*, 79:1110, 1997.

[77] B. Doucot and J. Vidal. *Phys. Rev. Lett.*, 88:227005, 2002.

[78] V. Cataudella M. Rizzi and R. Fazio. *Phys. Rev. B*, 73:R100502, 2006.

[79] P. Schuck G. Ropke, A. Schnell and P. Nozieres. *Phys. Rev. Lett.*, 80:3177, 1998.

[80] C.J. Wu. *Phys. Rev. Lett.*, 95:266404, 2002.

[81] A.A. Nersesyan A.O. Gogolin and A.M. Tsvelik. *Bosonization and Strongly Correlated Systems.* Cambridge University Press, United Kingdom, first edition, 1998.

[82] U. Ledermann and K. Le Hur. *Phys. Rev. B*, 61:2479, 2000.

[83] D. Senechal. cond-mat/9908262, 1999.

[84] E. Orignac and T. Giamarchi. *Phys. Rev. B*, 57:11713, 1998.

[85] H. J. Schulz. *Phys. Rev. B*, 52:R2959, 1996.

[86] M. Fabrizio. *Phys. Rev. B*, 37:325, 1993.

[87] L Balents and M.P.A. Fisher. *Phys. Rev. B*, 53:12133, 1996.

[88] E. Arrigoni. *Phys. Status Solidi B*, 195:425, 1996.

[89] L Balents H.H. Lin and M.P.A. Fisher. *Phys. Rev. B*, 56:6569, 1997.

[90] K. Le Hur U. Ledermann and T.M. Rice. *Phys. Rev. B*, 62:16383, 1997.

[91] L Balents H.-H. Lin and M.P.A. Fisher. *Phys. Rev. B*, 66:075105, 2002.

[92] W. Chen M.-S. Chang and H.-H. Lin. *Progress of Theoretical Physics*, 160:79, 2005.

[93] H.-H. Lin A. Seidel and D.-H. Lee. *Phys. Rev. B*, 71:220501, 2005.

[94] H.-H. Lin D. Chang W. Chen, M.-S. Chang and C.-Y. Mou. *Phys. Rev. B*, 70: 205413, 2004.

[95] H. J. Schulz. *Phys. Rev. Lett.*, 47:1840, 1981.

[96] T. Giamarchi. *Quantum Physics in One Dimension.* Oxford Science Publication, United Kingdom, first edition, 2004.

[97] F.D.H. Haldane. *Phys. Rev. Lett.*, 47:1840, 1981.

[98] A. Osterloh, L. Amico, G. Falci, , and R. Fazio. *Nature*, 416:608, 2005.

[99] I. Affleck and A.W.W. Ludwig. *Phys. Rev. Let.*, 67:161, 1991.

[100] I. Affleck, D. Gepner, H.J. Schulz, and T. Ziman. *J. Phys. A Math. Gen.*, 22:511, 1989.

[101] S. Eggert and I. Affleck. *Phys. Rev. B*, 46:10866, 1992.

[102] G. Refael and J. E. Moore. *Phys. Rev. Lett.*, 93:260602, 2004.

[103] G. C. Levine. *Phys. Rev. Lett.*, 93:226402, 2004.

[104] H.-Q. Zhou, T. Barthel, J. Fjaerestad, and U. Schollwöck. 2006.

[105] S. Y. Cho and R. H. McKenzie. *Phys. Rev. A*, 73:012109, 2006.

[106] A. C. Hewson. *The Kondo Problem to Heavy Fermions.* Cambridge University Press, 2000.

[107] J. Gan. *J. Phys. Condens. Matter*, 6:4547, 1994.

[108] E. S. Sørensen and I. Affleck. *Phys. Rev. B*, 53:9153, 1996.

[109] V. Barzykin and I. Affleck. *Phys. Rev. B*, 57:432, 1998.

[110] I. Affleck and P. Simon. *Phys. Rev. Lett.*, 86:2854, 2001.

[111] E. S. Sørensen and I. Affleck. *Phys. Rev. Lett.*, 94:086601, 2005.

[112] P. Nozières. *J. Low Temp. Phys.*, 17:31, 1974.

[113] I. Affleck. *Nucl. Phys. B*, 336:517, 1990.

[114] I. Affleck and A. W. W. Ludwig. *Nucl. Phys. B*, 352:849, 1991.

[115] I. Affleck and A. W. W. Ludwig. *Nucl. Phys. B*, 360:641, 1991.

[116] I. Affleck. *Nucl. Phys. B*, 360:641, 1991.

[117] J.L. Cardy H.W.J. Blote and M.P. Nightingale. *Phys. Rev. Lett.*, 56:742, 1986.

[118] I. Affleck. *Phys. Rev. Lett.*, 56:746, 1986.

[119] I. S. Gradshteyn and I. M. Ryzhik. *Table of Integrals, Series, and Products.* Academic Press, 2000.

[120] S. W. Tsai and J. B. Marston. *Phys. Rev. B*, 62:5546, 2000.

[121] V. Barzykin and I. Affleck. *J. Phys. A*, 32:867, 1999.

[122] I. Affleck. *J. Phys. A*, 31:4573, 1998.

Appendix A

$4k_F$ density operators

The higher order components of the density operator is known in 1D [97] but it's not clear what's the generalization to ladder systems. Here we will derive the higher harmonic moments of density operators through the process of integrating out the large momentum modes in the perturbative fashion. The density operator on the a^{th} leg can be written:

$$n_a(x) = \sum_{\alpha} c^{\dagger}_{a,\alpha} c_{a,\alpha} = \sum_{\alpha,i,j} S_{ai} S_{aj} \psi^{\dagger}_{i,\alpha} \psi_{j,\alpha}. \tag{A.1}$$

Using Eq. (1.14), we decompose $n_a(x)$ into components that oscillate with various phase factors $k_{Fi} \pm k_{Fj}$. We refer generically to all the components that oscillate with phases $\pm(k_{Fi} + k_{Fj})$ as "$2k_F$" terms. Naively, these appear to be all the components of the density operators. However, there are actually additional $4k_F$ (and higher) components. These arise from considering more carefully the RG transformation which leads to the low energy effective Hamiltonian. This transformation corresponds to integrating out, within the Feynman path integral, the "fast modes" of the fermion fields; i.e. all Fourier modes except for narrow bands, of width Λ, near each Fermi point, $\pm k_{Fi}$. We consider in detail how this produces $4k_F$ terms in $n_a(x)$, in lowest order in the Hubbard interaction, U. Consider calculating some Green's function involving $n_a(x)$, or $< n_a(x) >$ with open boundary conditions. Expanding the exponential of the action, to first order in U, inside the path integral effectively adds an extra term to $n_a(x)$:

$$n_a(x,\tau) \to n_a(x,\tau)[1 + U \int d\tau' \sum_{x'=1}^{L} \sum_{b=1}^{4} n_{b,\uparrow}(x',\tau') n_{b,\downarrow}(x',\tau')]. \tag{A.2}$$

We now expand the second term, of $O(U)$ in band fermions using:

$$n_a(x,\tau) = \sum_{i,j,\alpha,p,q} S_{ai} S_{aj} e^{iqx} \psi^{\dagger}_{i\alpha}(p) \psi_{j\alpha}(q+p), \tag{A.3}$$

$$\sum_{x'=1}^{L} \sum_{b=1}^{4} n_{b,\uparrow}(x') n_{b,\downarrow}(x')$$

$$= \sum_{b,i_1,i_2,i_3,i_4,p_1,p_2,p_3} C_{i_1,i_2,i_3,i_4} \psi^{\dagger}_{i_1\uparrow}(p_1 - p_2 + p_3) \psi_{i_2\uparrow}(p_1) \psi^{\dagger}_{i_3,\downarrow}(p_2) \psi_{i_4,\downarrow}(p_3). \tag{A.4}$$

Here:

$$C_{i_1,i_2,i_3,i_4} \equiv S_{ai_1} S_{ai_2} S_{ai_3} S_{ai_4}, \tag{A.5}$$

and we have suppressed the imaginary time labels τ, τ' which are not too important. Each fermion field, $\psi_{i\alpha}(p)$, may either be a slow mode with $|p-k_{Fi}| < \Lambda$ or $|p+k_{Fi}| < \Lambda$ or it may be a fast mode with $|p \pm k_{Fi}| > \Lambda$. Doing the functional integral over the fast modes eliminates some of the fermion fields from the correction, $\delta n_a(x)$, to the density operator, $n_a(x)$, replacing them by their expectation value. To generate $4k_F$ terms in $n_a(x)$ we take the case where four of the six fields in $n_a H_{int}$ are slow modes and two of them are fast modes. For instance consider the case where:

$$\begin{aligned} p &= -k_{F1} + \tilde{p}, \quad i = 1 \\ q &= k_{F1} + k_{F2} + k_{F3} + k_{F4} + \tilde{q} \\ p_1 &= k_{F4} + \tilde{p}_1, \quad i_1 = 4 \\ p_2 &= -k_{F2} + \tilde{p}_2, \quad i_2 = 2 \\ p_3 &= k_{F3} + \tilde{p}_3, \quad i_3 = 3 \end{aligned} \tag{A.6}$$

where all the $\tilde{p}$ and $\tilde{p}_i$ obey $|\tilde{p}| < \Lambda$ and $\tilde{q}$ is also small, of $O(\Lambda)$. Then four of the fields are slow modes but $\psi_{j\alpha}(p+q)$ and $\psi^\dagger_{i_1\uparrow}(p_1-p_2+p_3)$ are fast modes. Note that we have chosen the band index to correspond to the momentum range for all slow modes. This would be necessary if we assume that the momentum range Λ around each Fermi momentum is smaller than the difference of Fermi momenta between different bands. The product of fast mode fields gets replaced by its expectation value during the RG transformation:

$$< \psi_{j\alpha}(p+q)\psi^\dagger_{i_1\uparrow}(p_1-p_2+p_3) > \propto \delta_{ji_1}\delta_{\alpha\uparrow}\delta(p+q-p_1+p_2-p_3). \tag{A.7}$$

From Eq. (A.6) we see that the last δ-function in Eq. (A.7) can be written:

$$\delta(p+q-p_1+p_2-p_3) = \delta(\tilde{p}+\tilde{q}-\tilde{p}_1+\tilde{p}_2-\tilde{p}_3). \tag{A.8}$$

Thus the extra term in the density operator can be written schematically as:

$$\begin{aligned} \delta n_a(x) \;\propto\; & U\exp[i(k_{F1}+k_{F2}+k_{F3}+k_{F4})x] \sum_{j,\tilde{p},\tilde{p}_1,\tilde{p}_2,\tilde{p}_3} S_{a1}S_{aj}C_{j423}\exp[i(-\tilde{p}+\tilde{p}_1-\tilde{p}_2+\tilde{p}_3)x] \\ & \times\psi^\dagger_{1\uparrow}(-k_{F1}+\tilde{p})\psi_{4\uparrow}(k_{F4}+\tilde{p}_1)\psi^\dagger_{2\downarrow}(-k_{F2}+\tilde{p}_2)\psi_{3\downarrow}(k_{F3}+\tilde{p}_3) \\ =\; & U\exp[i(k_{F1}+k_{F2}+k_{F3}+k_{F4})x]S_{a1}S_{a2}S_{a3}S_{a4}\psi^\dagger_{L1\uparrow}(x)\psi_{R4\uparrow}(x)\psi^\dagger_{L2\downarrow}(x)\psi_{R3\downarrow}(x). \end{aligned} \tag{A.9}$$

Naturally, a large number of other such $4k_F$ terms are generated by choosing other momentum ranges for the slow and fast modes. It turns out all the terms allowed by the symmetry will be generated in the low energy continuum limit, which is what we expected.

Appendix B

RG Initial Values and the RG Potential Form

Here we explicitly give the bare coupling values in Eq. (4.2) in terms of the interactions in Eq.(1.8) and (1.9) for general doped N-leg ladders. By using $\vec{\sigma}_{\alpha\beta}\cdot\vec{\sigma}_{\gamma\delta} = 2\delta_{\alpha\delta}\delta_{\beta\gamma}-\delta_{\alpha\beta}\delta_{\gamma\delta}$, Eq. (4.2) can be written as

$$H_{int} = \sum_{\alpha\beta}\sum_{ij}\sum_{x}[\frac{1}{4}(\tilde{c}^{\rho}_{ij}+\tilde{c}^{\sigma}_{ij})\psi^{\dagger}_{Ri\alpha}\psi_{Rj\alpha}\psi^{\dagger}_{Li\beta}\psi_{Lj\beta} - \frac{1}{2}\tilde{c}^{\sigma}_{ij}\psi^{\dagger}_{Ri\alpha}\psi_{Rj\beta}\psi^{\dagger}_{Li\beta}\psi_{Lj\alpha}$$
$$+\frac{1}{4}(\tilde{f}^{\rho}_{ij}+\tilde{f}^{\sigma}_{ij})\psi^{\dagger}_{Ri\alpha}\psi_{Ri\alpha}\psi^{\dagger}_{Lj\beta}\psi_{Lj\beta} - \frac{1}{2}\tilde{f}^{\sigma}_{ij}\psi^{\dagger}_{Ri\alpha}\psi_{Ri\beta}\psi^{\dagger}_{Lj\beta}\psi_{Lj\alpha}], \qquad \text{(B.1)}$$

where i and j are running from 1 to N. Note that we have a factor of $1/2$ difference from the definition of operator J_{ij} in Ref. [89]. Expand Eq. (1.8) and (1.9) in terms of the chiral fermions Eq. (1.14) and we have

$$\begin{aligned} H_{U,V} &= \sum_{\alpha\beta}\sum_{ijkl}\sum_{x}\sum_{P_i}[\frac{V}{2}A_{ijkl}e^{(-iP_3k_{F_k}+iP_4k_{F_l})} + \frac{V_{\perp}}{2}(B^1_{ijkl}+B^2_{ijkl}+B^3_{ijkl})]\times \\ & e^{i(-P_1k_{F_i}+P_2k_{F_j}-P_3k_{F_k}+P_4k_{F_l})x}\psi^{\dagger}_{P_1i\alpha}\psi_{P_2j\alpha}\psi^{\dagger}_{P_3k\beta}\psi_{P_4l\beta} \\ & +\sum_{ijkl}\sum_{x}\sum_{P_i}A_{ijkl}Ue^{i(-P_1k_{F_i}+P_2k_{F_j}-P_3k_{F_k}+P_4k_{F_l})x}\psi^{\dagger}_{P_1i\uparrow}\psi_{P_2j\uparrow}\psi^{\dagger}_{P_3k\downarrow}\psi_{P_4l\downarrow}, \qquad \text{(B.2)} \end{aligned}$$

where $P_i = \pm$ for R/L fermions and with the S_{jm} in Eq. (1.10)

$$\begin{aligned} A_{ijkl} &= \sum_{m=1}^{N} S^*_{im}S_{jm}S^*_{km}S_{lm}, \\ B^m_{ijkl} &= S^*_{mi}S_{mj}S^*_{m+1,k}S_{m+1,l}. \end{aligned}$$

The $1/2$ factor for V and $V_{\perp}$ in Eq. (1.9) will put them in an equal footing with U. Now we just have to compare the coefficients in Eq. (4.2) and (B.2) for the same interaction then we can obtain the bare initial values of the RG interactions. Recall that $\tilde{f}_{ij} = \tilde{f}_{ji}$, $\tilde{c}_{ij} = \tilde{c}_{ji}$ and $\tilde{f}_{ii} = 0$. Following the convention in Ref. [89], the RG equations are written down for $\tilde{c}_{ii}$, $\tilde{c}_{ij}$ and $\tilde{f}_{ij}$ where $i < j$. It will be convenient to define the following quantity for OBC:

$$S_{ijkl} = \sum_{m=1}^{N-1} B^m_{ijkl}.$$

In this basis, we write down the general form for the initial values in the RG equations:

$$\tilde{c}^{\rho}_{ii} = 2[(2-\cos 2k_{F_i})VA_{iiii} + V_{\perp}S_{iiii} + UA_{iiii}], \tag{B.3}$$
$$\tilde{c}^{\sigma}_{ii} = 2(VA_{ijij}\cos 2k_{F_i} + V_{\perp}S_{iiii} + UA_{iiii}), \tag{B.4}$$
$$\tilde{c}^{\rho}_{ij} = 4\{VA_{ijij}[2\cos(k_{F_i}-k_{F_j}) - \cos(k_{F_i}+k_{F_j})] + V_{\perp}S_{ijij} + UA_{ijij}\}, \tag{B.5}$$
$$\tilde{c}^{\sigma}_{ij} = 4[VA_{ijij}\cos(k_{F_i}+k_{F_j}) + V_{\perp}S_{ijij} + UA_{ijij}], \tag{B.6}$$
$$\tilde{f}^{\rho}_{ij} = 4\{VA_{ijij}[2-\cos(k_{F_i}+k_{F_j})] + V_{\perp}(2S_{iijj} - S_{ijij}) + UA_{ijij}\}, \tag{B.7}$$
$$\tilde{f}^{\sigma}_{ij} = 4[VA_{ijij}\cos(k_{F_i}+k_{F_j}) + V_{\perp}S_{iijj} + UA_{ijij}]. \tag{B.8}$$

where $i<j$ here. Eq. (B.3)-(B.8) are not the basis such that the RG potential exists. In practice, we always deal with the RG equations in the potential basis. Therefore, we rescale Eq. (B.3)-(B.8) into the RG potential basis (without tilde) by

$$\tilde{c}^{\rho}_{ii} = 4\sqrt{2}(2\pi v_i)c^{\rho}_{ii}, \tag{B.9}$$
$$\tilde{c}^{\sigma}_{ii} = 4\sqrt{\frac{2}{3}}(2\pi v_i)c^{\sigma}_{ii}, \tag{B.10}$$
$$\tilde{a}^{\rho}_{ij} = 4\sqrt{v_i v_j}(2\pi)a^{\rho}_{ij}, \tag{B.11}$$
$$\tilde{a}^{\sigma}_{ij} = \frac{4}{\sqrt{3}}\sqrt{v_i v_j}(2\pi)a^{\sigma}_{ij}, \tag{B.12}$$

here a is c or f and again $i<j$. After this rescaling, the explicit form of RG potential is:

$$\begin{aligned}
V(\vec{g}) = & -\sum_i \frac{4\sqrt{2}}{3\sqrt{3}}(c^{\sigma}_{ii})^3 - \sum_{i<j}\frac{4}{3\sqrt{3}}\gamma_{ij}(f^{\sigma}_{ij})^3 \\
& + \sum_{i<j}(c^{\rho}_{ij})^2\left[-\frac{1}{\sqrt{2}}c^{\rho}_{ii} - \frac{1}{\sqrt{2}}c^{\rho}_{jj} + \gamma_{ij}f^{\rho}_{ij}\right] \\
& + \sum_{i<j}(c^{\sigma}_{ij})^2\left[-\frac{1}{\sqrt{2}}c^{\rho}_{ii} - \frac{1}{\sqrt{2}}c^{\rho}_{jj} + \gamma_{ij}f^{\rho}_{ij}\right] \\
& + \sum_{i<j}(c^{\sigma}_{ij})^2\left[-\frac{\sqrt{2}}{\sqrt{3}}c^{\sigma}_{ii} - \frac{\sqrt{2}}{\sqrt{3}}c^{\sigma}_{jj} - \frac{2}{\sqrt{3}}\gamma_{ij}f^{\sigma}_{ij}\right] \\
& + \sum_{i<j}c^{\rho}_{ij}c^{\sigma}_{ij}\left[-\sqrt{2}c^{\sigma}_{ii} - \sqrt{2}c^{\sigma}_{jj} + 2\gamma_{ij}f^{\sigma}_{ij}\right] \\
& - \sum_{i<j<k}c^{\rho}_{ij}c^{\rho}_{jk}c^{\rho}_{ik} - \frac{2}{\sqrt{3}}\sum_{i<j<k}c^{\sigma}_{ij}c^{\sigma}_{jk}c^{\sigma}_{ik} \\
& - \sum_{i<j<k}\left[c^{\rho}_{ij}c^{\sigma}_{jk}c^{\sigma}_{ik} + c^{\sigma}_{ij}c^{\rho}_{jk}c^{\sigma}_{ik} + c^{\sigma}_{ij}c^{\sigma}_{jk}c^{\rho}_{ik}\right],
\end{aligned} \tag{B.13}$$

where the parameters γ_{ij} is defined as

$$\gamma_{ij} = \frac{2\sqrt{v_i v_j}}{v_i + v_j}. \tag{B.14}$$

With all the above results, we have the bare initial values for the RG equations derived from simply taking the derivative of the RG potential in Eq. (B.13).

Appendix C

Dimerization Derivation

The energy density for XXZ antiferromagnetic spin chains:

$$\langle h_r \rangle = \left\langle (S_r^+ S_{r+1}^- + S_r^- S_{r+1}^+)/2 + \Delta S_r^z S_{r+1}^z \right\rangle \tag{C.1}$$

is uniform in periodic chains. On the other hand, an open end breaks translational invariance and there will be a slowly decaying alternating term or "dimerization" in the energy density

$$\langle h_r \rangle = E_U(r) + (-1)^r E_A(r), \tag{C.2}$$

where $E_A(r)$ becomes nonzero near the boundary and decays slowly away from it. We can calculate $E_A(r)$ by Abelian bosonization modified by OBC [120]. In the critical region $|\Delta| \leq 1$, the low energy effective Hamiltonian is just a free massless relativistic boson.

The staggered part of $h_r \sim (-1)^{r+1}(\psi_R^\dagger \psi_L - \psi_L^\dagger \psi_R) \sim (-1)^{r+1} \sin(\sqrt{4\pi K}\phi)$. Here we basically follow the notations in Ref. [101] but define the Luttinger parameter as $K = \pi/(2(\pi - \cos^{-1}\Delta))$ so that $K = 1$ for an XY spin chain and $K = 1/2$ for the Heisenberg model. In a system with finite R and OBC,

$$E_A(r, R) \propto \left\langle \sin(\sqrt{4\pi K}\phi) \right\rangle \propto \frac{1}{[\frac{2R}{\pi} \sin(\frac{\pi r}{R})]^K}. \tag{C.3}$$

At the Heisenberg point, $\Delta = 1$, Eq. (C.3) will have some logarithmical corrections due to the presence of a marginally irrelevant operator $-(gv/2\pi)\vec{J}_L \cdot \vec{J}_R$ in the low energy Hamiltonian. The staggered energy density $E_A \sim \sin(\sqrt{2\pi}\phi)$ has the anomalous dimension

$$\gamma(g) = 1/2 - 3g/4. \tag{C.4}$$

With a boundary, the renormalization group equation for E_A is

$$[\partial/\partial(\ln r) + \beta(g)\partial/\partial g + \gamma(g)]E_A(r) = 0. \tag{C.5}$$

The presence of the boundary actually won't change the scaling dimension of $E_A(r)$ since we are looking at the case $r \gg 1$. This can be seen from considering the operator product expansion of the interaction term in the Hamiltonian Eq. (C.3) with $E_A(r)$. At short distances and away from the boundary, it's unaffected by the boundary. The general solution of Eq. (C.5) is

$$E_A(r) = F[g(r)] \exp\{-\int_{r_0}^{r} d(\ln r')\gamma[g(r')]\}, \tag{C.6}$$

where F is an arbitrary function of $g(r)$. With the second order beta function, $\beta = -g^2$, we easily get $E_A(r) \propto 1/[\sqrt{r}(\ln|r|)^{3/4}]$ [117]. One can push this a bit further following the similar calculation in Ref. [121, 122]. Provided with the beta function up to third order

$$\beta(g) = g^2 - (1/2)g^3, \tag{C.7}$$

the effective coupling solved from Eq. (C.7) is

$$\frac{1}{g(r)} - \frac{1}{g_0} = \{\ln(r/r_0) + \frac{1}{2}\ln[\ln(r/r_0)]\},$$

and expanding $E_A(r)$ in terms of $g(r)$, we can improve the solution as

$$E_A(r) = \frac{a_0}{\sqrt{r}[\ln(r/a_1) + \frac{1}{2}\ln\ln(r/a_1)]}\{1 + \frac{a_2}{[\ln(r/a_1)]^2}\}, \tag{C.8}$$

where the $1/[\ln(r/a_1)]$ term can be always absorbed by redefining a_1.